

Experiment and theory

Combination of experiment and theory to determine data and understanding on reactions for application in combustion

Transition state theory

Canonical

$$k(T) = \frac{k_B T}{h} \frac{Q^\ddagger}{Q_{\text{react}}} \exp(-E^\ddagger / k_B T)$$

Q - partition function

\ddagger indicates the transition state

ρ is the density of states (number of states per unit energy range)

N^\ddagger is the sum of states at the transition state from energy zero to E

Properties of transition state (and reactants if necessary) determined from electronic structure calculations

Microcanonical

$$k(E) = \frac{N^\ddagger(E)}{h\rho_{\text{react}}(E)}$$

CH₃ Vibrational energy levels / cm⁻¹

1. Stretch , 3004 (A1')
2. Out of plane bend 606 (A2'')
3. stretch, 3161 (E')
4. deformation, 1396 (E')

quanta	OOP bend	deformation	stretches
0	0	0	0
1	606	1396(2)	3004 3161(2)
2	1212	2792(3)	
3	1818	3988(4)	
4	2424		
5	3030	$E = h\nu c$ $1000 \text{ cm}^{-1} \equiv 11.96 \text{ kJ mol}^{-1}$	
6	3636		

Sums and densities of states for CH₃

Energy range/cm ⁻¹	Density / 500cm ⁻¹	Sum of states
0 - 499	1	1
500 - 999	1	2
1000 - 1499	3	5
1500 - 1999	1	6
2000 - 2499	1	7
2500 - 2999	4	11
3000 - 3499	4	15
3500 - 3999	5	20

Thermodynamic Formulation of TST

Equilibrium Constant = ratio of Partition Functions

$$K = \frac{Q_{\text{products}}}{Q_{\text{reactants}}} = \exp\left(-\frac{\Delta G}{k_B T}\right)$$

Klippenstein p11

$$k(T) = \frac{k_B T}{h} \frac{Q^\ddagger}{Q_{\text{reac}}} \exp(-E^\ddagger / k_B T)$$

$$k(T) = \frac{k_B T}{h} \exp\left(-\frac{\Delta G^\ddagger}{k_B T}\right)$$

Variational =>
Maximize ΔG^\ddagger

$$k(T) = \frac{k_B T}{h} \exp\left(-\frac{\Delta H^\ddagger}{k_B T}\right) \exp(\Delta S^\ddagger)$$

Maximize ΔH^\ddagger
Minimize ΔS^\ddagger

Canonical Partition Functions Klippenstein p13

Rigid Rotor Harmonic Oscillator (RRHO)

$$Q = Q_{trans} Q_{rot} Q_{vib} Q_{elec}$$

$$Q_{trans} = \left(\frac{2\pi M k_B T}{h^2} \right)^{3/2} V$$

Last lecture - determination of data for calculation of Qs from spectroscopy and electronic structure calcs

$$Q_{rot} = \frac{\pi^{1/2}}{\sigma} \left(\frac{8\pi^2 I_a k_B T}{h^2} \right)^{1/2} \left(\frac{8\pi^2 I_b k_B T}{h^2} \right)^{1/2} \left(\frac{8\pi^2 I_c k_B T}{h^2} \right)^{1/2}$$

$$Q_{vib}^{quan} = \prod_{i=1}^n \frac{\exp(-h\nu_i/2k_B T)}{1 - \exp(-h\nu_i/k_B T)}$$

$$Q_{vib}^{class} = \prod_{i=1}^n \frac{k_B T}{h\nu_i}$$

$$Q_{elec} = \sum_{i=1} g_i \exp\left(-\frac{E_i}{k_B T}\right)$$

At 300 K
 $kT/hc = 208 \text{ cm}^{-1}$

Statistical Mechanics, D. A. McQuarrie, Harper & Row

Kinetic Accuracy

Klippenstein p24

Kinetic Accuracy ~ Factor of 2

Energy to chemical accuracy

Transition State Theory

RRHO Energy Levels

Eckart Tunneling

Subkinetic Accuracy ~ 20% Accuracy

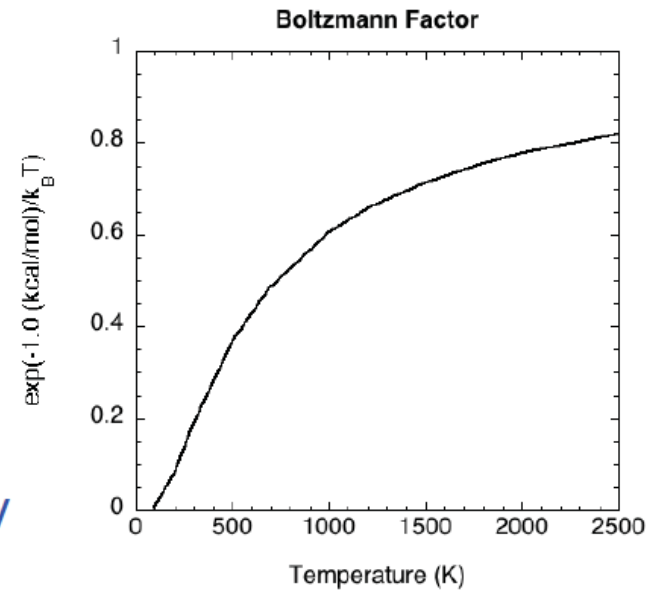
Many factors

Multidimensional Tunneling; Variational Effects

Anharmonicities; Transition State Recrossing

Energy Transfer Probabilities; 2D Master Equation

Empirical Normalization - Adjust some parameter to reproduce experiment hope for good interpolation/extrapolation

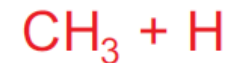


Radical + radical reactions
e.g. $\text{CH}_3 + \text{H}$, $\text{CH}_3 + \text{CH}_3$
No barrier on surface. Transition states
determined variationally

Where is the Transition State?

Calculate $Q(T,R)$ or $N(E,R)$ as function of R

Transition State is at position of minimum in Q or N



Radical - Molecule

Saddle Point

$\text{Exp}(-\beta E)$ dominates

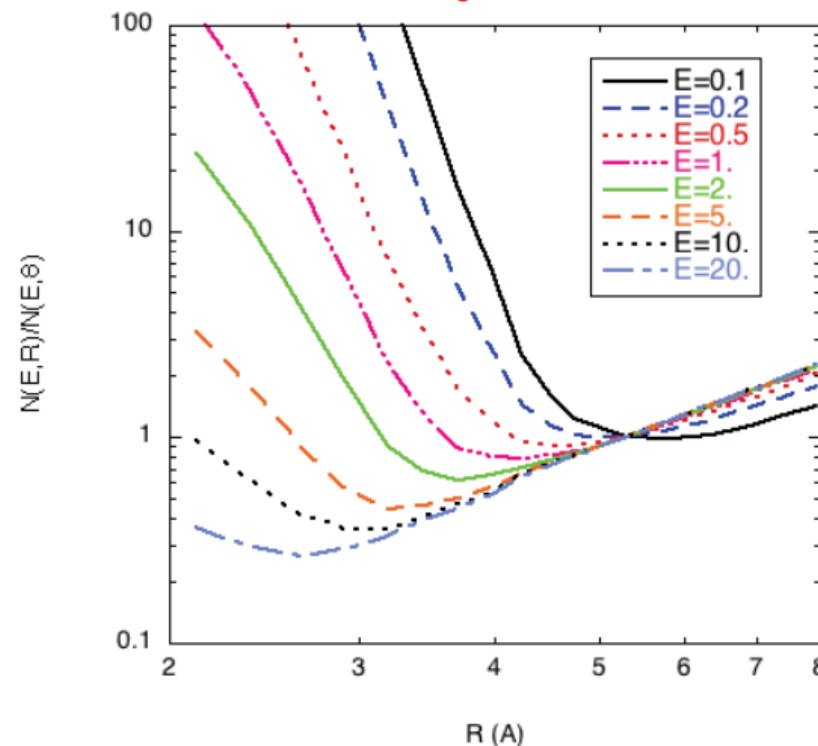
Radical - Radical

No Saddle Point

With Decreasing R

Entropy Decreases

$\text{Exp}(-\beta V_{\min})$ Increases



Correlation of reactant and product modes for CH_3+H

- Conserved Modes – Vibrations of Fragments
- Transitional Modes – Fragment Rotations, Orbital Motion, and Reaction Coordinate

Vibrational frequencies / cm^{-1}

CH_3

A_1'	3004
A_2''	606
E'	3161
E'	1396

CH_4

A_1	2917
E	1534
T_2	3019
T_2	1306

Methyl and Ethane frequencies

CH₃

A ₁ '	3004
A ₂ "	606
E'	3161
E'	1396

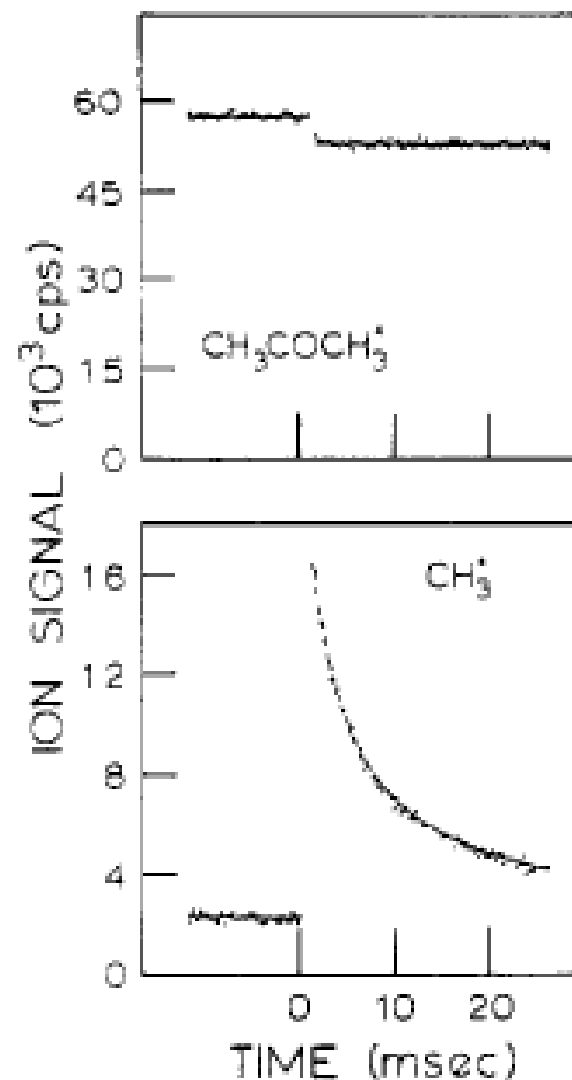
C₂H₆

A _{1g}	2896	E _g	2969
A _{1g}	1388	E _g	1468
A _{1g}	995	E _g	1190
A _{1u}	289	E _u	2974
A _{2u}	2915	E _u	1460
A _{2u}	1370	E _u	822

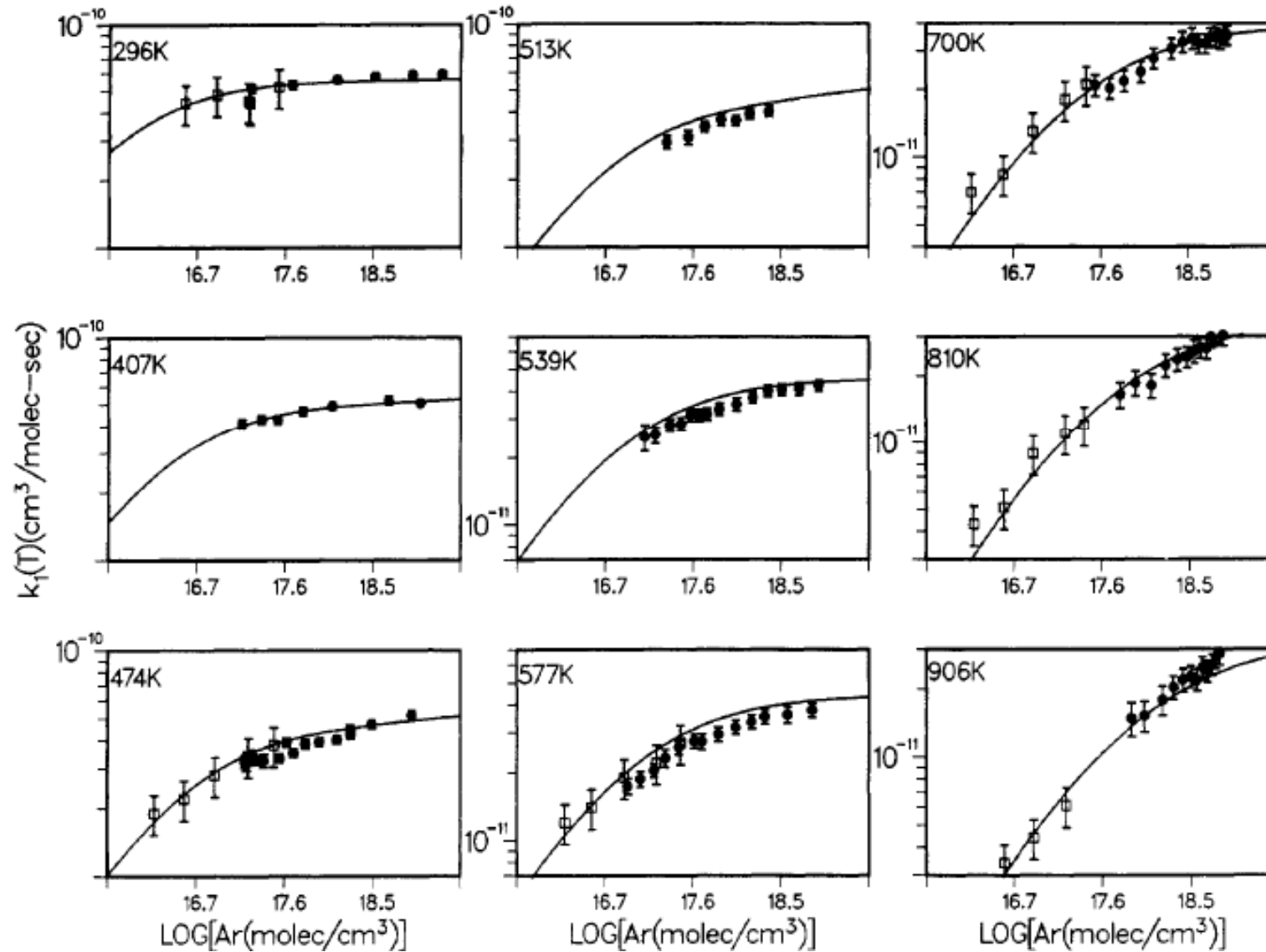


Slagle et al. *J. Phys. Chem.* 1988, 92, 2455-2462

- Laser flash photolysis + photionization mass spectrometry (PIMS) at low pressures and absorption spectroscopy (AS) at high pressures.
- Reaction is second order in radical - so absolute, not relative, concentration needed. Use absorption cross section for AS (see *J. Phys. Chem.* 1985, 89, 2268-2274) and calibration for PIMS, against loss of precursor.



Rate coefficient vs pressure

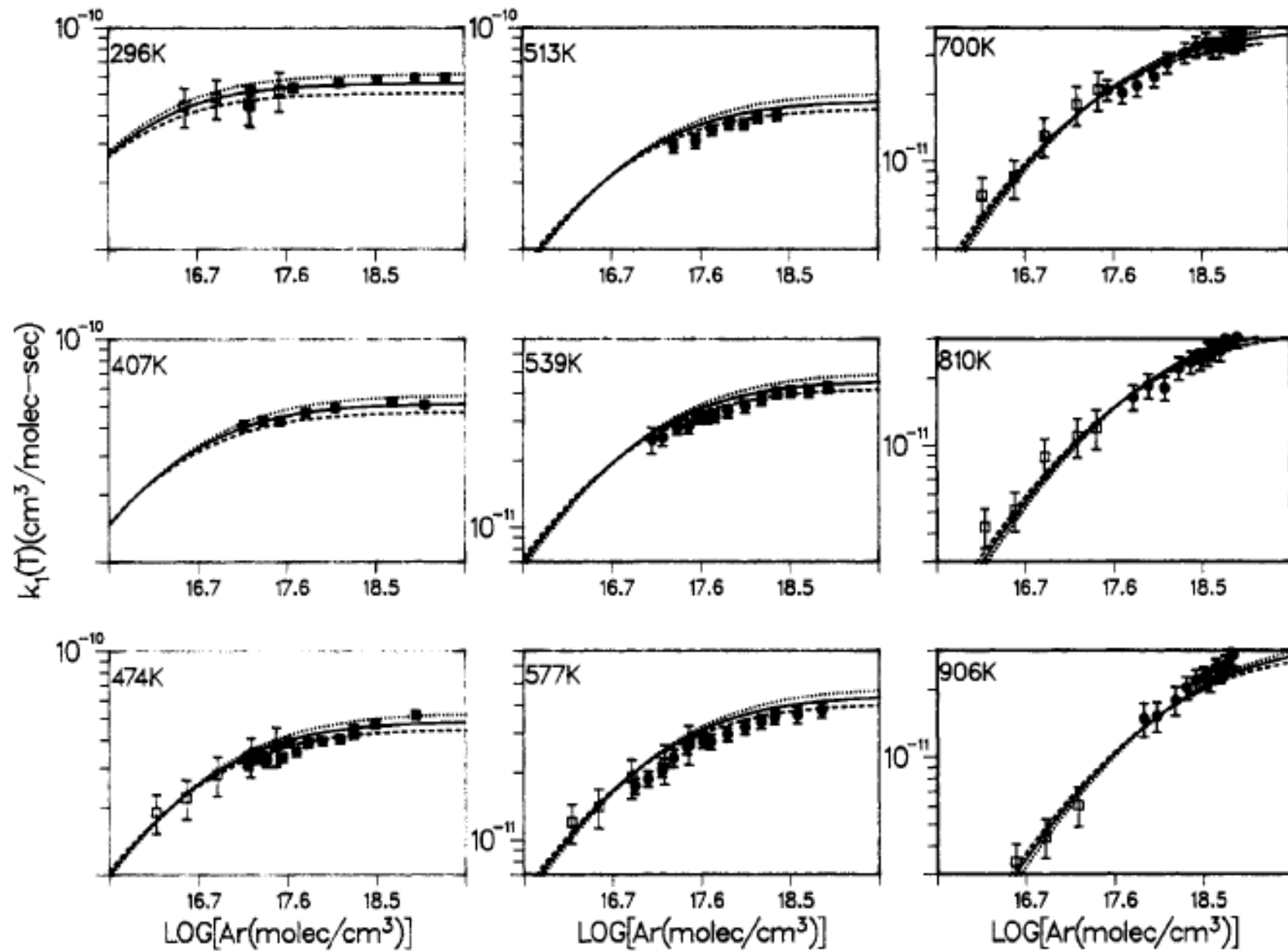


Theory - Wagner and Wardlaw,
J. Phys. Chem. 1988, 92, 2462-2471

- Applied flexible transition state theory to calculate microcanonical rate constants, $k(E, J)$ with a RRKM model:

$$k_1(T, [M]) = \left(\frac{1}{4}\right) \frac{1}{Q(T)^2} \int_0^\infty \int_0^\infty dJ dE N(E, J) \frac{k_s[M]}{k_s[M] + k(E, J)} e^{-E/kT}$$

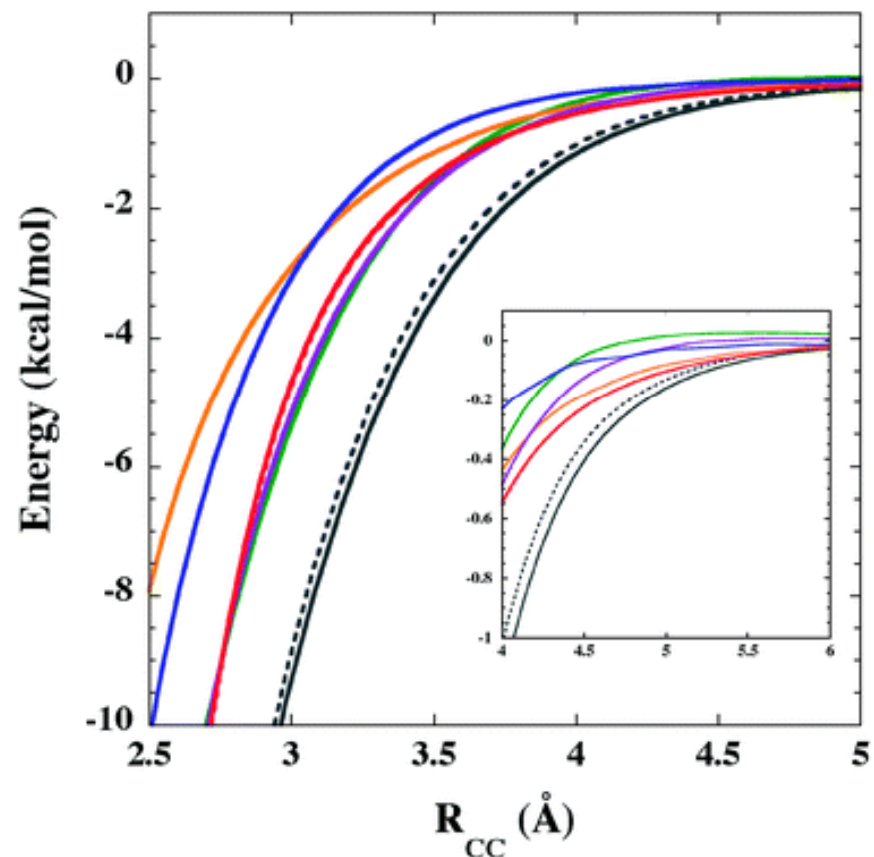
- Two adjustable parameters linked to (i) efficiency of collisional energy transfer and (ii) the evolution of the transitional modes.
- Obtained best fit to experimental data and then fitted to the Troe parameterisation.



More recent calculations, based on ab initio surfaces

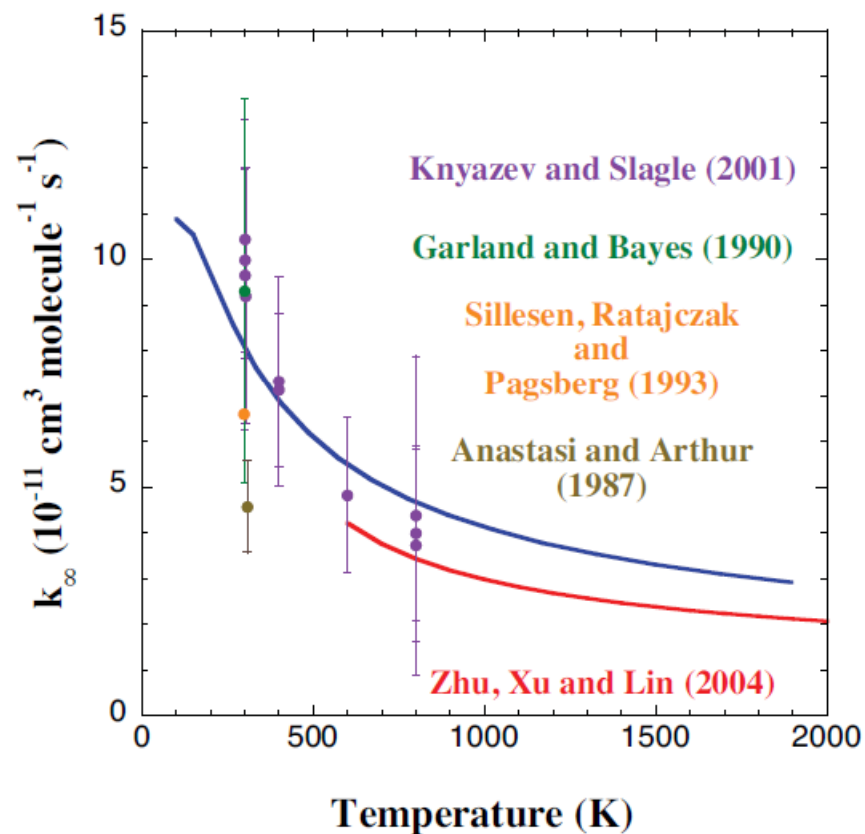
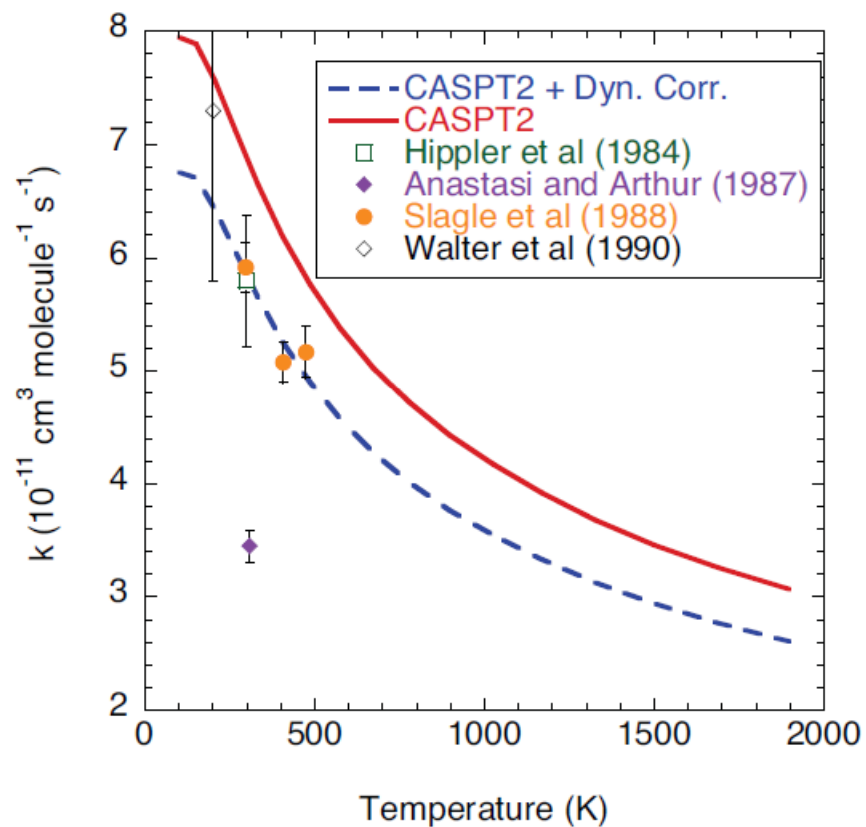
Harding et al Phys. Chem. Chem. Phys., 2008, 9,4055

- k_{∞} depends sensitively on potential energy, V , as radicals approach.
- V_{calc} depends on the level of theory used.
- Calculated $k_{\infty}(T)$ varies by > factor of 10 as level of theory is changed.
- $k_{\infty}(T)_{\text{calc}}$ may be more accurate than $k_{\infty}(T)_{\text{expt}}$, because the latter depends on extrapolation



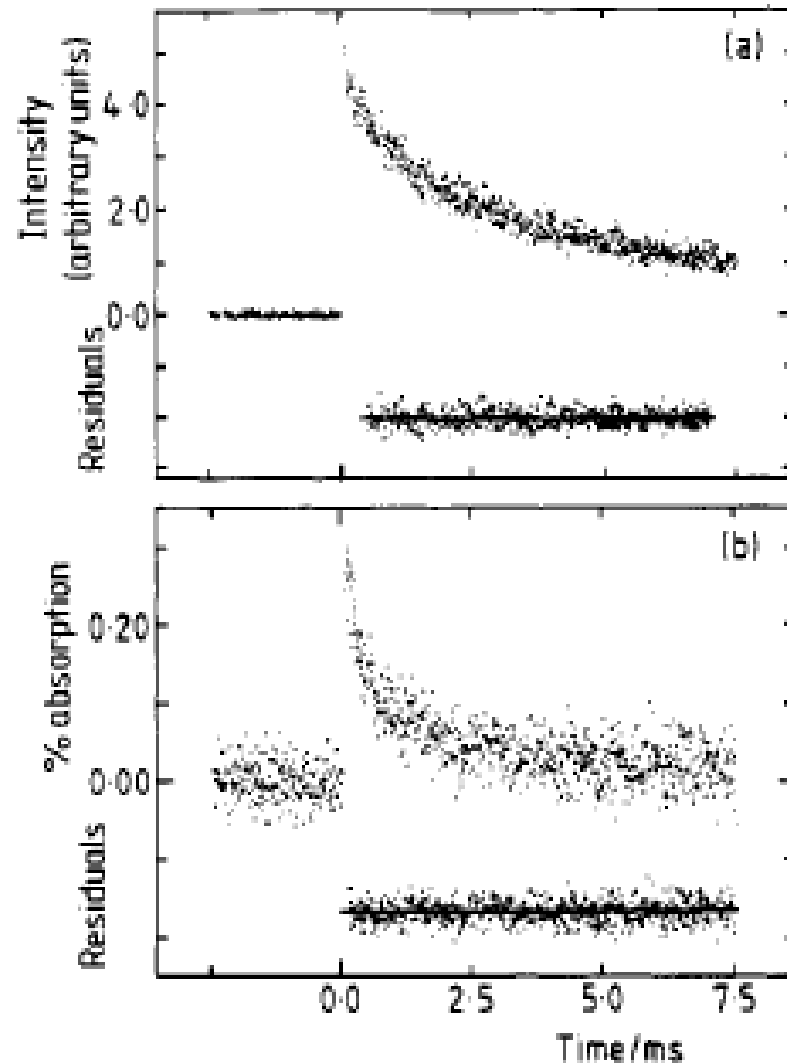


Klippenstein p122



Experimental determination of $k(\text{CH}_3 + \text{H})$

- Laser flash photolysis producing H and CH₃ with $[\text{H}] \ll [\text{CH}_3]$
- H by resonance fluorescence, CH₃ by absorption. Need absolute [CH₃], since $k(\text{H}) = k[\text{CH}_3]$
- Brouard et al. J. Phys. Chem. 1989, 93, 4047-4059



Experimental results for $\text{CH}_3 + \text{H}$

CH_2 absorption analysed via

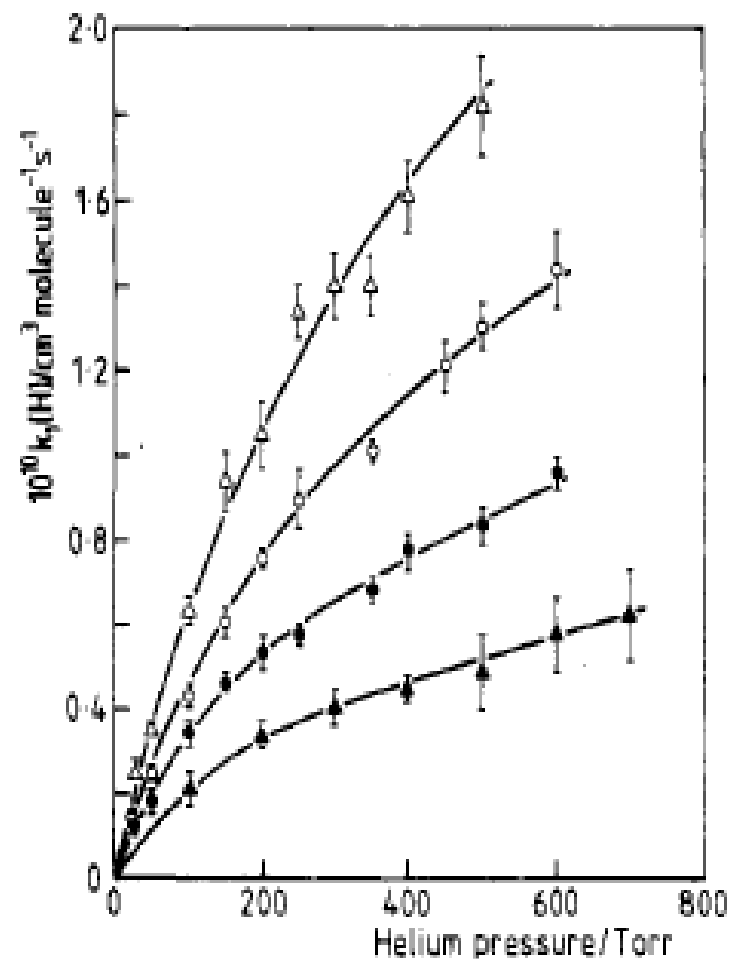
$$D(t) = 1 - \exp\{-(\Delta_0^{-1} - 2k_2t/\sigma L)^{-1}\}$$

Where $D(t) = \Delta I/I_0$

H fluorescence analysed via

$$[\text{H}]' = [\text{H}_0]' \left\{ 1 + \frac{2k_2}{\sigma} \frac{\Delta_0}{L} t \right\}^{-1} \exp(-k_3 t)$$

- Where k_2 refers to $\text{CH}_3 + \text{CH}_3$ and k_3 to other 1st order loss processes for H
- Plot show rate coefficients vs p at 300, 400, 500, 600 K.



CH₃ + H. Parameterisation and determination of k[∞]

- Parameterisation using Troe method (see earlier)

TABLE III: Limiting Rate Coefficients Obtained from Fitting the Data for k₁(H) Using the Troe Factorization Procedure^{36,37}

T/K	10 ¹⁰ k ₁ [∞] (H)/ cm ³ molecule ⁻¹ s ⁻¹	10 ²⁹ k ₁ ⁰ (H)/ cm ³ molecule ⁻¹ s ⁻¹	F _{sc} ^{cent}	β _c
300	7.6 ± 1.6	2.7 ± 0.4	0.659	0.45
400	4.7 ± 1.2	3.1 ± 0.6	0.627	0.39
500	3.1 ± 0.6	3.0 ± 0.5	0.599	0.34
600	1.8 ± 0.6	2.5 ± 0.8	0.566	0.30

Optimum k[∞] obtained from uncorrelated mVRRKM-master equation analysis (10⁻¹⁰ cm³ molecule⁻¹ s⁻¹)

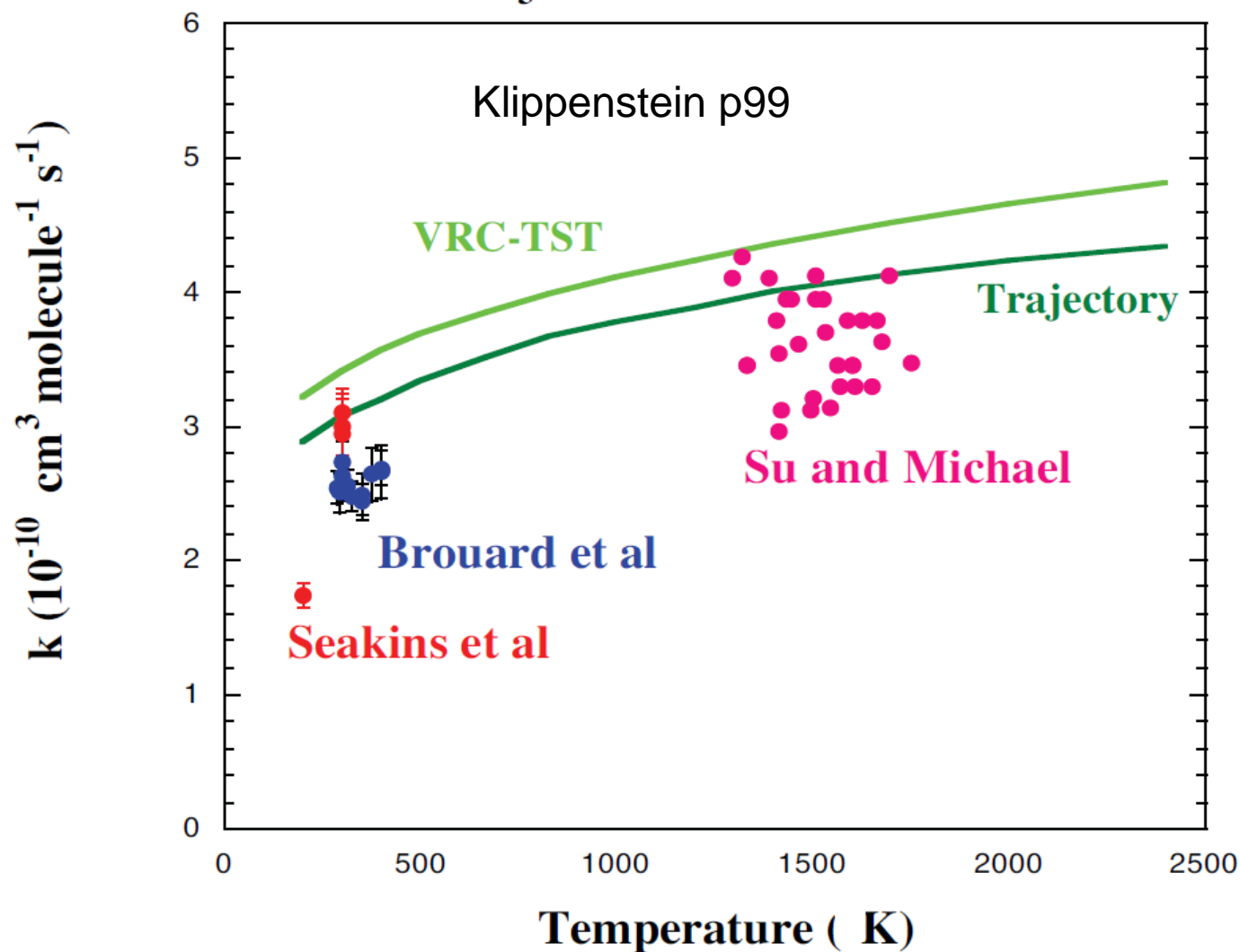
300 K: 4.7

400 K: 4.5

500 K: 4.6

600 K: 4.4

CH₃ + H : High Pressure



Positive T dependence for k_{∞} : contrast –ve dependence for CH₃+CH₃

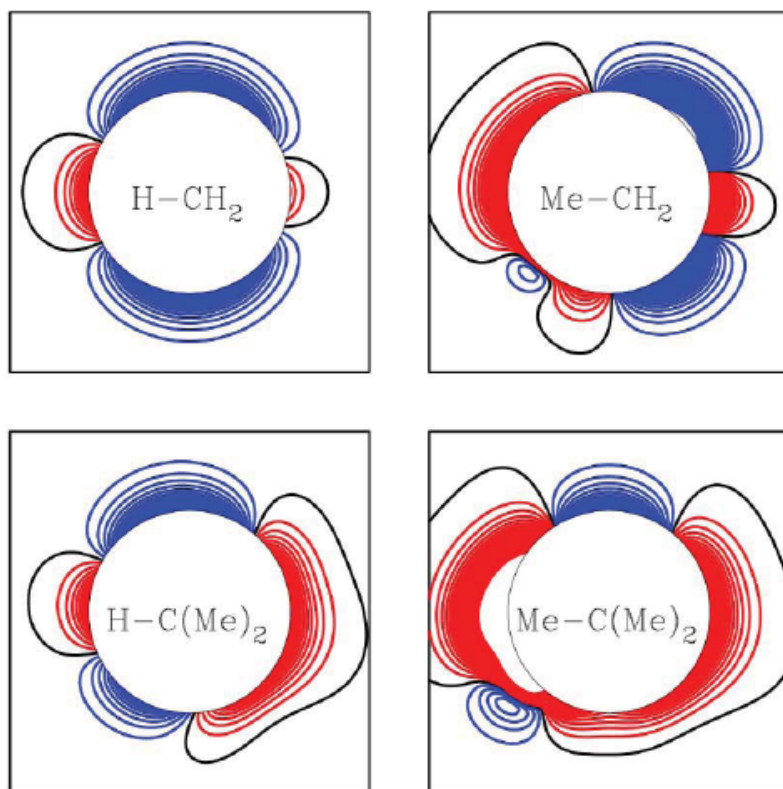
Su and Michael, Proc Comb Inst 2002, 29, 1219

Shock tube study of the thermal decomposition of $C_2D_5I/CH_3I/Kr$ mixtures which generated D atoms and CH_3 radicals. $[H]$ and $[D]$ were monitored by ARAS. A rate constant of $2.20 \cdot 10^{-10} \text{ cm}^3 \text{ molecule}^{-1} \text{ s}^{-1}$ was measured for the reaction $CH_3 + D \rightarrow CH_2D + H$. This rate constant was converted to the high pressure limit for $CH_3 + H \rightarrow CH_4$ using the theoretical ratio of 1.6 determined theoretically by Klippenstein, Georgieskii, and Harding. (Proc. Comb. Inst. 2002, 29, 1229.)

H + Alkyl Radical

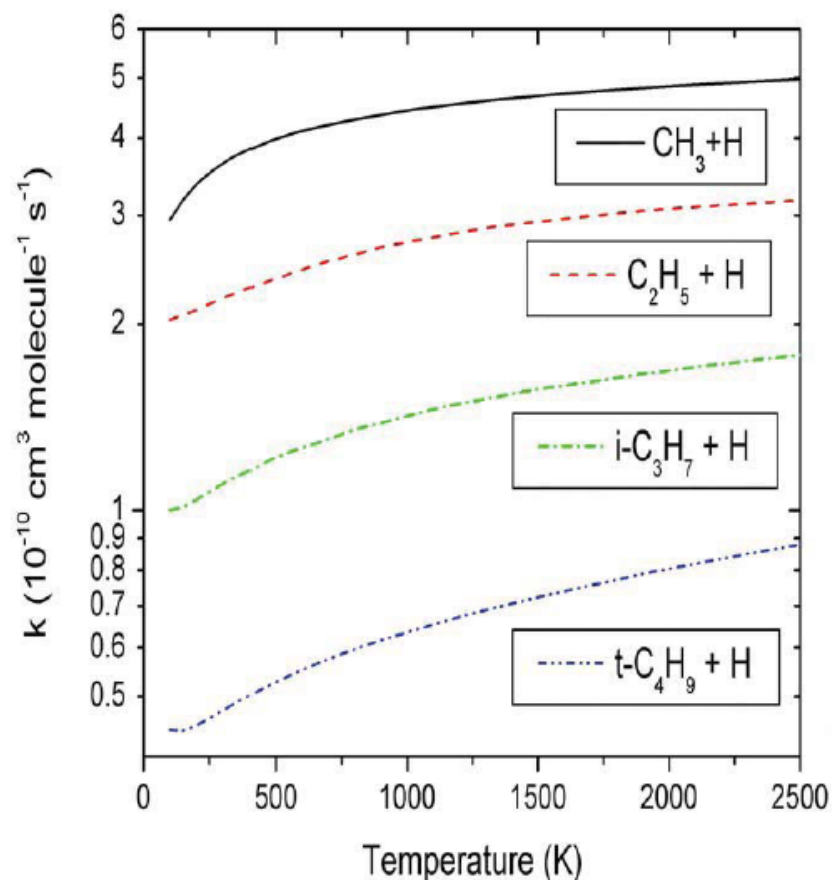
Klippenstein p106

Potential Energy Surface



Blue = attractive contours

Red = repulsive contours

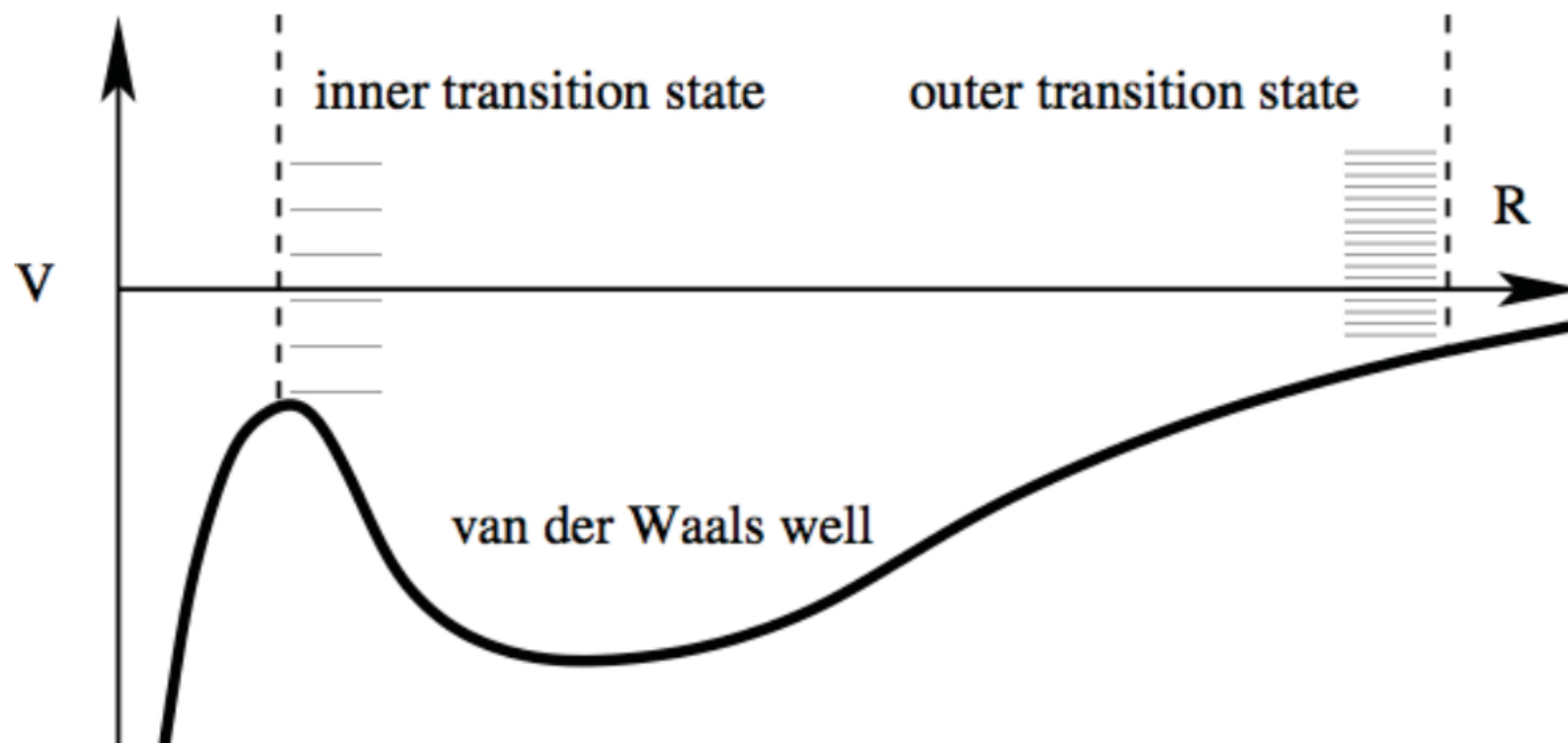


Gorin model (D M Golden)
Excluded angles of approach

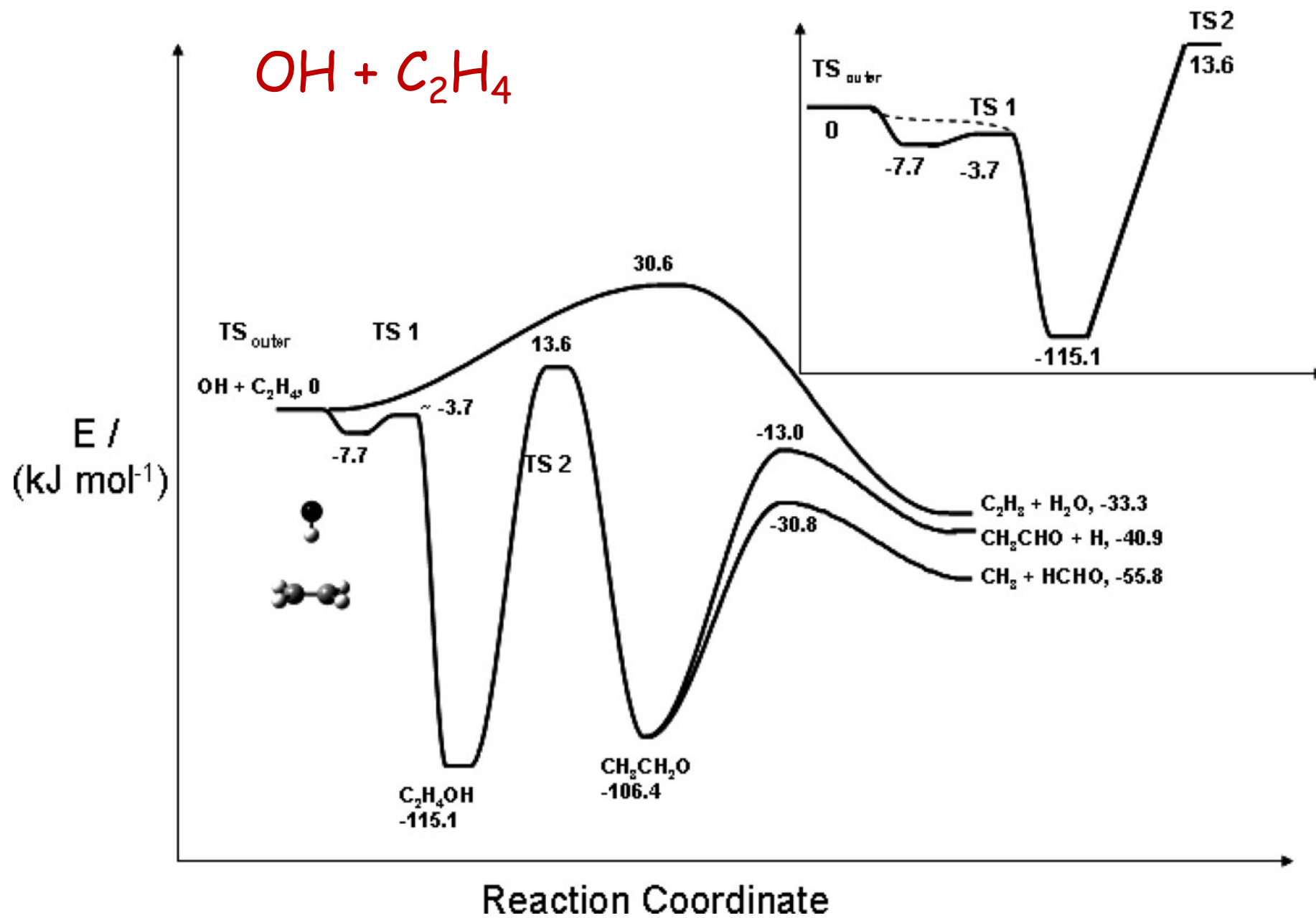
Two Transition States

Schematic Potential Energy Surface for Radical Molecule Addition

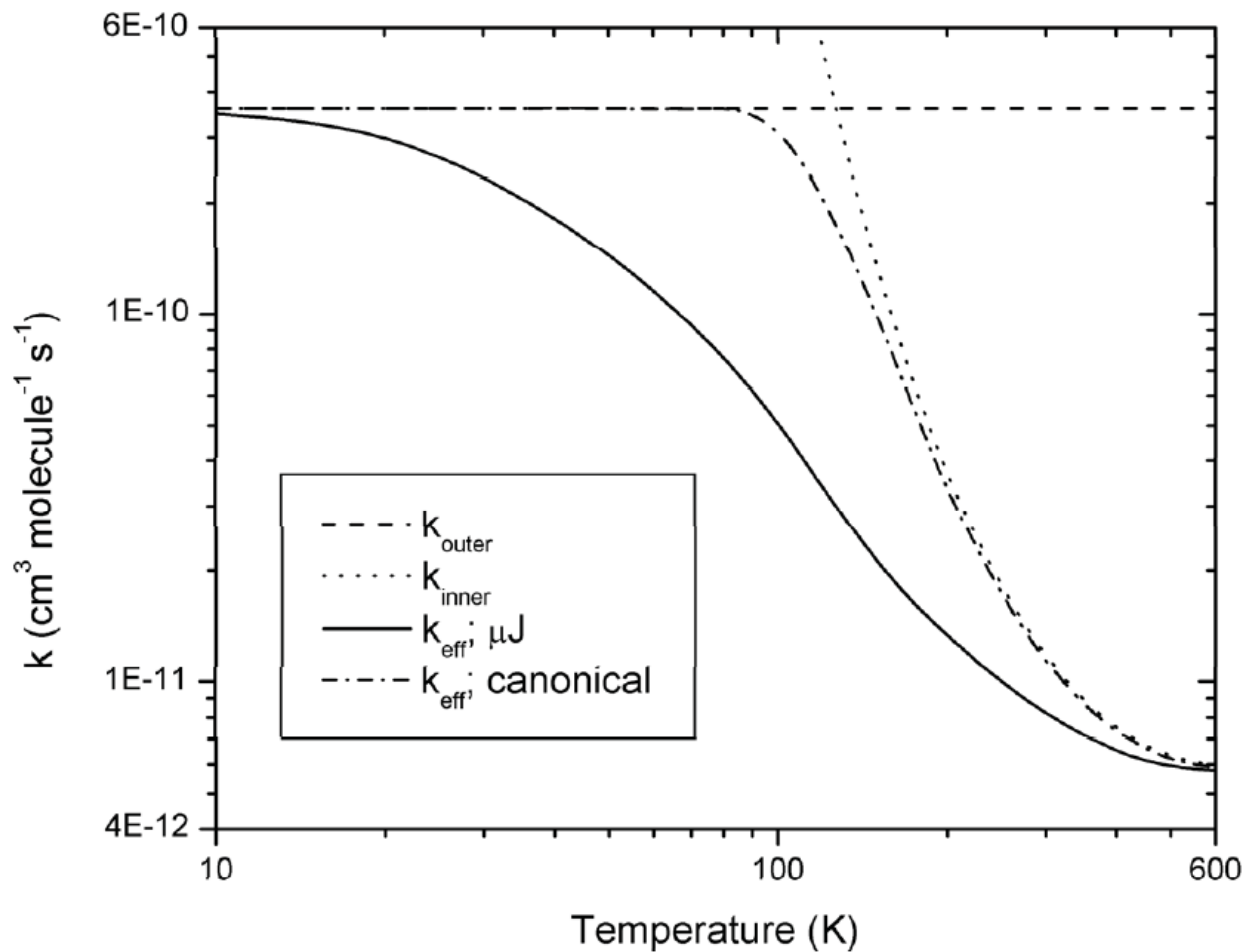
Klippenstein p137



- Inner TS
 - Entropic Barrier
 - Covalent Bond Formation
 - Rigid Rotor Harmonic Oscillator
- Outer TS
 - Long Range TST
- Effective TS
$$1/N_{\text{eff}} = 1/N_{\text{inner}} + 1/N_{\text{outer}}$$

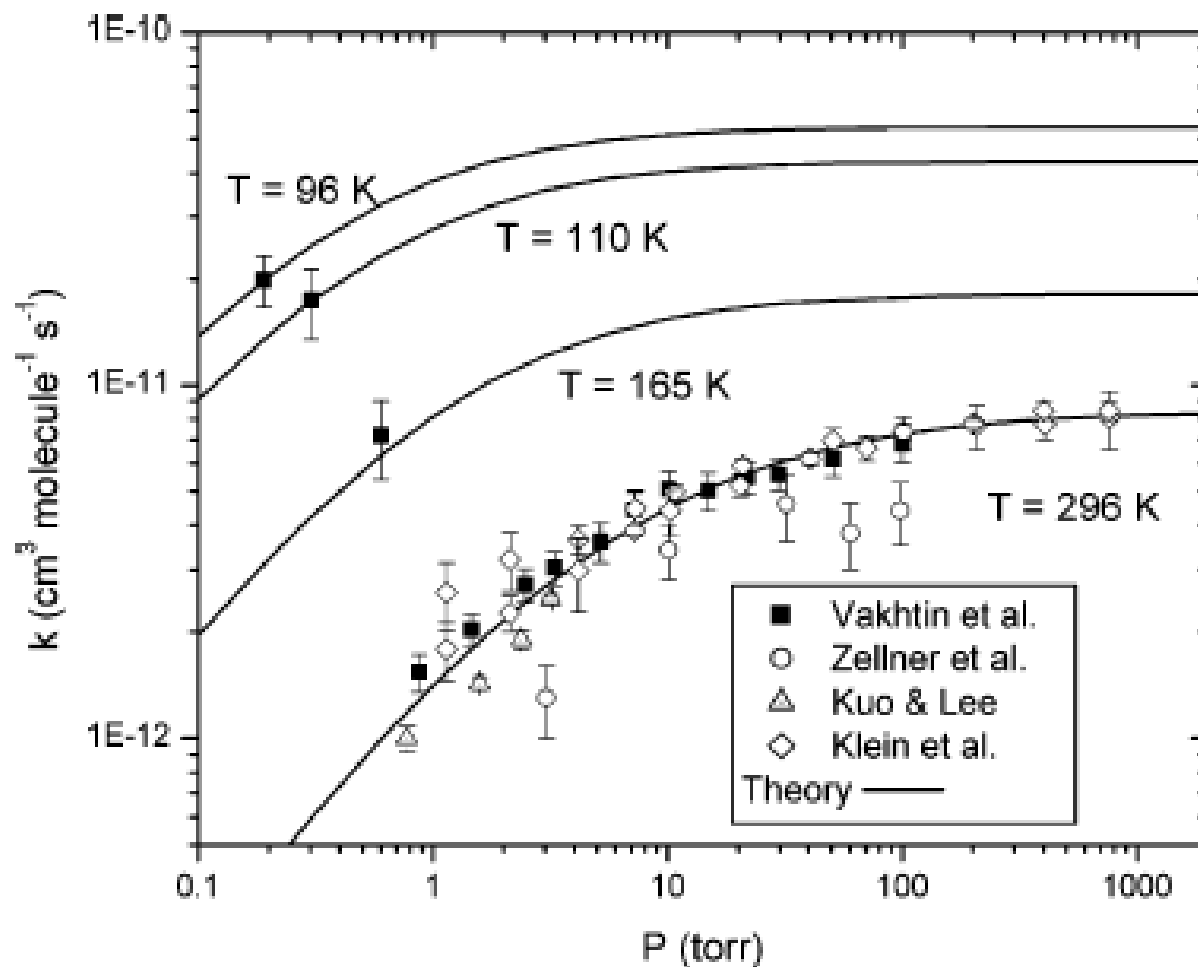


$C_2H_4 + OH$ High P Limit

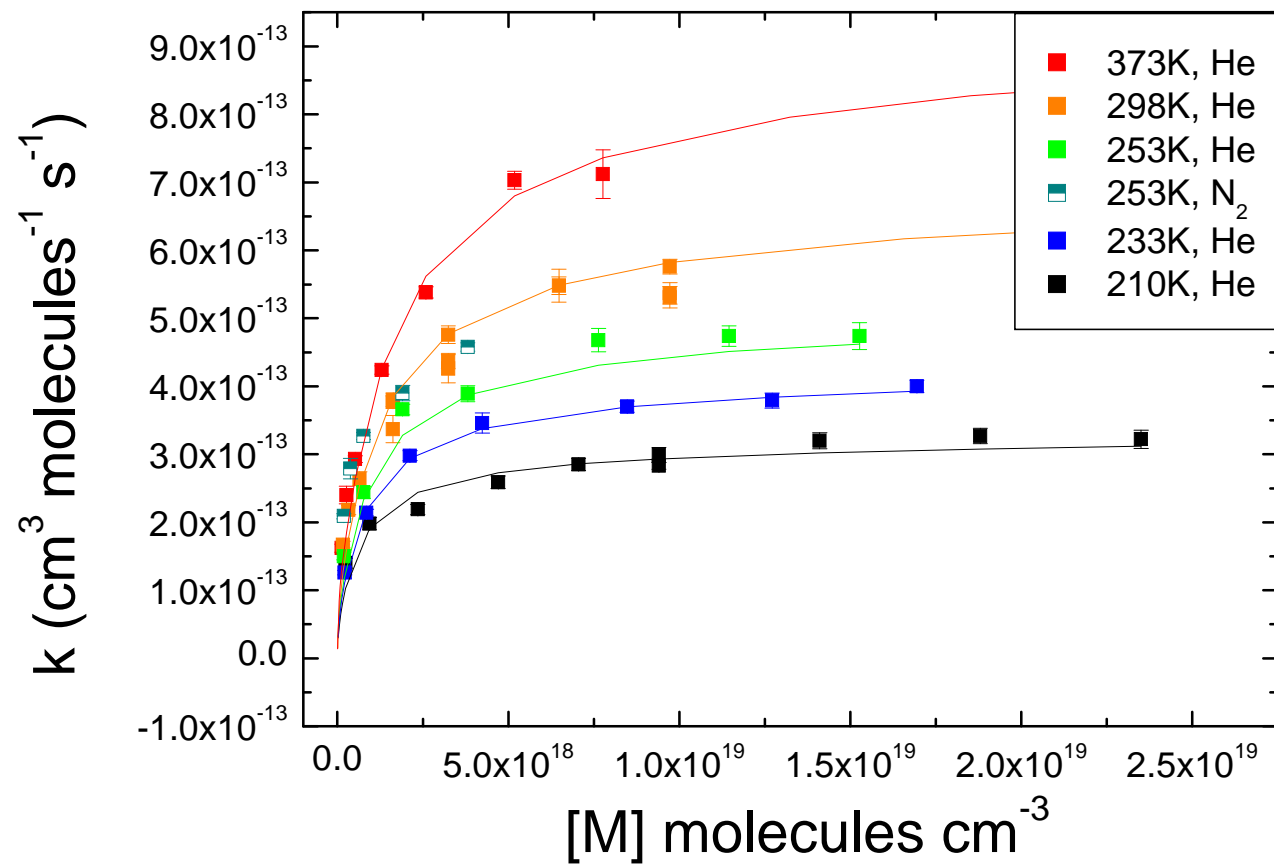


E. E. Greenwald, S. W. North, Y. Georgievskii and S. J. Klippenstein, J. Phys. Chem. A, 2005, 109, 6031–6044.

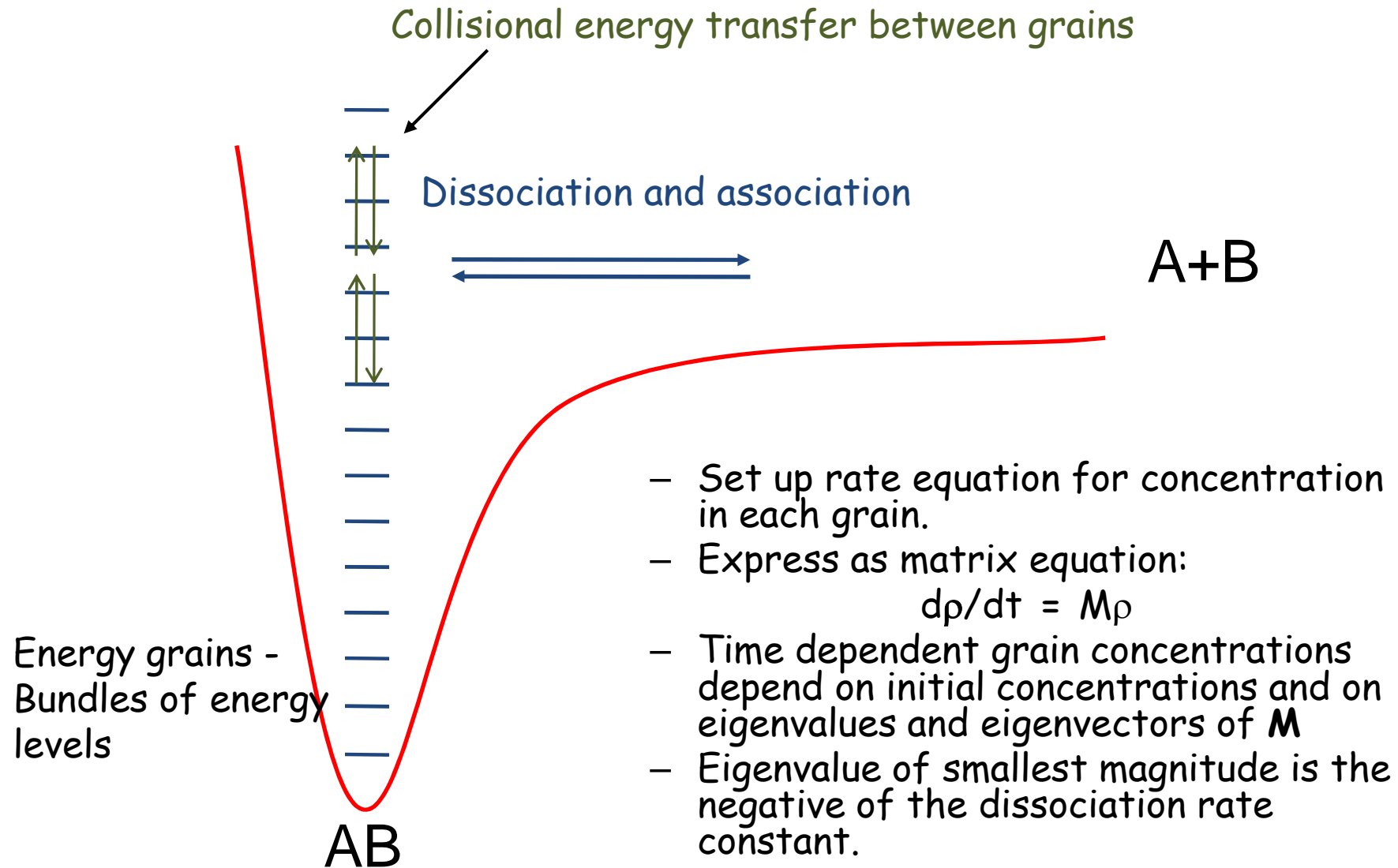
Fits to available data slight adjustment of inner TS energy



Contrast OH + C₂H₂ (yesterday)



Modelling dissociation and association reactions - master equation analysis



Master equation for dissociation

$$\frac{\partial}{\partial t} \rho(E, t) = \omega \sum_{E'} P(E|E') \rho(E', t) - \omega \rho(E, t) - k(E) \rho(E, t).$$

$$P(E|E') = A(E) \exp(-\alpha(E' - E)) \quad E' \geq E,$$

$$P(E|E') = A(E') \exp(-\alpha(E - E')) (f(E')/f(E)) \quad E < E'.$$

$$\frac{\partial}{\partial t} \rho(E, t) = \hat{M} \rho(E, t),$$

Solution: $\rho(E, t) = \sum_i c_i \varphi_i(E) \exp(\lambda_i t)$

$$\frac{d[A]}{dt} = -k_u [A], \quad [A](t) = [A]_0 \sum_E \rho(E, t) \quad k_u = -\lambda_1.$$

Association reaction



$$\frac{\partial}{\partial t} \rho(E, t) = \hat{M} \rho(E, t) + g(E, t).$$

$$g(E, t) = R(t) \phi(E) = k_{a,\infty} [B](t) [C](t) \phi(E),$$

$$\phi(E) = \frac{k(E) f(E)}{\int k(E) f(E) dE}.$$

$$k_a = \frac{-\lambda_2}{[C] + 1/K_{eq}}$$

$$k_u = \frac{-\lambda_2}{1 + K_{eq}[C]}.$$

$$\begin{pmatrix} M_{11}^A & \cdots & M_{1n}^A & k_1 f_1 K_{eq}[C] \\ \vdots & \ddots & \vdots & \vdots \\ M_{n1}^A & \cdots & M_{nn}^A & k_n f_n K_{eq}[C] \\ k_1 & \cdots & k_n & -k_{a,\infty}[C] \end{pmatrix}.$$

$$k_a = \frac{-\lambda_2}{[C] + 1/K_{eq}}$$

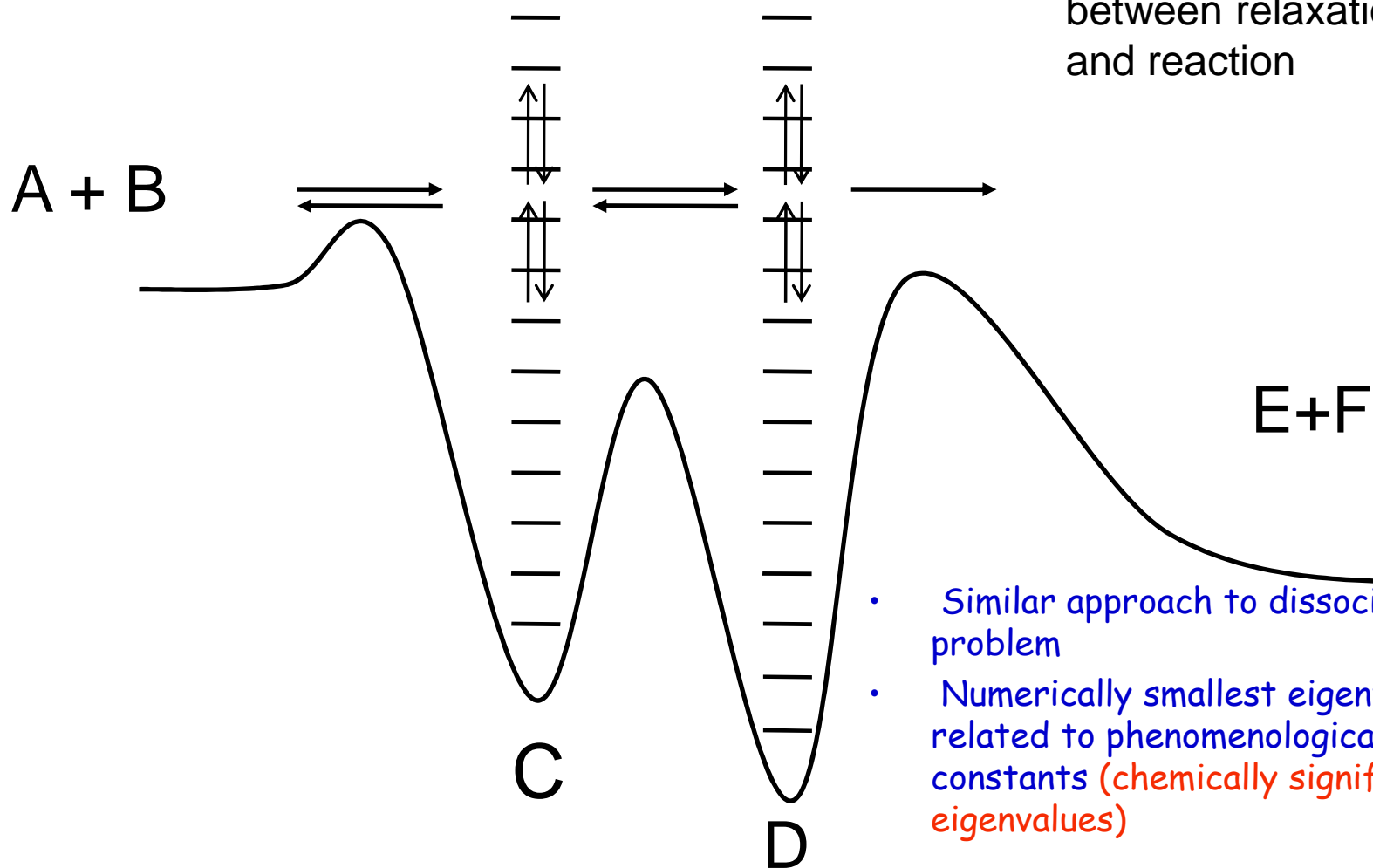
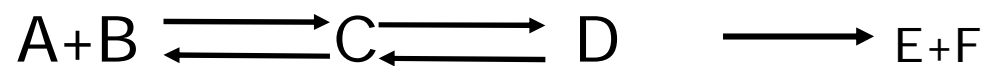
$$k_u = \frac{-\lambda_2}{1 + K_{eq}[C]}.$$

Structure of \mathbf{M} for an isomerisation reaction

$$\frac{\partial}{\partial t} \rho^A(E, t) = \omega \sum_{E'} P(E|E') \rho^A(E', t) - \omega \rho^A(E, t) - k^A(E) \rho^A(E, t) + k^B(E) \rho^B(E, t),$$

$$\begin{pmatrix} M_{11}^A & \omega P_{12}^A & \dots & \omega P_{1n}^A & 0 & \dots & 0 & 0 \\ \omega P_{21}^A & M_{22}^A & \dots & \omega P_{2n}^A & \vdots & \ddots & \vdots & \vdots \\ \vdots & \vdots & \ddots & \vdots & 0 & \dots & k_{l-1}^B & 0 \\ \omega P_{n1}^A & \omega P_{n2}^A & \dots & M_{nn}^A & 0 & \dots & 0 & k_l^B \\ 0 & \dots & 0 & 0 & M_{11}^B & \omega P_{12}^B & \dots & \omega P_{1l}^B \\ \vdots & \ddots & \vdots & \vdots & \omega P_{21}^B & M_{22}^B & \dots & \omega P_{2l}^B \\ 0 & \dots & k_{n-1}^A & 0 & \vdots & \vdots & \ddots & \vdots \\ 0 & \dots & 0 & k_n^A & \omega P_{l1}^B & \omega P_{l2}^B & \dots & M_{ll}^B \end{pmatrix}$$

More complex reactions.

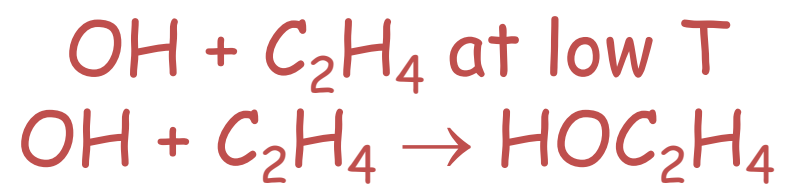


Master equation code

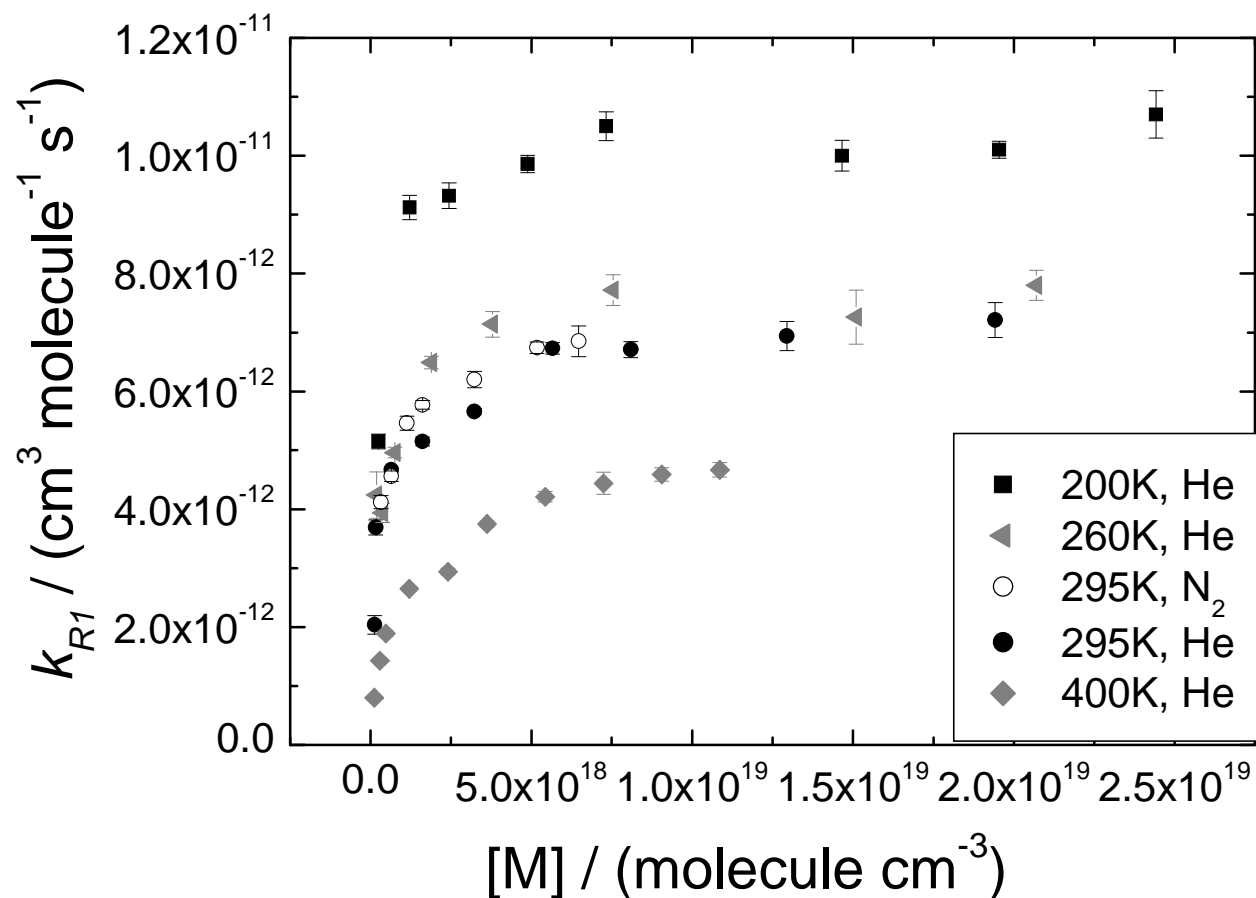
MESMER

Master Equation Solver for Multi-Energy Well Reactions), 2008; an object oriented C++ program for carrying out ME calculations and eigenvalue-eigenvector analysis on arbitrary multiple well systems.

<http://sourceforge.net/projects/mesmer>



$\text{OH} + \text{C}_2\text{H}_4$ (Cleary et al, *Phys. Chem. Chem. Phys.*, 2007, 8, 5633-5642) Data fitted using master equation, with $k(E)$ for dissociation of HOC_2H_4 obtained by inverse Laplace transformation



Inverse Laplace transform and association rate coefficients

$$\mathcal{L}^{-1}\{F(s)\} = f(t) = \frac{1}{2\pi i} \lim_{T \rightarrow \infty} \int_{\gamma - iT}^{\gamma + iT} e^{st} F(s) ds,$$

$$\begin{aligned} k_{\infty}(T) &= \frac{\int_0^{\infty} k(E_R) N(E_R) \exp(-\beta E_R) dE_R}{\int_0^{\infty} N(E_R) \exp(-\beta E_R) dE} \\ &= \int_0^{\infty} k(E_R) N(E_R) \exp(-\beta E_R) dE / Q_R \end{aligned}$$

- Inverting this relationship allows $k(E)$ to be determined from the high pressure limiting rate constant. Most effectively performed using the association rate constant.
- Davies et al. Chem Phys Letters, 1986, 126, 373-379.

Microcanonical dissociation rate constants from inverse Laplace transform of canonical association rate constant

$\beta = 1/RT$ $Q(\beta)$ is the rovibronic partition function, $K(\beta)$ is the equilibrium constant and $N(E)$ is the rovibronic density of states of the association complex. N_p is the convoluted densities of states of the reactant species



$$k_{\infty}(\beta) = A'_{\infty} \left(\frac{1}{\beta} \right)^{n_{\infty}} \exp(-\beta E_{\infty})$$

$$k(E) = \mathcal{L}^{-1} [Q(\beta) K(\beta) k_{\infty}(\beta)] / N(E) \quad E > 0$$

$$k(E) = \frac{A^{\infty} C'}{N(E) \Gamma(n^{\infty} + 1.5)} \int_0^{E - E^{\infty} - \Delta H_0^0} N_p(x) \exp(-\beta x) dx$$

$$\times [(E - E^{\infty} - \Delta H_0^0) - x]^{n^{\infty} + 0.5} dx$$

$$C' = \left(\frac{2\pi(M_A M_B)}{h^2(M_A + M_B)} \right)^{3/2}$$

Comparison of master equation fits with theory of Greenwald et al.

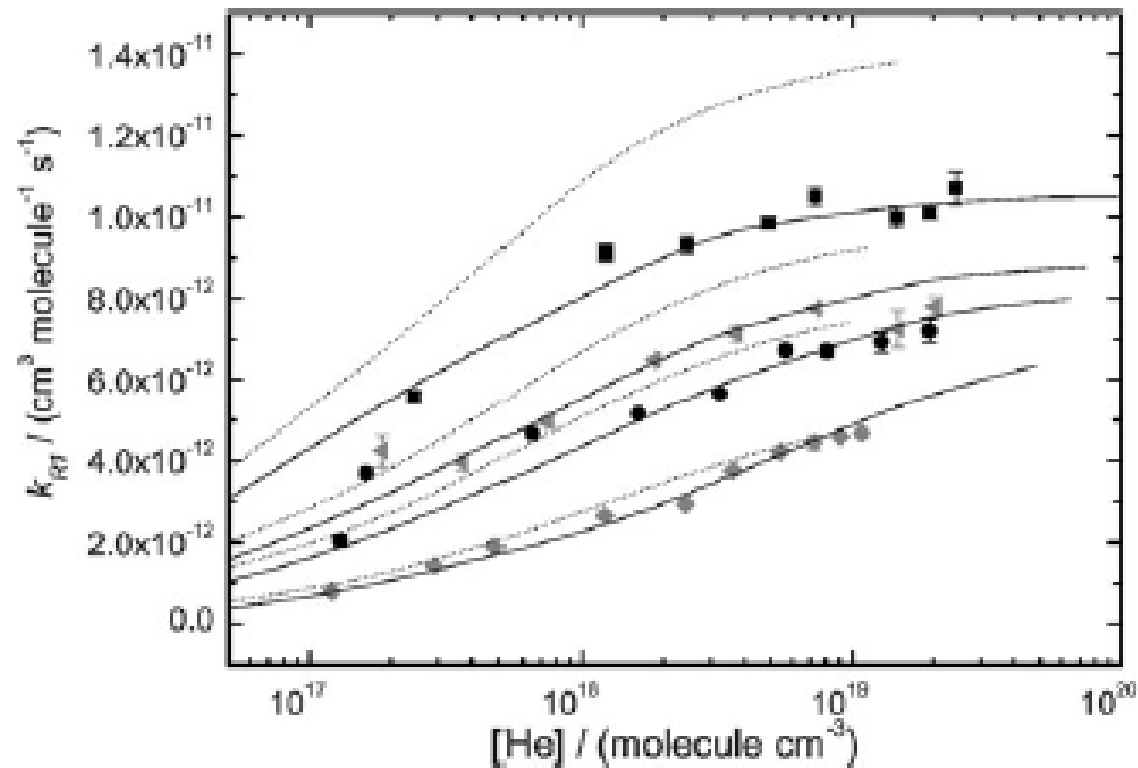
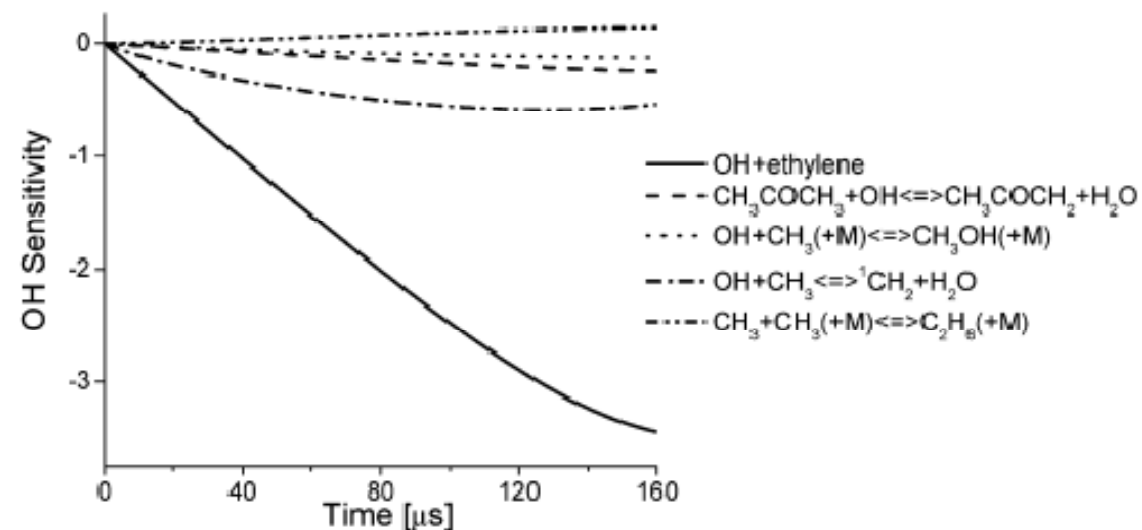
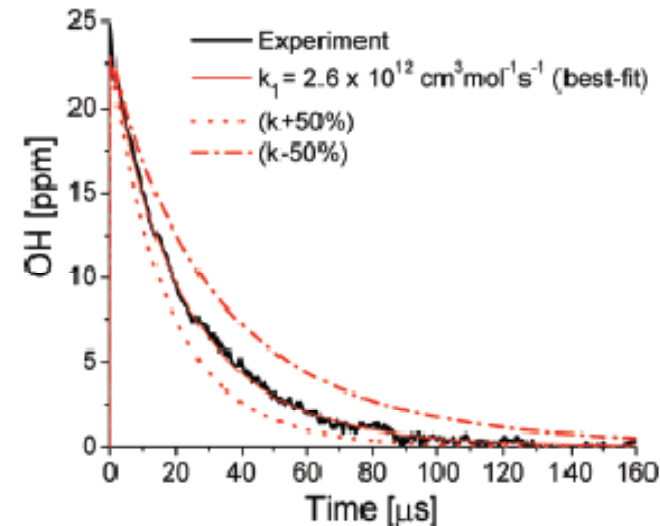


Fig. 9 Bold lines are ME calculations fit to the He data from Table 1, at 200 (■), 260 (grey ◄), 295 (●) and 400 K (grey ◆). The dotted lines are the theoretical results using the Greenwald *et al.*¹⁸ expression for the temperature dependence of k_{∞} .

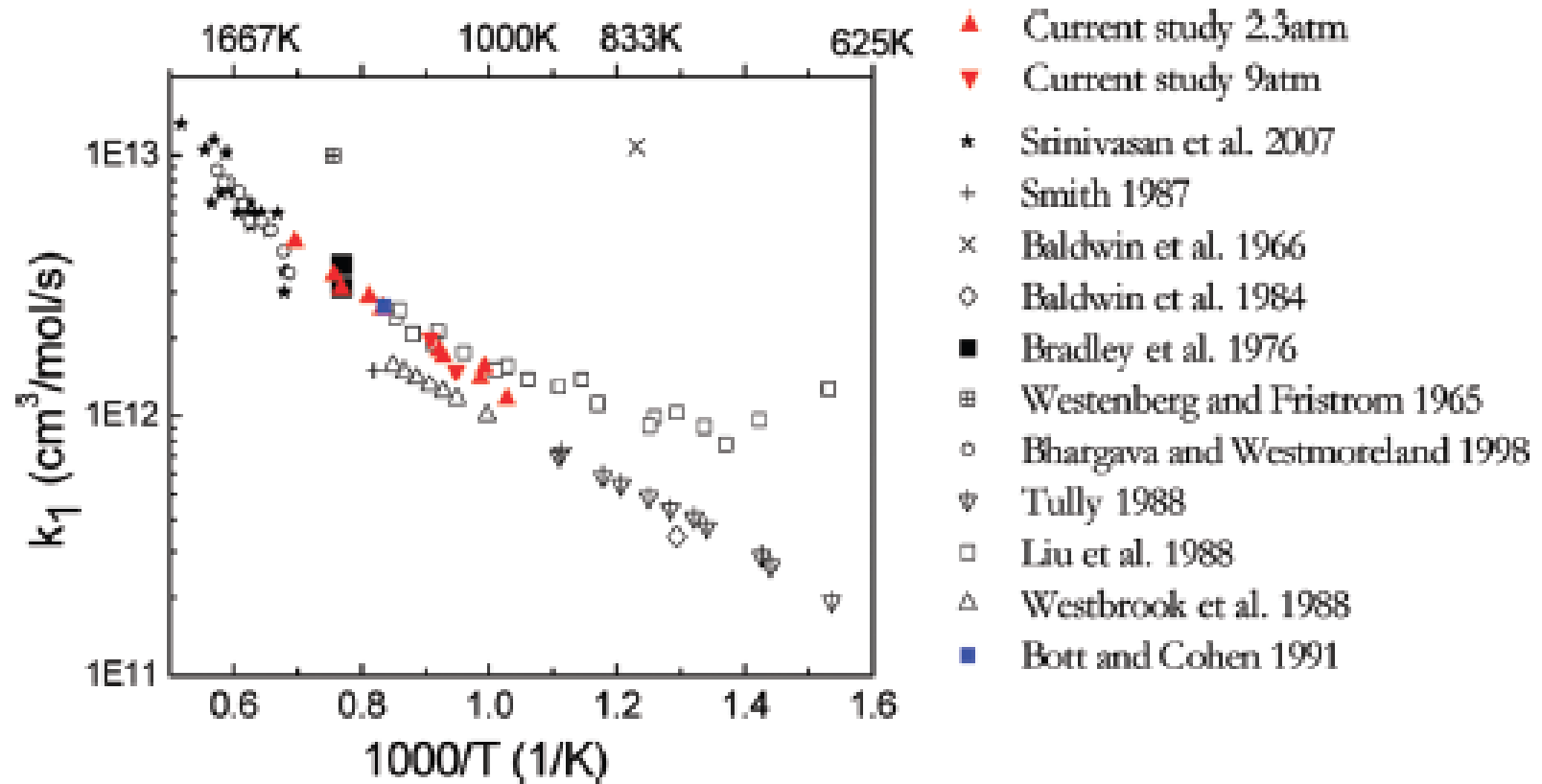
High temperature, OH + C₂H₄
 Hanson group (Vasu et al. *J. Phys. Chem. A* 2010, 114, 11529-11537)

1201 K

- OH radicals were produced by shock-heating t-butyl hydroperoxide, Me₃COOH, and monitored by laser absorption near 306.7 nm
- 890 -1366 K, 2.3 atm



OH + C₂H₄ (Vasu et al.)



Uncertainty contributions in the determination of $\text{OH} + \text{C}_2\text{H}_4$

- Contributions from uncertainty in rate coefficients:

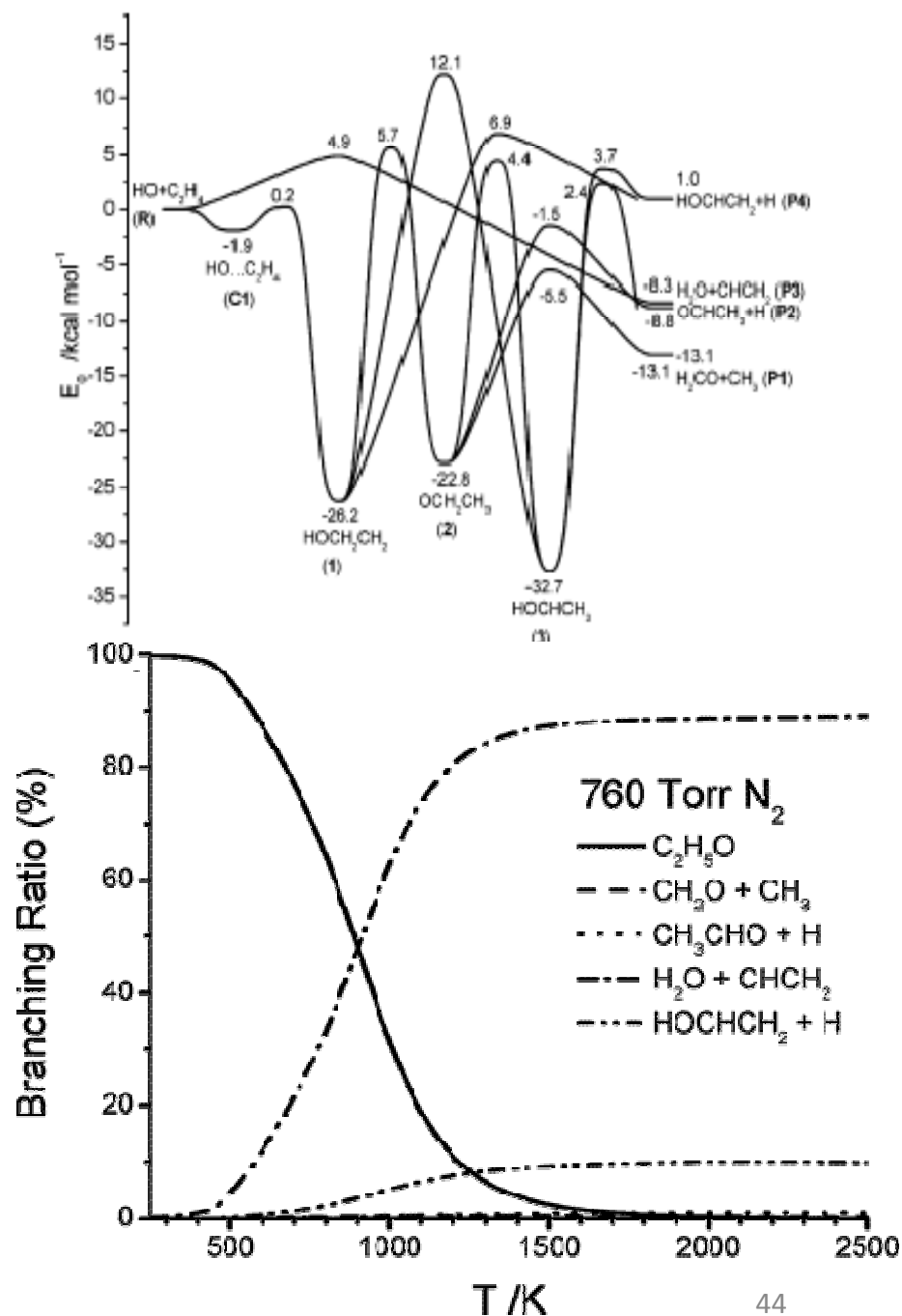
$\text{CH}_3\text{COCH}_3 + \text{OH}$ (fractional uncertainty 0.3)	0.1%
$\text{CH}_3 + \text{OH} \rightarrow {}^3\text{CH}_2 + \text{H}_2\text{O}$ (factor 2)	3.9%
$\text{CH}_3 + \text{OH} \rightarrow \text{CH}_3\text{OH}$ (factor of 2)	1.5%
$\text{CH}_3 + \text{CH}_3 \rightarrow \text{C}_2\text{H}_6$ (Factor of 2)	1.5%

Also contributions from temperature, fitting process, OH absorption coefficient, mixture concentration, wavemeter reading

Overall uncertainty: 22.8%

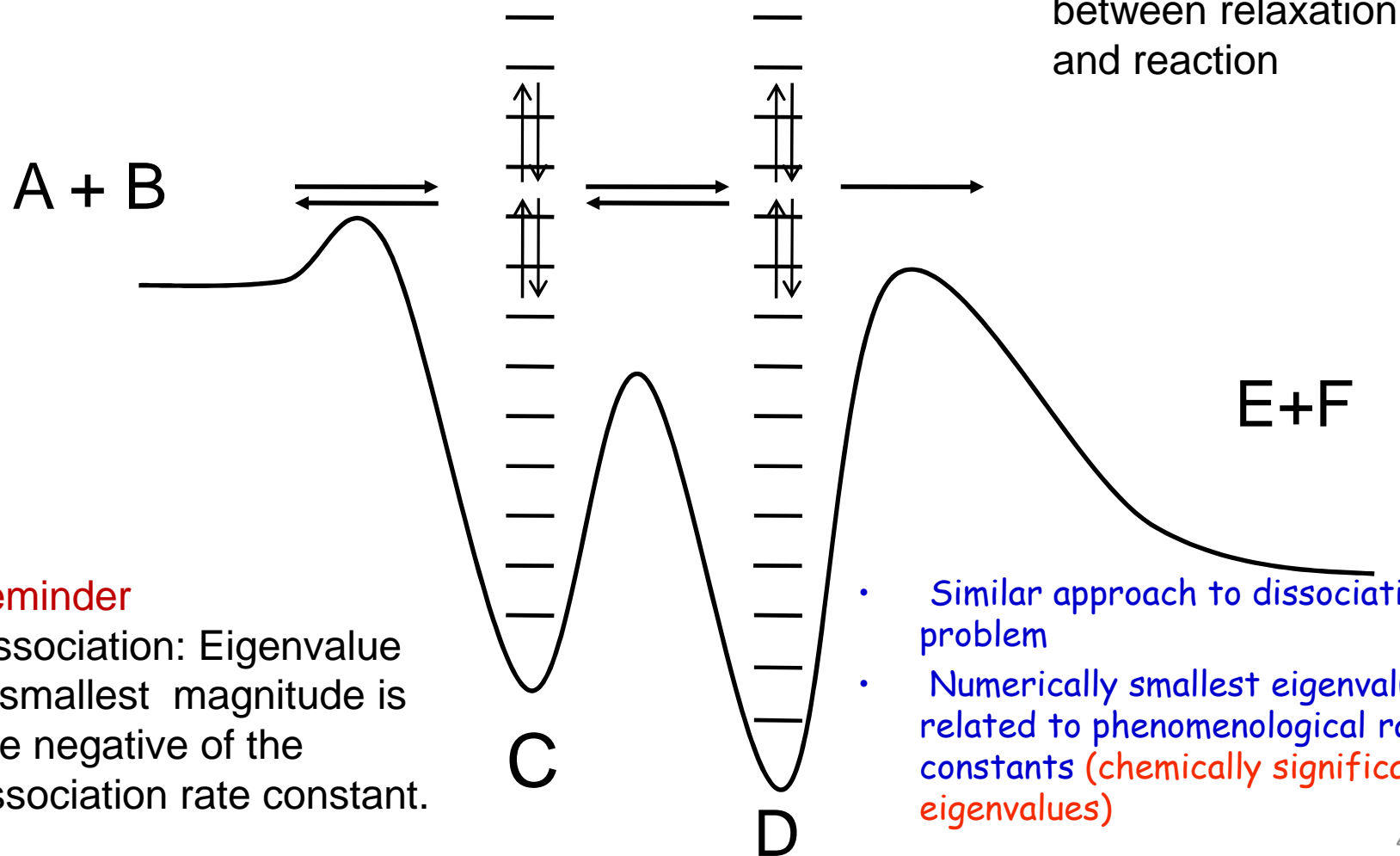
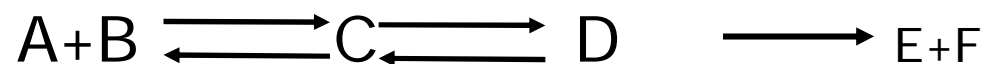
Product yields - contribution from theory

- Senosiaian et al, *J. Phys. Chem. A* 2006, 110, 6960-6970
- Slight tuning of surface (~ 0.4 kcal mol $^{-1}$) by reference to experimental data.
- Note formation of vinyl alcohol >800 K, Confirmed by Taatjes et al.
- Srinivasan et al. *Phys. Chem. Chem. Phys.*, 2007, 9, 4155-4163



Master equation
Chemically significant eigenvalues

More complex reactions.



Reminder

Dissociation: Eigenvalue of smallest magnitude is the negative of the dissociation rate constant.

- Similar approach to dissociation problem
- Numerically smallest eigenvalues related to phenomenological rate constants (chemically significant eigenvalues)

Chemically significant eigenvalues for isomerisation



Two species, two CSEs
System is conservative,
so $\lambda_1 = 0$

Reaction system relaxes to equilibrium state. Relaxation rate constant $= |\lambda_2| = k_f + k_r$
Relaxation time $= \tau$

$$\tau = (k_f + k_r)^{-1}$$

$$\frac{d[A]}{dt} = -k_f[A] + k_r[B]$$

$$\frac{d[B]}{dt} = k_f[A] - k_r[B],$$

$$\mathbf{c} = \begin{pmatrix} [A] \\ [B] \end{pmatrix}.$$

$$\frac{d\mathbf{c}}{dt} = \mathbf{M}_c \mathbf{c},$$

$$\mathbf{M}_c = \begin{pmatrix} -k_f & k_r \\ k_f & -k_r \end{pmatrix}.$$

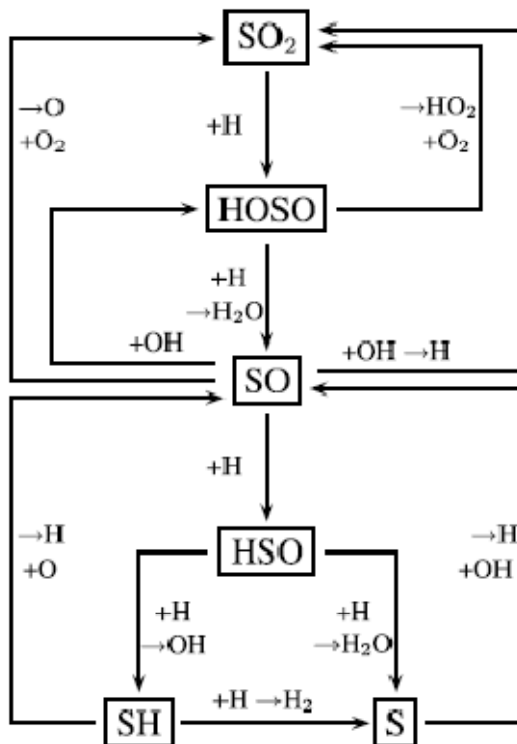
$$-\lambda_2 = k_f + k_r.$$

$$k_f/k_r = K_{eq}, \quad k_f = \frac{-\lambda_2}{1 + 1/K_{eq}}$$
$$k_r = \frac{-\lambda_2}{1 + K_{eq}}.$$



Effect of sulfur oxides on fuel oxidation

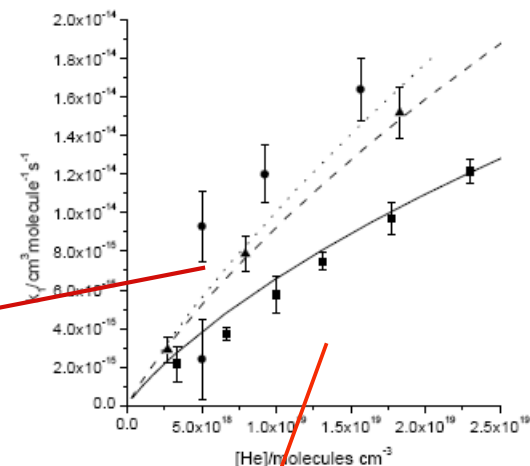
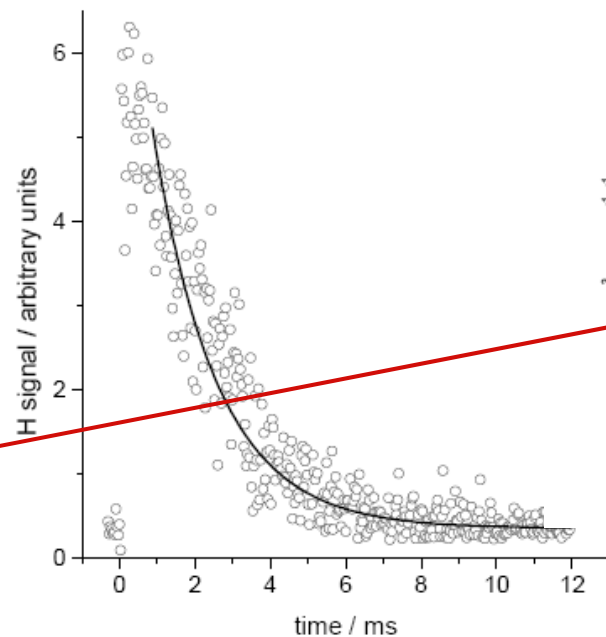
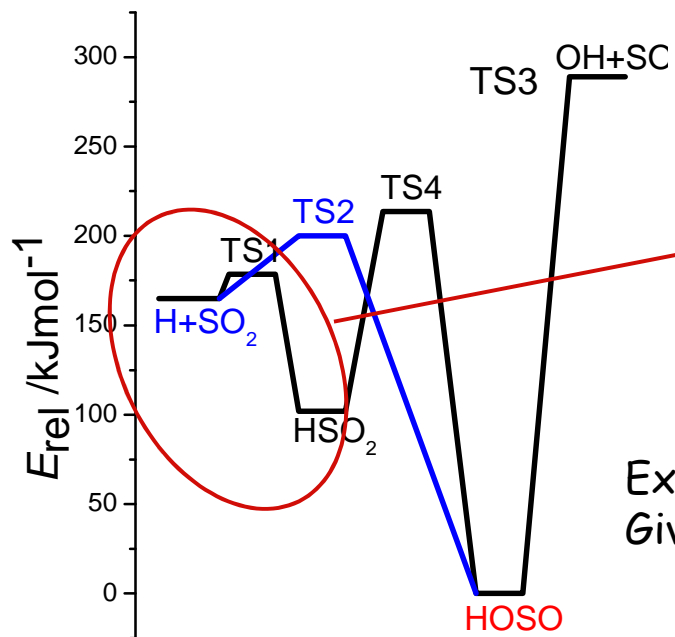
Peter Glarborg Hidden interactions—Trace species governing combustion and emissions. 31st Symposium



- $SO_2 + H (+M) \rightleftharpoons HOSO (+M)$ (R1)
- $HOSO + H \rightleftharpoons SO + H_2O$ (R2)
- $SO + O_2 \rightleftharpoons SO_2 + O$ (R3)

- How do we provide rate data for reactions of this sort?
- Are there hidden complexities in a simple association reaction like (R1)?

H + SO₂ experiment + theory

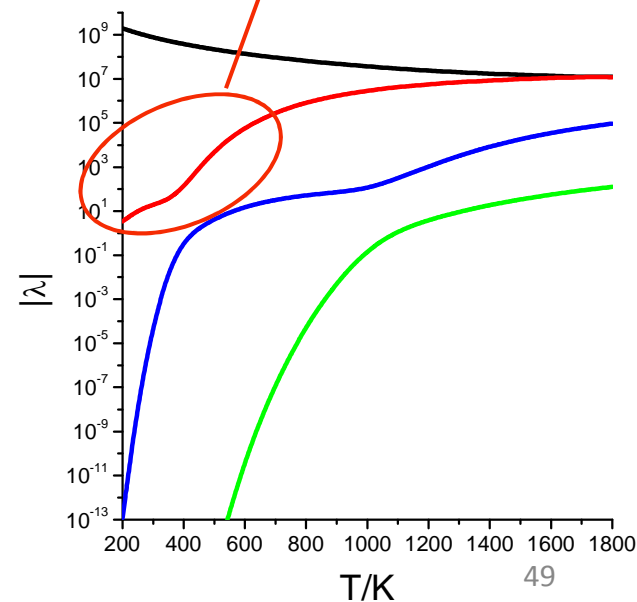


k vs p at T = 295,
363 and 423 K

Experimental decays trace for H + SO₂
Gives k at selected p and T.

- Potential energy surface for H + SO₂, from electronic structure calcs
- Approach: Experimental investigation using vuv LIF for H
- Master equation analysis, constrained to experimental data

Eigenvalues
from ME
analysis.
Red - TS1
Blue TS2
Green TS3



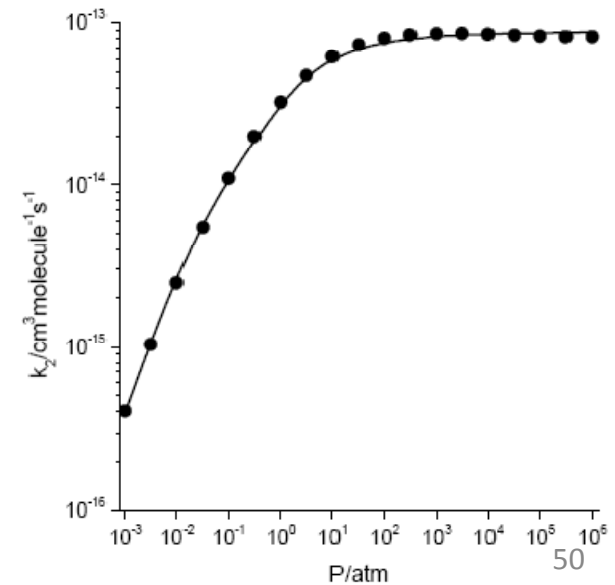
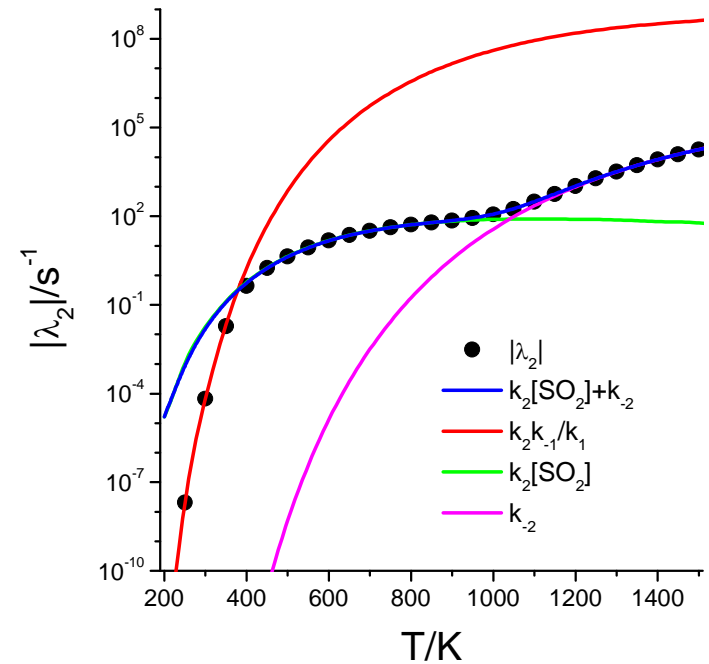
Determination of individual phenomenological rate constants from eigenvalues / eigenvectors

Total number of eigenvalues is equal to the total number of grains.

The 3 eigenvalues of smallest magnitude relate to the phenomenological eigenvalues of the macroscopic chemical system (*chemically significant eigenvalues*)

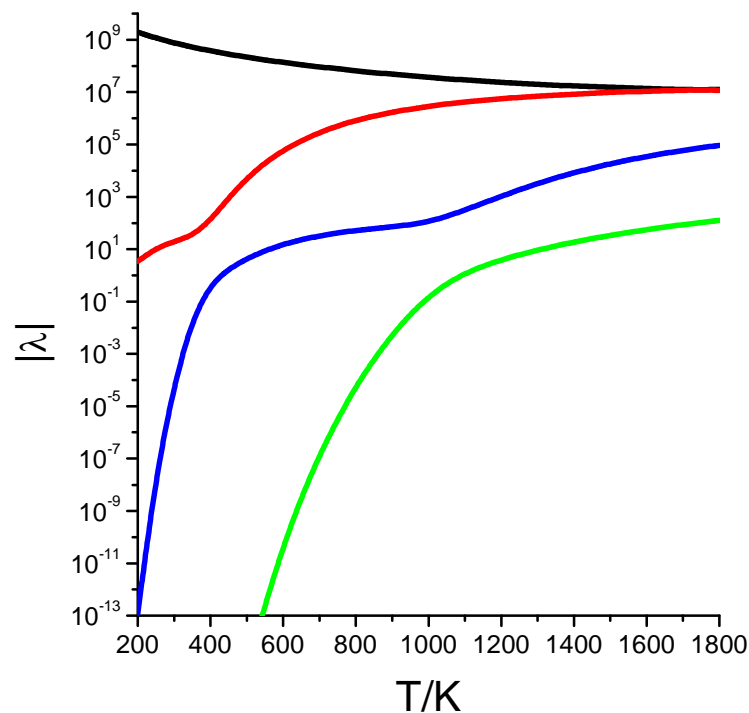


$$dc/dt = \begin{pmatrix} -k_{-1} & -k_4 & -k_5 & k_{-4} & k_1 \\ k_4 & -k_{-4} & -k_{-2} & -k_6 & k_2 \\ k_{-1} & k_{-2} & -k_1 & -k_2 & -k_3 \end{pmatrix} \begin{pmatrix} [\text{HSO}_2] \\ [\text{HOSO}] \\ [\text{H}] \end{pmatrix}$$

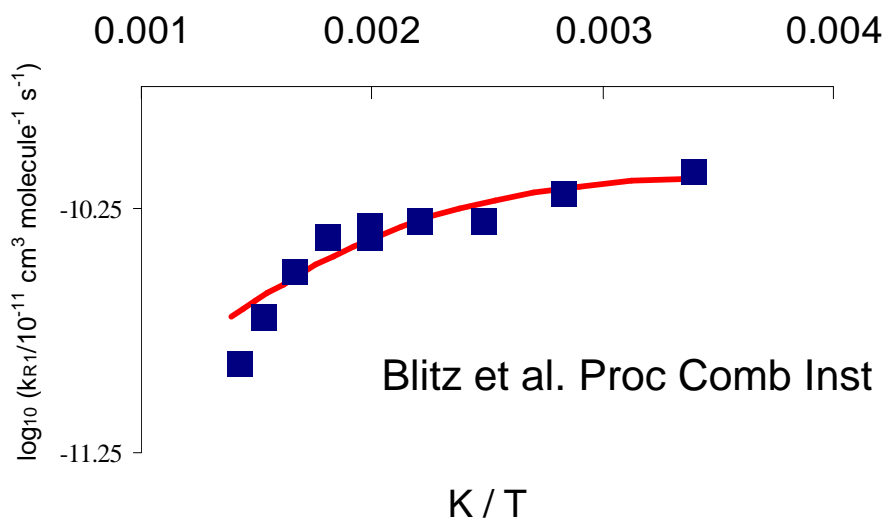


Experimental characterisation of the TS2 and TS3 regions of the surface

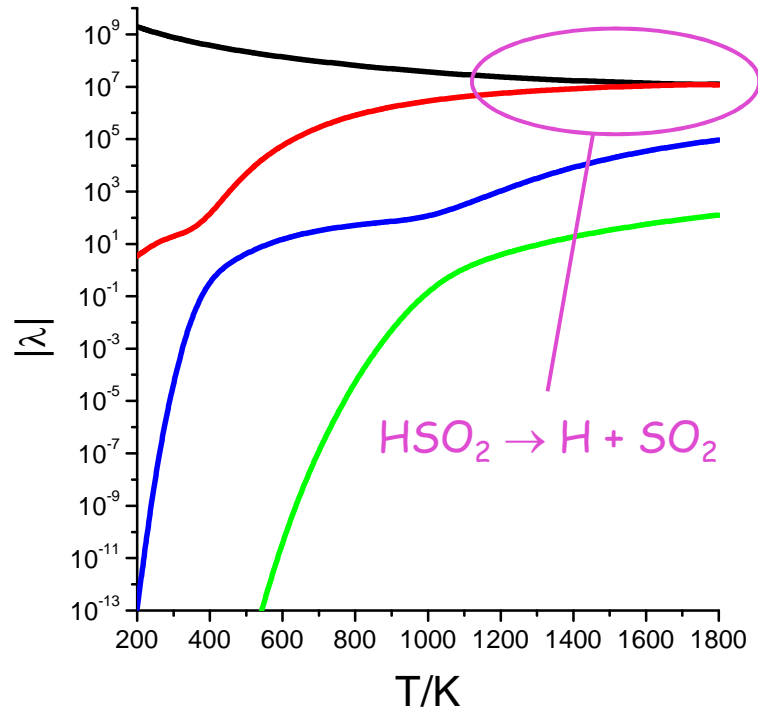
- TS2 is significant in the 400 - 800 K region.
- Difficult to study experimentally using LFP.
- ?Characterise using flow reactor methods?



- TS3 is even more difficult to investigate. Use the reverse reaction, $\text{OH} + \text{SO}$, via detailed balance



Issues



- Overlap of chemically significant eigenvalues with energy relaxation eigenvalues: can lead to problems in defining rate constants (e.g. Tsang et al, Robertson et al in alkyl radical decomposition).
- Use of OH + SO to calculate forward ks using detailed balance. Does detailed balance always apply - are the forward and reverse rate constants always related through the equilibrium constant? (Miller and Klippenstein, Miller et al. Phys. Chem. Chem. Phys., 2009, 11, 1128-1137)
- Important issue in combustion - e.g. CHEMKIN generally introduces forward and reverse reactions, linked via thermodynamics.

Detailed balance in multiple-well chemical reactions
Phys. Chem. Chem. Phys., 2009, 11, 1128-1137

- 'In this Perspective we address the issue of whether or not (and to what extent) detailed balance is satisfied by rate constants obtained from solutions [of the master equation for multiple well systems]It is extremely unlikely that the rate constants of interest satisfy detailed balance exactly (there is no reason to believe that they do). However, the discrepancies are expected to be vanishingly small, as observed in practice.'

Low T (<1000 K) R1,R-1,R2, R-2 dominate

$$\lambda_{2,3} = (-p \pm \sqrt{p^2 - 4q})/2$$

$$p = k_1 + k_{-1} + k_2 + k_{-2}$$

$$q = k_1 k_{-2} + k_{-1}(k_2 + k_{-2})$$

$$|\lambda_3| \approx k_1 + k_{-1} + k_2 + k_{-2} \approx k_1[\text{SO}_2] + k_{-1}$$

and

$$|\lambda_2| \approx \frac{k_1 k_{-2} + k_{-1}(k_2 + k_{-2})}{k_1 + k_{-1}} = k_{-2} + \frac{k_2}{1 + K_1[\text{SO}_2]} \quad (1)$$

where $K_1 = k_1/k_{-1}$.



System conservative: $\lambda_1=0$

High T (>1000 K), $k_{-1} \gg k_1[\text{SO}_2]$: $[\text{HSO}_2] \sim 0$



$|\lambda_3|$ is now very large and the associated timescale is much less than the experimental timescale.

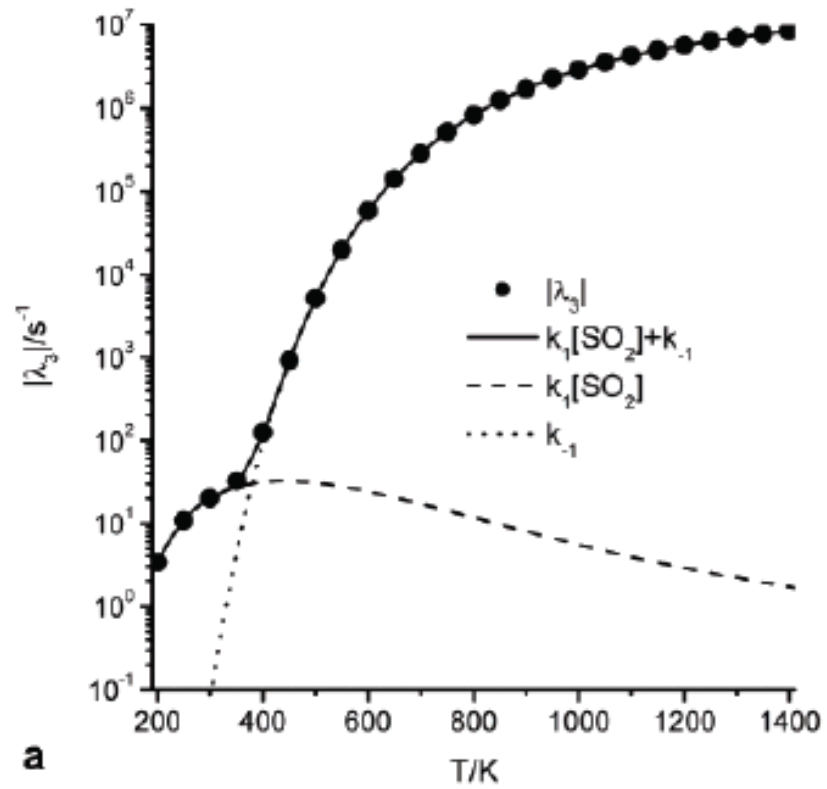
The system reduces to 2 species (H, HOSO) with OH + SO as a sink.

Solution has same form as before, and gives:

$$|\lambda_2| \approx k_2 + k_{-2} + k_3 + k_6 \approx k_2[\text{SO}_2] + k_{-2}$$

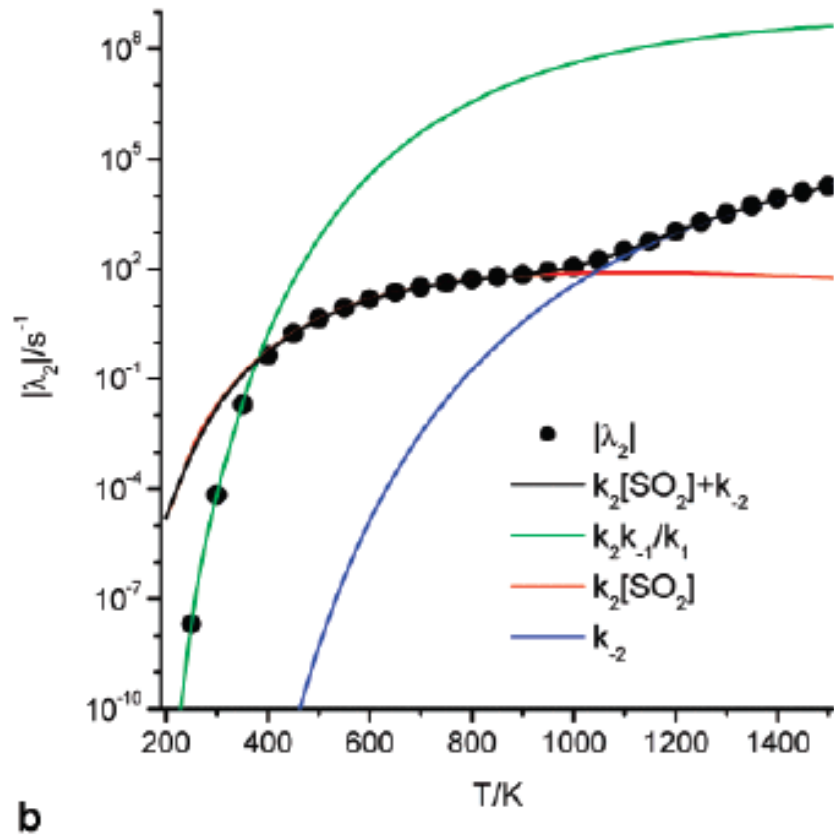
$$|\lambda_1| \approx \frac{k_2 k_6 + k_3(k_{-2} + k_6)}{k_2 + k_{-2}} \approx \frac{k_3[\text{SO}_2] + k_6 K_2[\text{SO}_2]}{1 + K_2[\text{SO}_2]}$$

λ_3

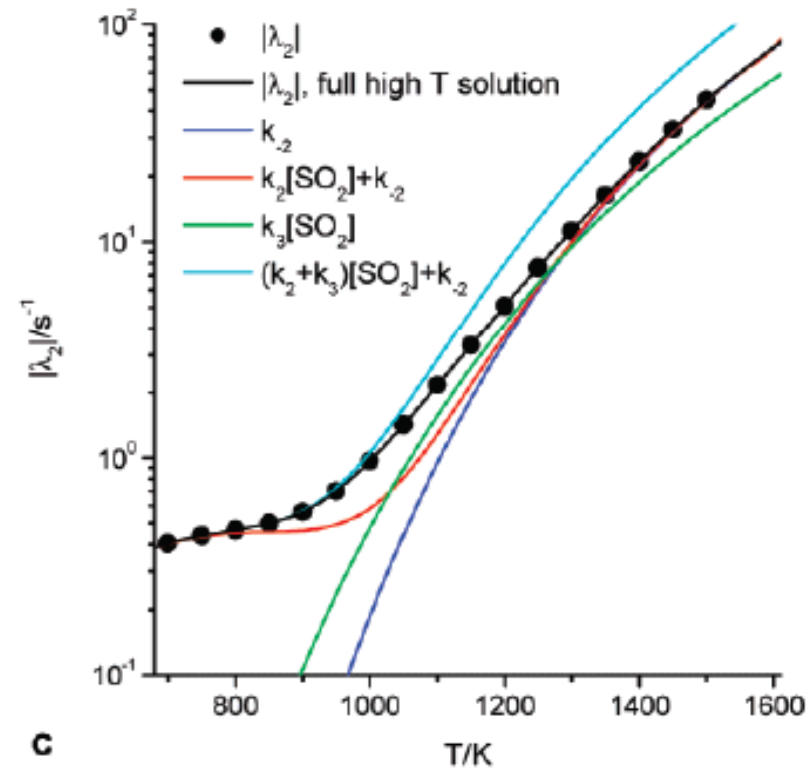


1 atm

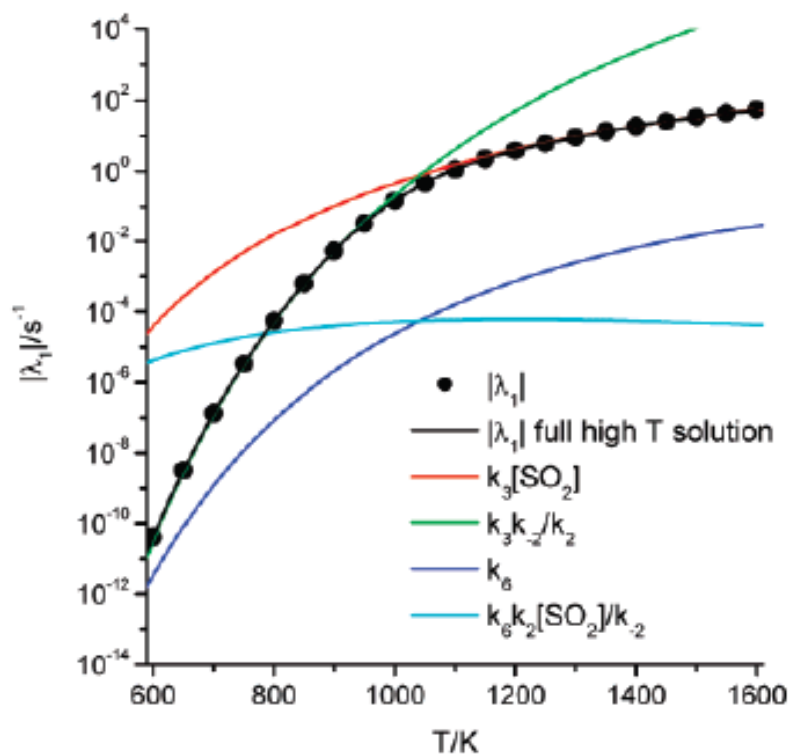
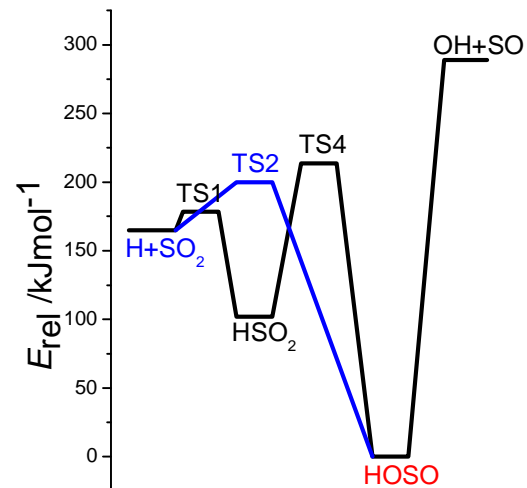
λ_2



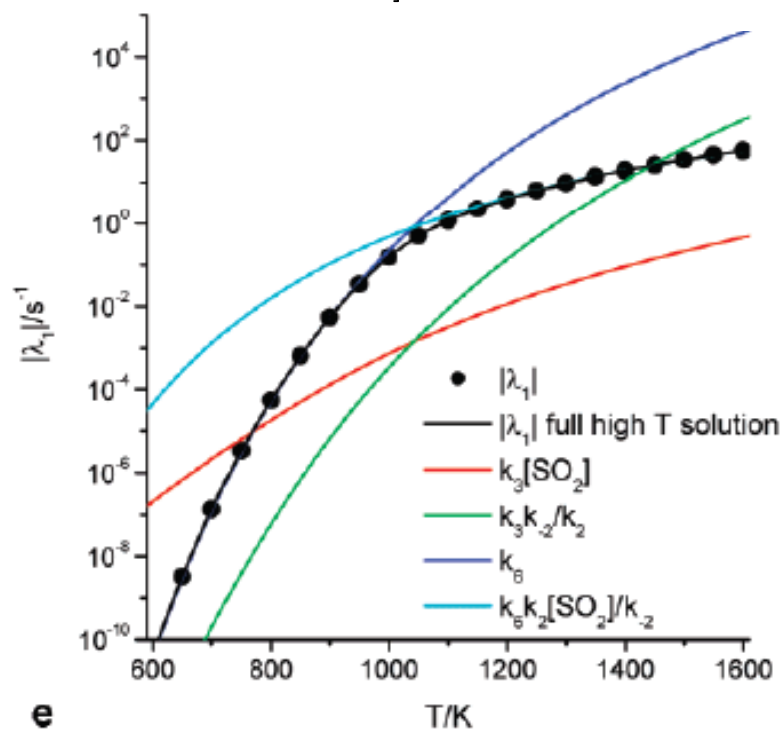
1 atm



0.001 atm

λ_1 

d

1 atm

e

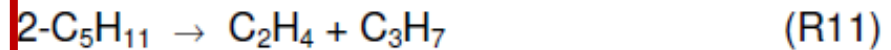
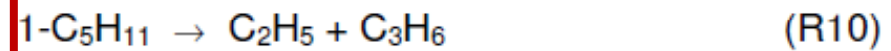
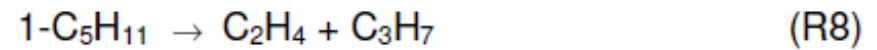
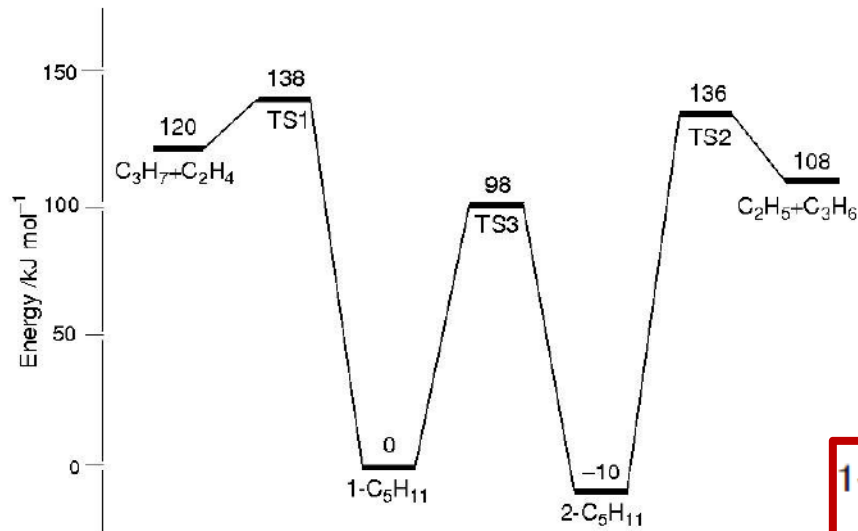
10⁶ atm

Eigenpair analysis to return macroscopic rate constants

Macroscopic rate-coefficients are combinations of the Chemically Significant eigenvalues and vectors of the collision matrix

- J. T. Bartis and B. Widom, *J. Chem. Phys.*, 1974, 60, 3474
- J. A. Miller and S. J. Klippenstein, *J. Phys. Chem. A*, 2006, 110, 10528, J. A. Miller and S. J. Klippenstein, *J. Phys. Chem. A*, 2002 106, 9267, J. A. Miller and S. J. Klippenstein, *J. Phys. Chem. A*, 2003, 107, 2680.
- Robertson et al. *Phys. Chem. Chem. Phys.*, 2007, 9, 4085-4097

1,2-Pentyl isomerisation and dissociation

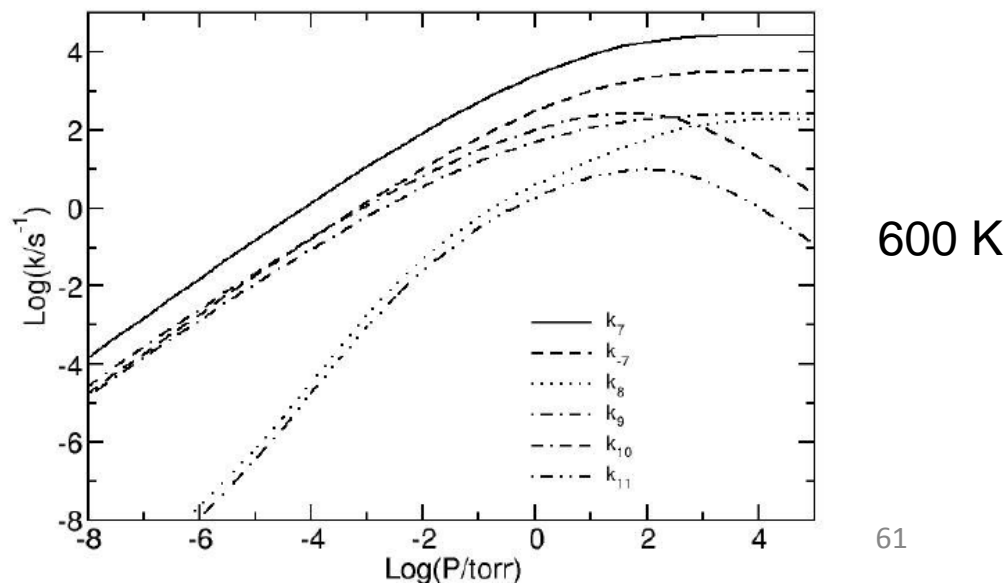
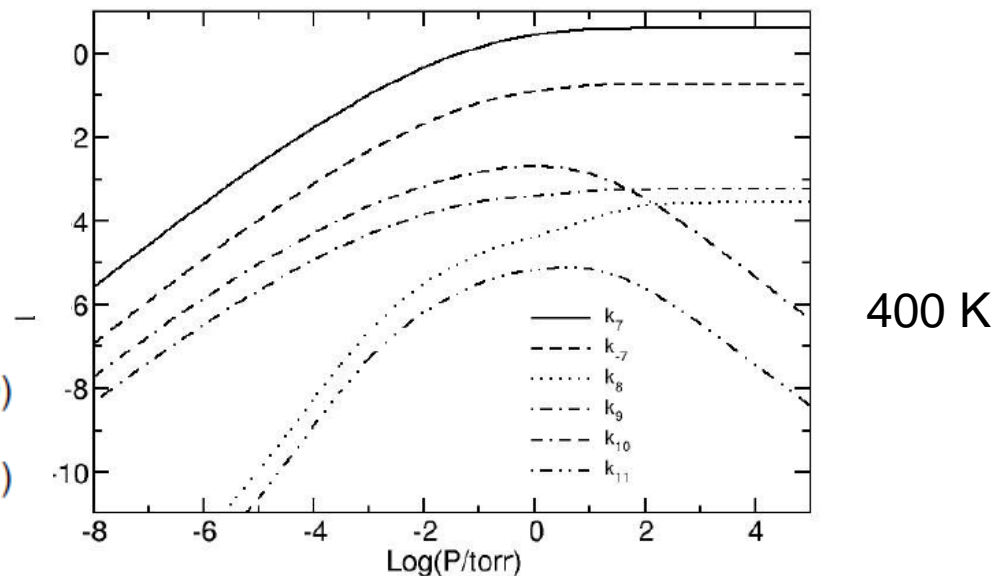
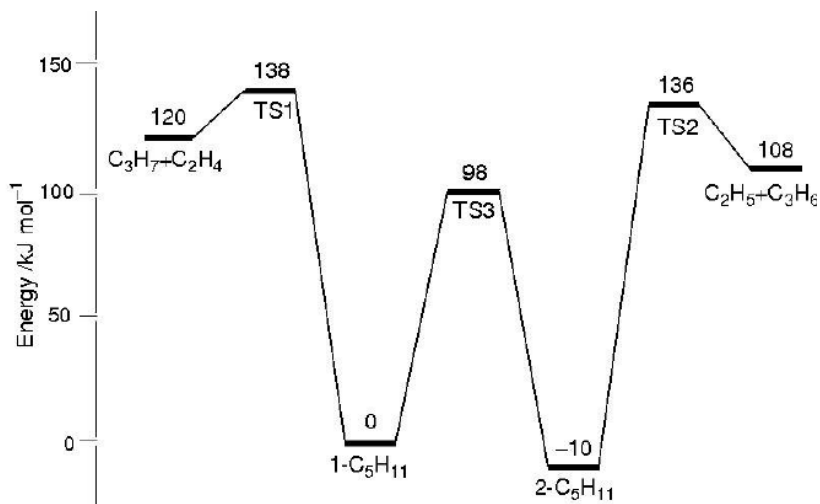
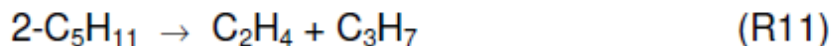
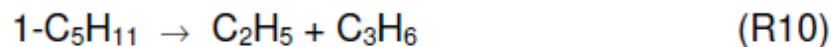
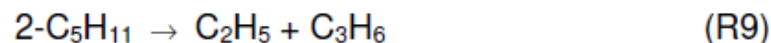
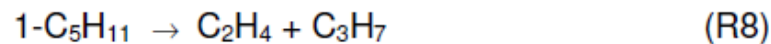
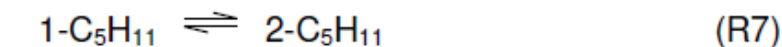


$$\lambda_{1,2} = \frac{-(k_C + k_D) \pm \sqrt{(k_C + k_D)^2 - 4(k_C k_D - k_7 k_{-7})}}{2}$$

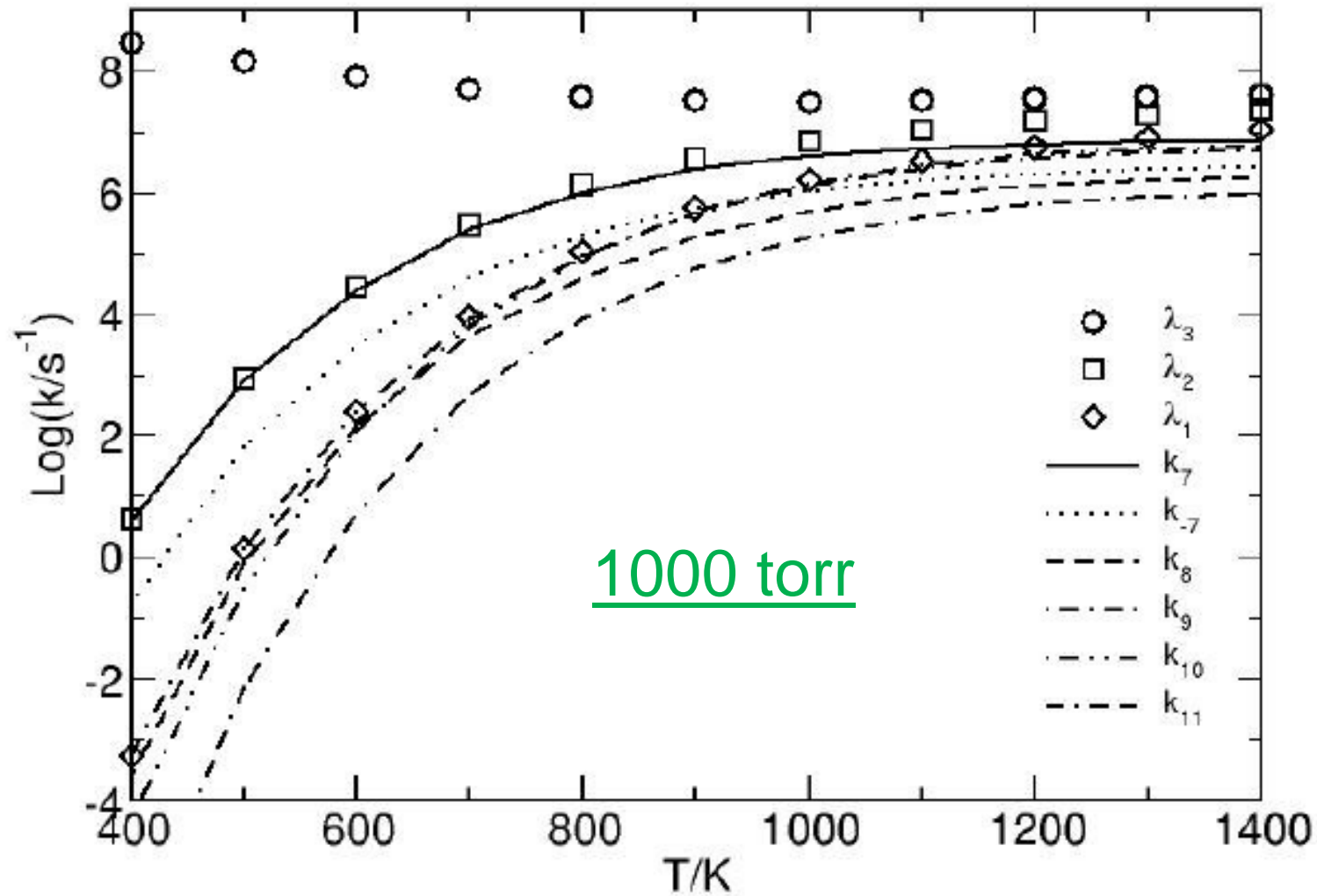
where $k_C = k_7 + k_8 + k_{10}$ and $k_D = k_{-7} + k_9 + k_{11}$.

1,2 pentyl isomerisation and dissociation

Rate coefficients extracted with Bartis Widom analysis,



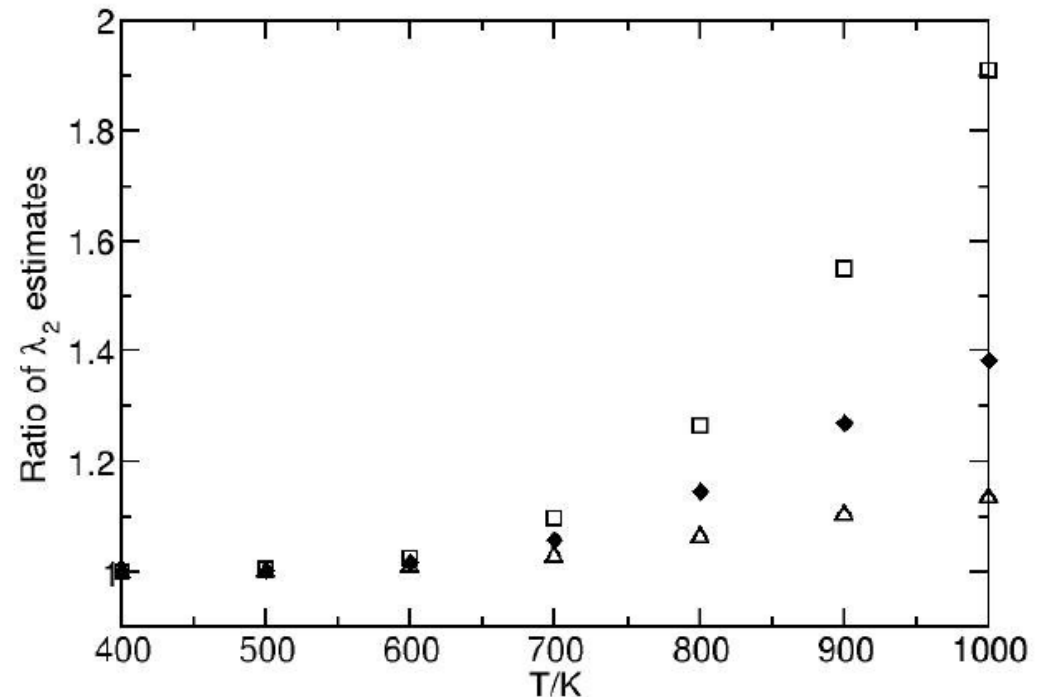
Behaviour at high temperatures: overlap of CS and relaxation eigenvalues



Binomial expansion of quadratic solution for λ_2

$$-\lambda_2 \approx k_7 + k_{-7} + k_8 + k_9 + k_{10} + k_{11} \approx k_7 + k_{-7} \quad \text{Low T}$$

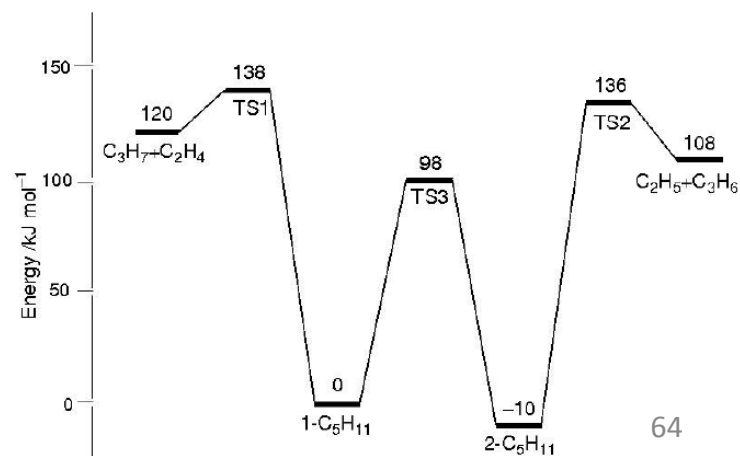
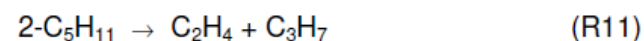
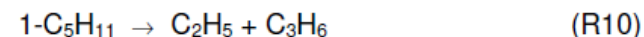
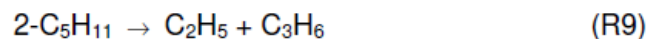
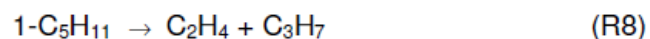
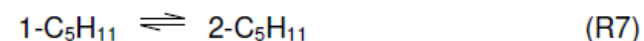
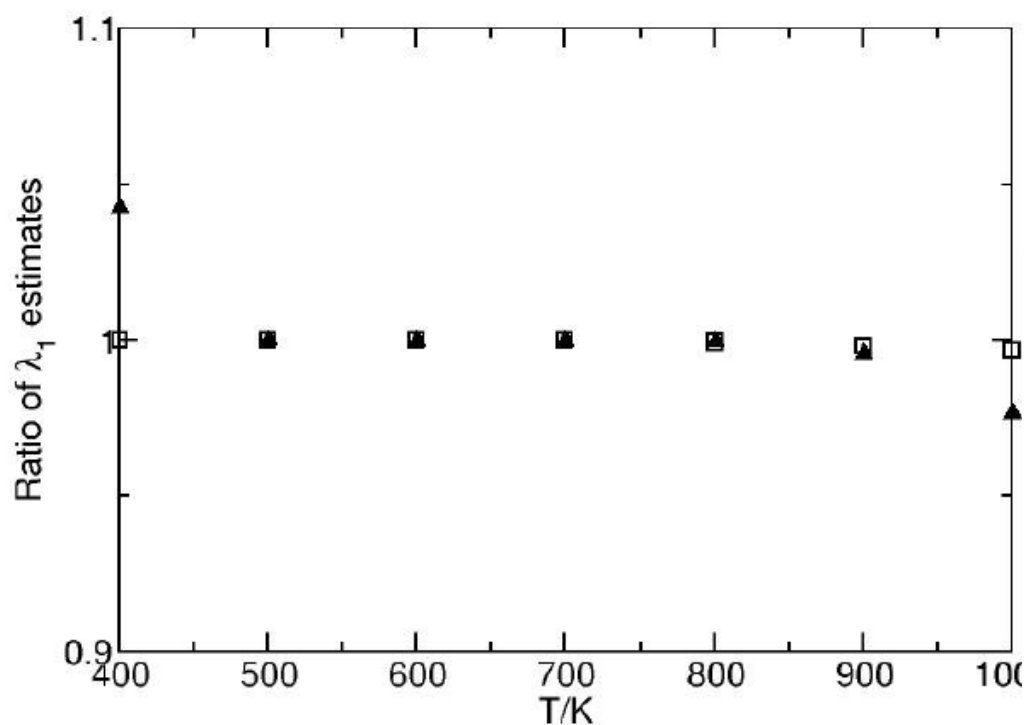
- full diamonds: ratio of λ_2 from full quadratic solution to λ_2 from the ME.
- Open triangles: ratio of λ_2 from Eq. full quadratic solution to λ_2 from equation above (full expression.)
- Open squares: ratio of $-\lambda_2$ from full quadratic expression to $(k_7 + k_{-7})$.



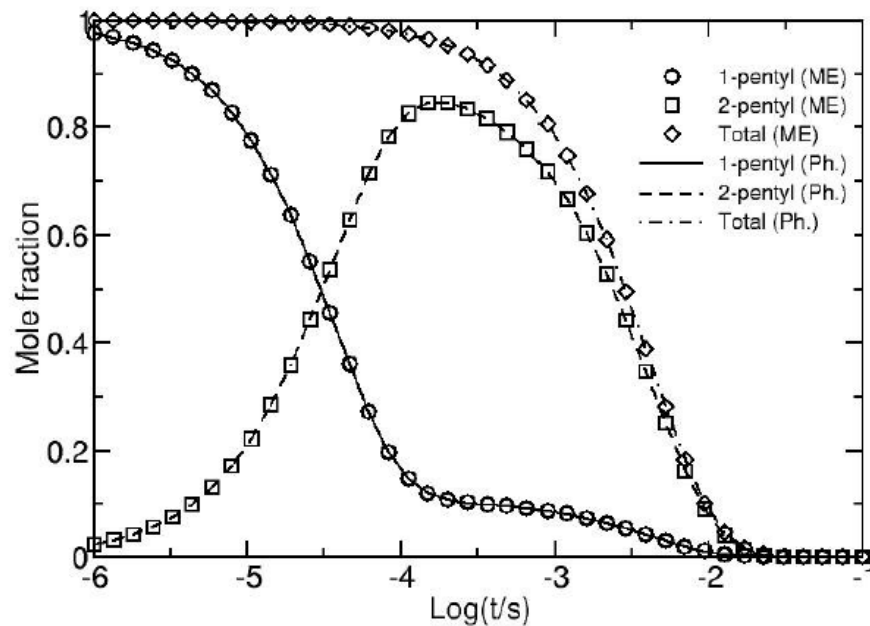
Binomial expansion of quadratic solution for λ_1

$$-\lambda_1 \approx \frac{k_8 + k_{10}}{1 + K_7} + \frac{k_9 + k_{11}}{1 + K_7^{-1}} \quad \text{where } K_7 = k_7/k_{-7}.$$

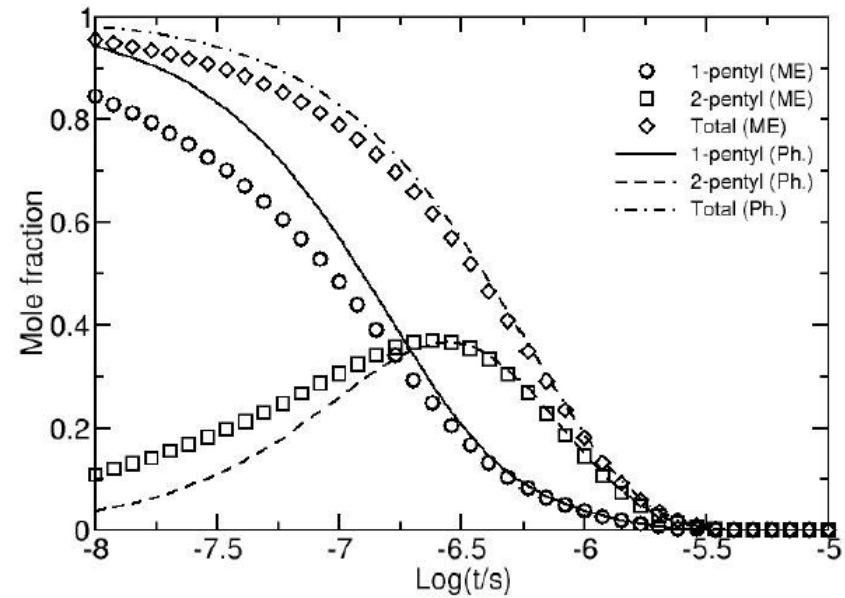
- Full triangles: ratio of λ_1 from the full quadratic solution to λ_1 from the ME.
- Open squares: ratio of λ_1 from the full quadratic solution to λ_1 from above approximation



Comparison of the time dependence of the mole fraction of the 1- and 2-pentyl isomers using the summed grain populations from the ME and using the phenomenological rate coefficients from the ME in a biexponential representation: (a) 600 K; (b) 1000 K.



a

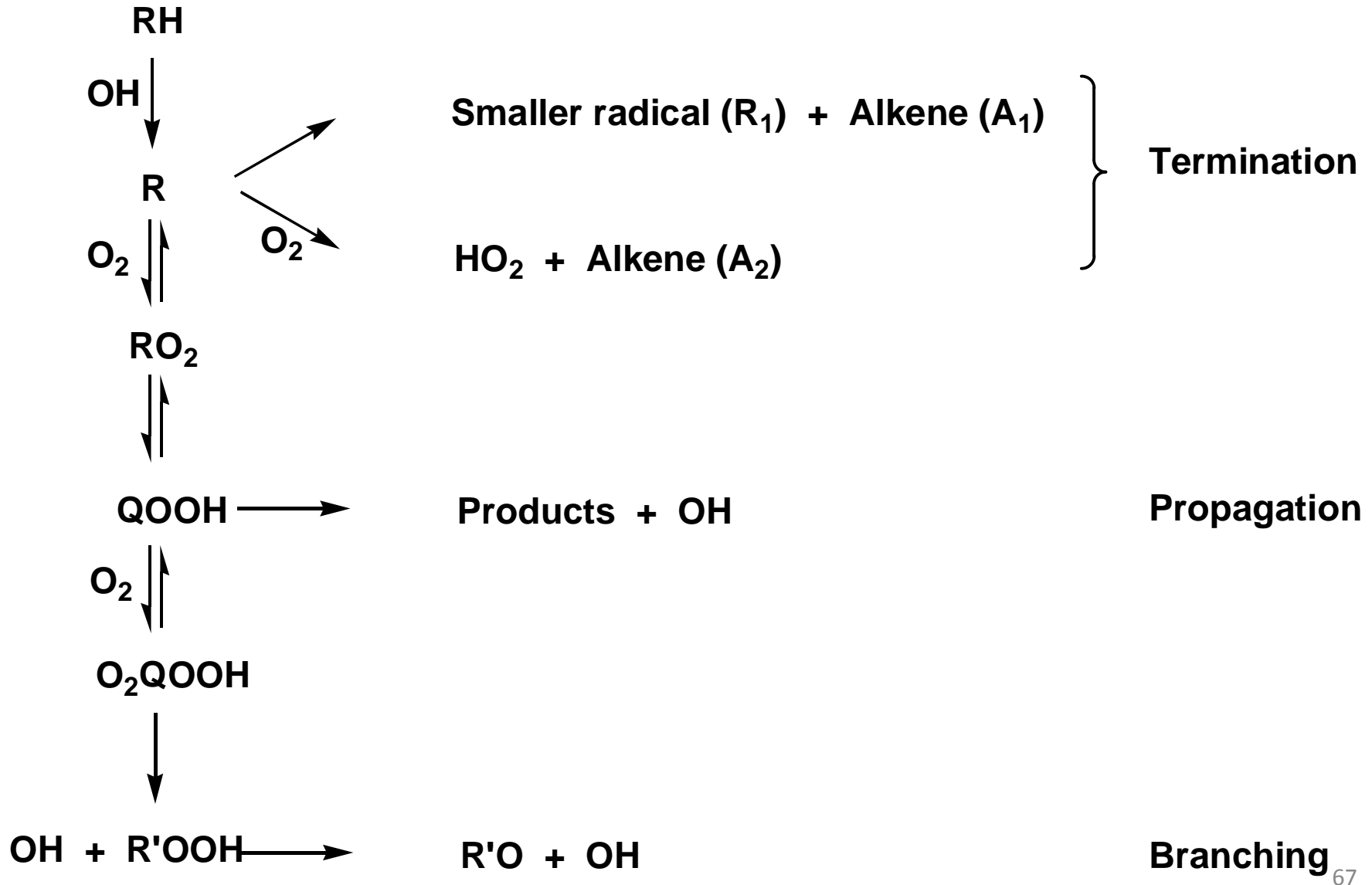


b

Conclusions

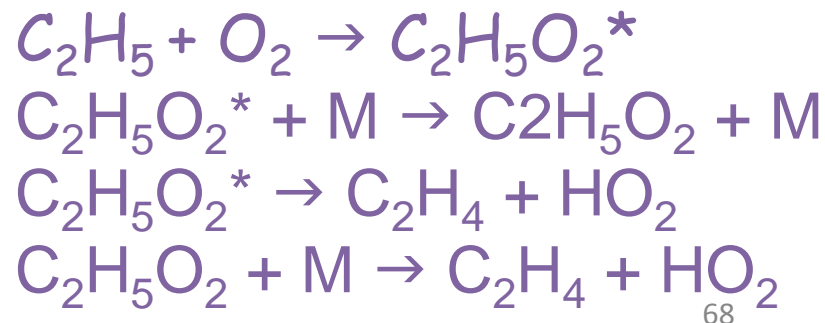
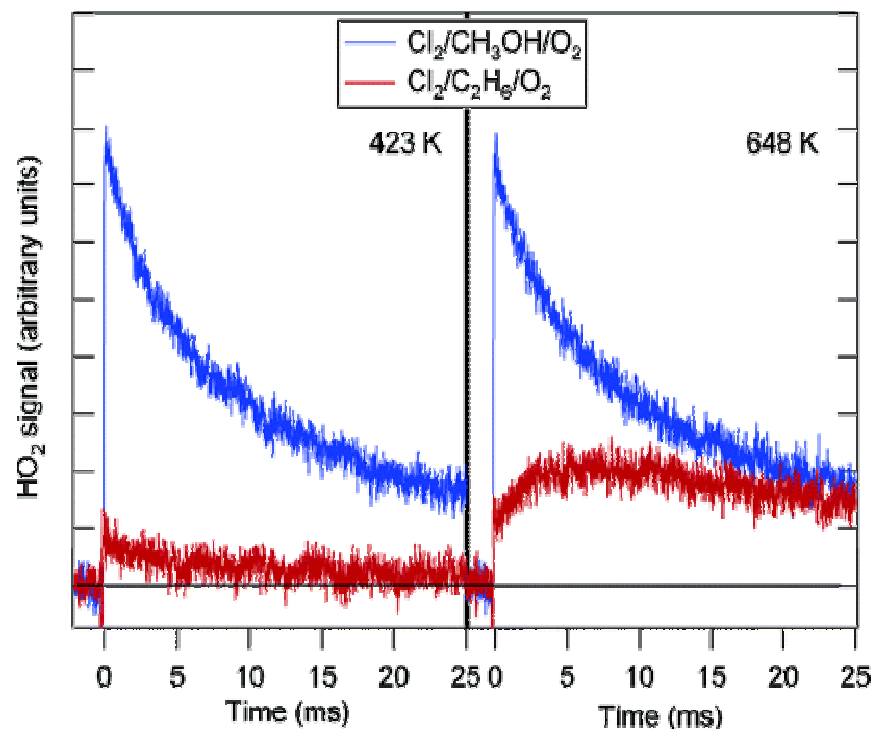
- All wells can contribute to all sink channels irrespective of whether they are directly connected to the transition state that leads to a given set of products.
- 'Well-skipping' is significant and is characterized by non-standard fall-off curves which exhibit a decline in rate coefficient with increasing pressure, indicative of the competition between collisional relaxation and reaction.
- Product yields are very sensitive to the difference in dissociation energies for 1- and 2-pentyl. The calculations give a difference of only 4 kJ mol⁻¹, and ancillary experiments are essential to define the system more accurately. Because of the complexity of the system, the experiments must be interpreted with a master equation analysis.

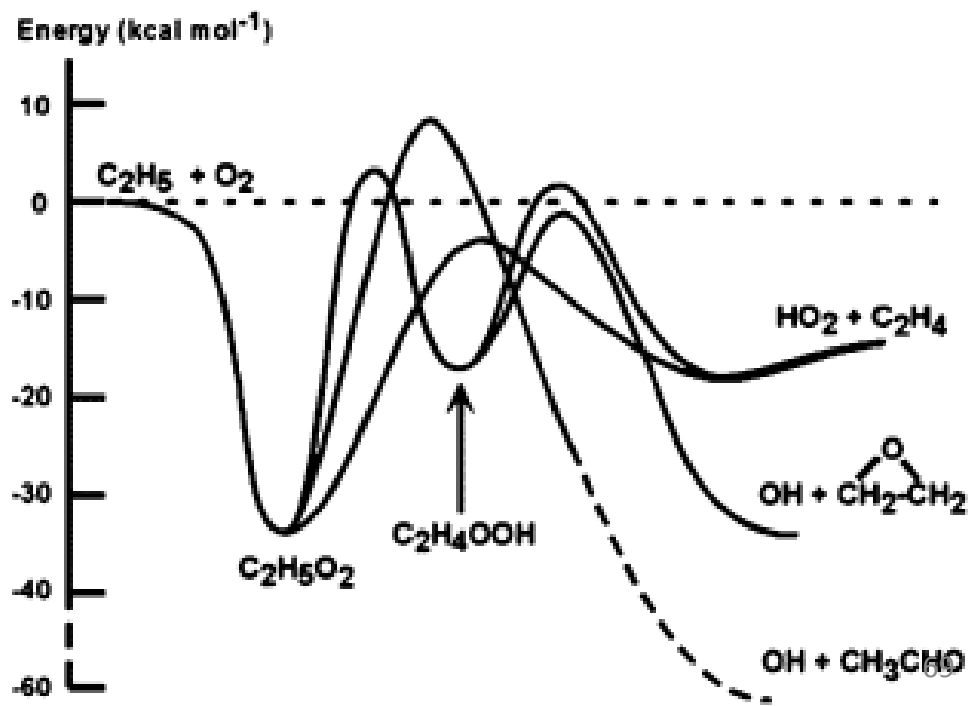
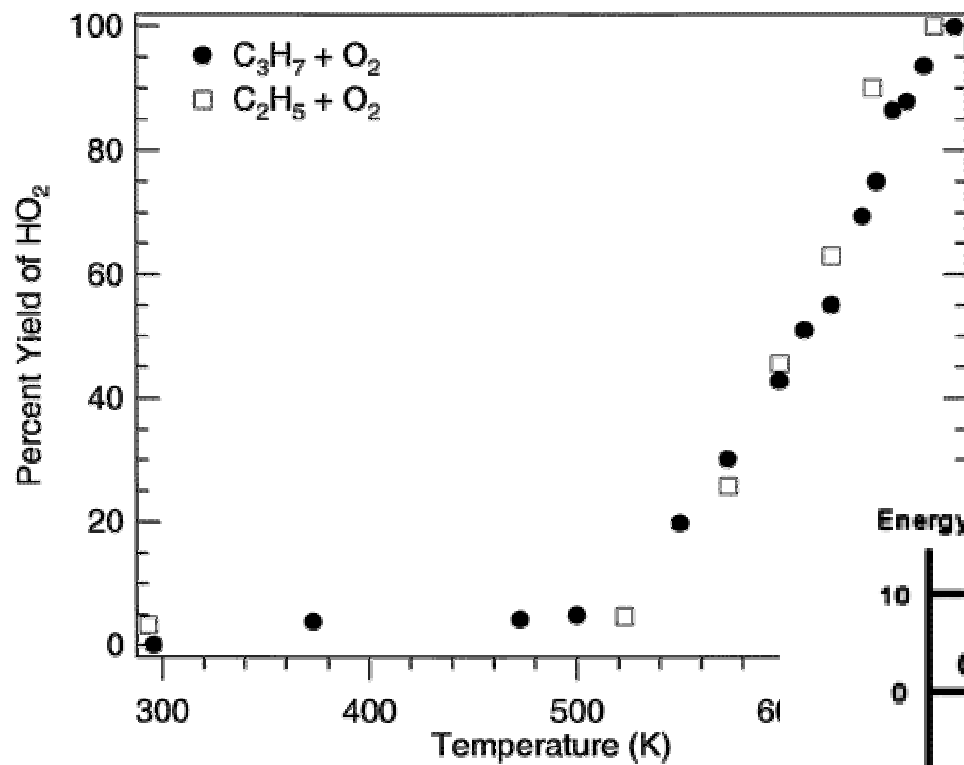
Autoignition chemistry



Determination of product yields in $C_2H_5 + O_2$

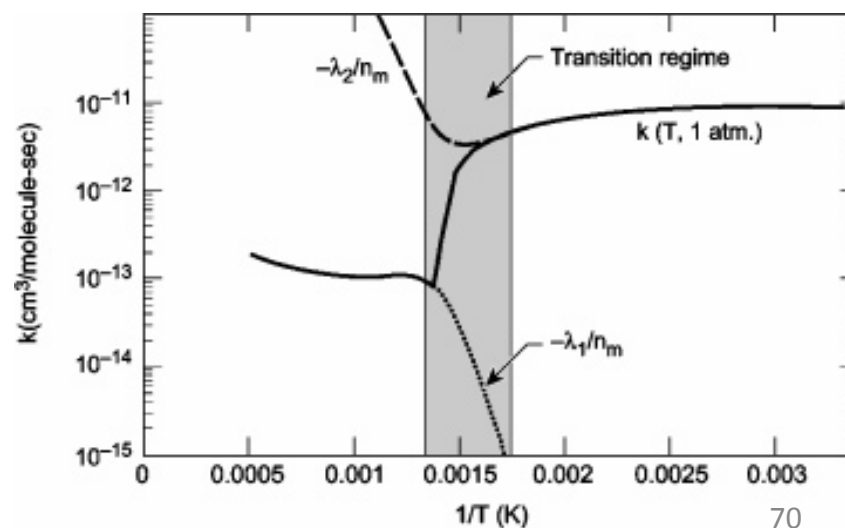
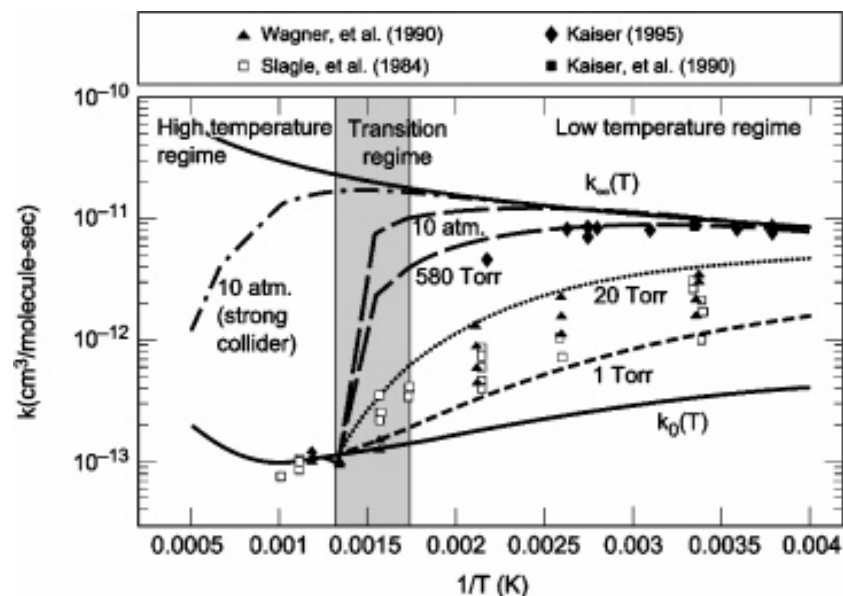
- Taatjes et al. (J. Phys. Chem. A 104 (2000) 11549 - 11560) observed the formation of OH and HO_2 , determining the fractional yields. Used 100% yield of HO_2 from $CH_2OH + O_2$ to calibrate the system.
- HO_2 yield \uparrow as $T \uparrow$ and $p \downarrow$
- Two timescales at higher T
- OH yield is small.
- Theoretical interpretation and relevance to autoignition chemistry will be discussed later





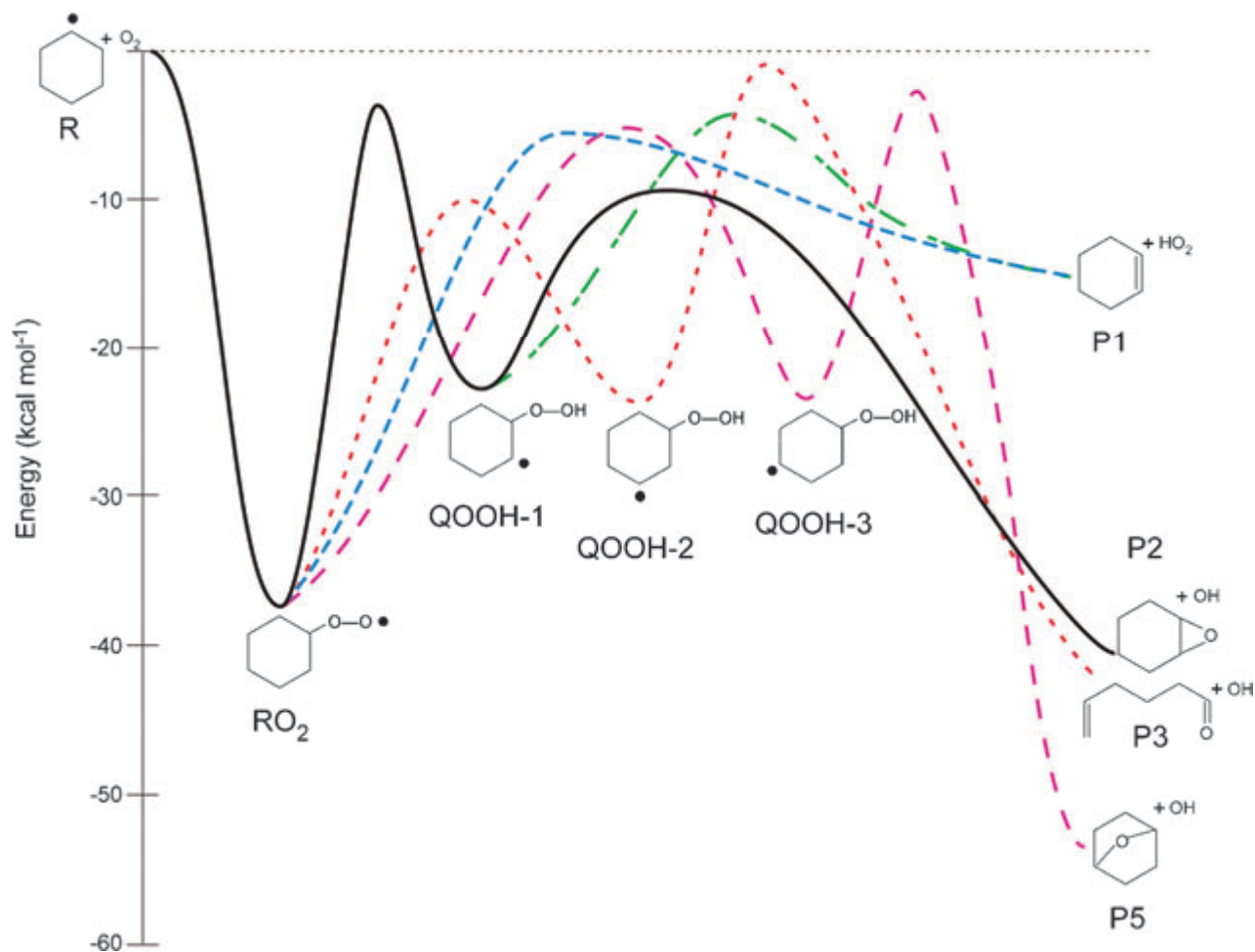
Master equation analysis: Miller and Klippenstein, Int J Chem Kinet 33: 654-668, 2001

- 3 regimes, low, transition, high T.
- In transition region, thermal rate constant jumps from one eigenvalue to the other - the two eigenvalues are mixed in this region.
- At high T, the reaction exclusively forms HO_2 via a largely thermalised RO_2 . k is, in practical terms, independent of p .
- At low T, reaction involves the pressure dependent formation of RO_2 and direct formation of HO_2

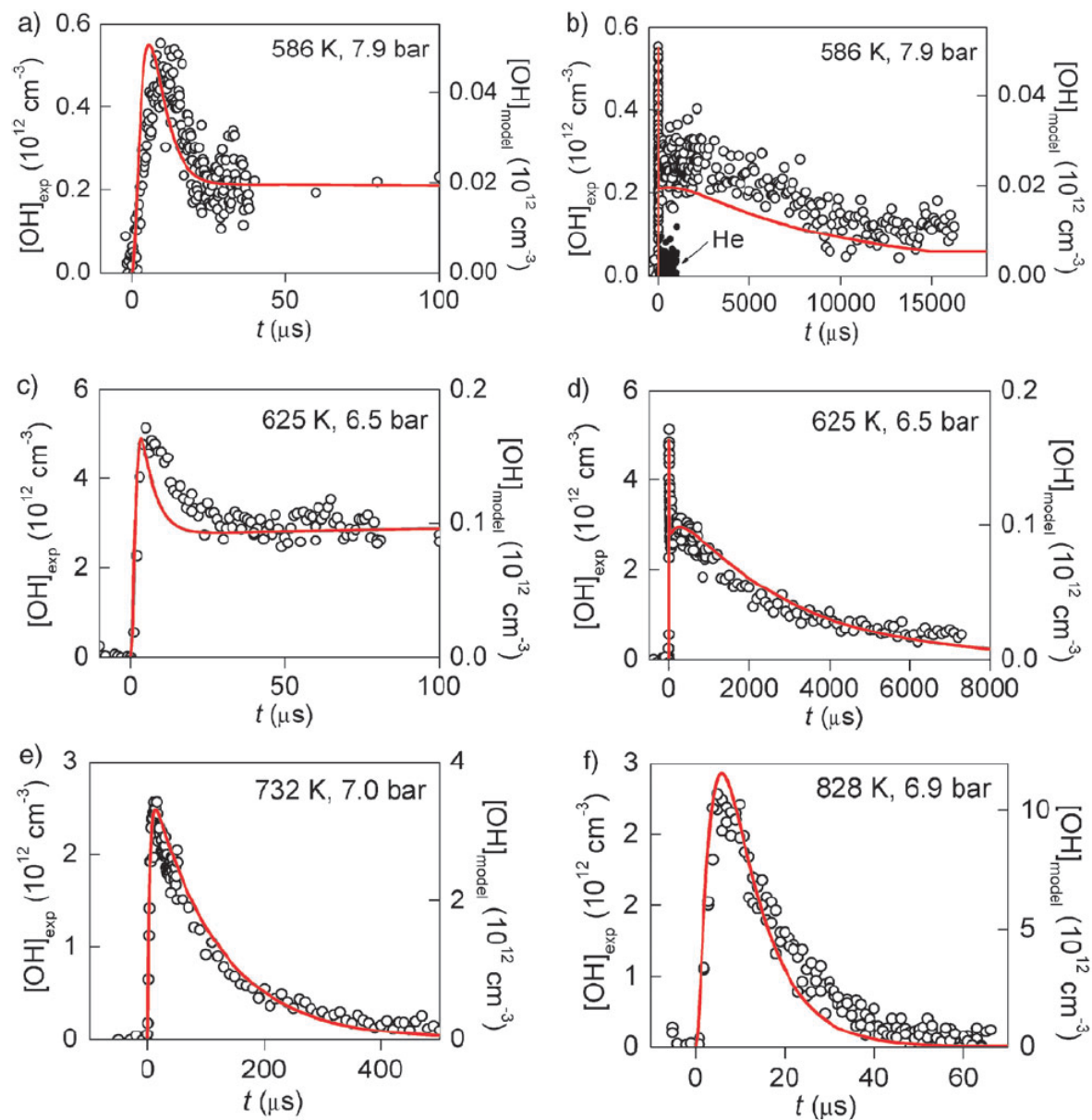


Cyclohexyl + O₂

Fernandes et al. Phys Chem. Chem. Phys., 2009, 11, 1302 - 1307



Time dependence of OH formation



Importance of formally direct route to OH

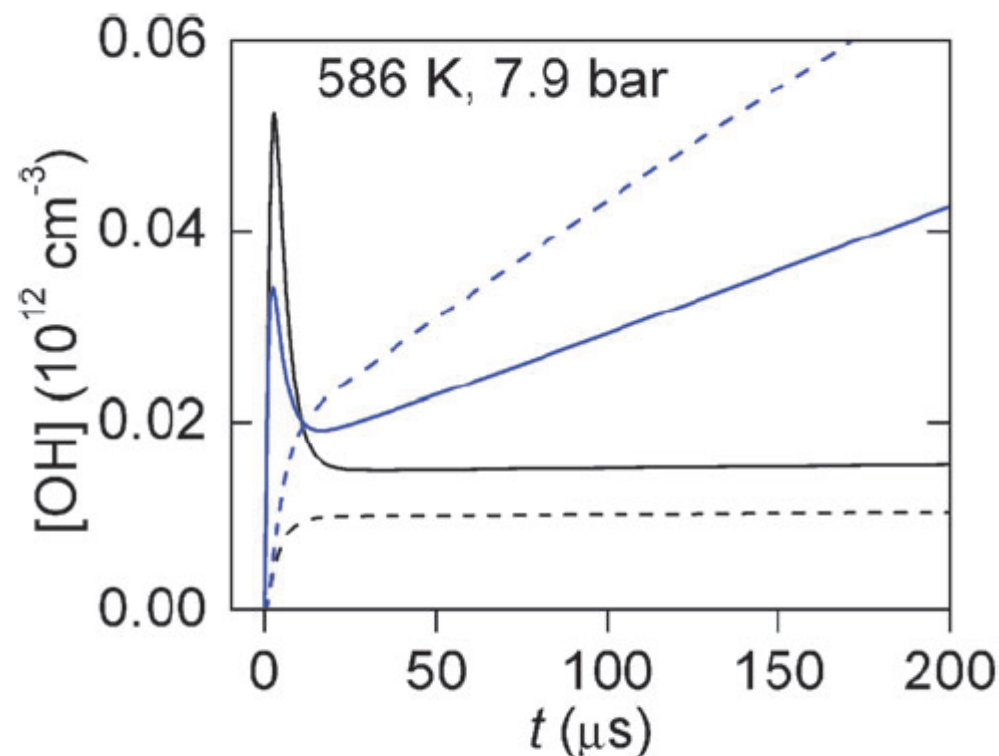
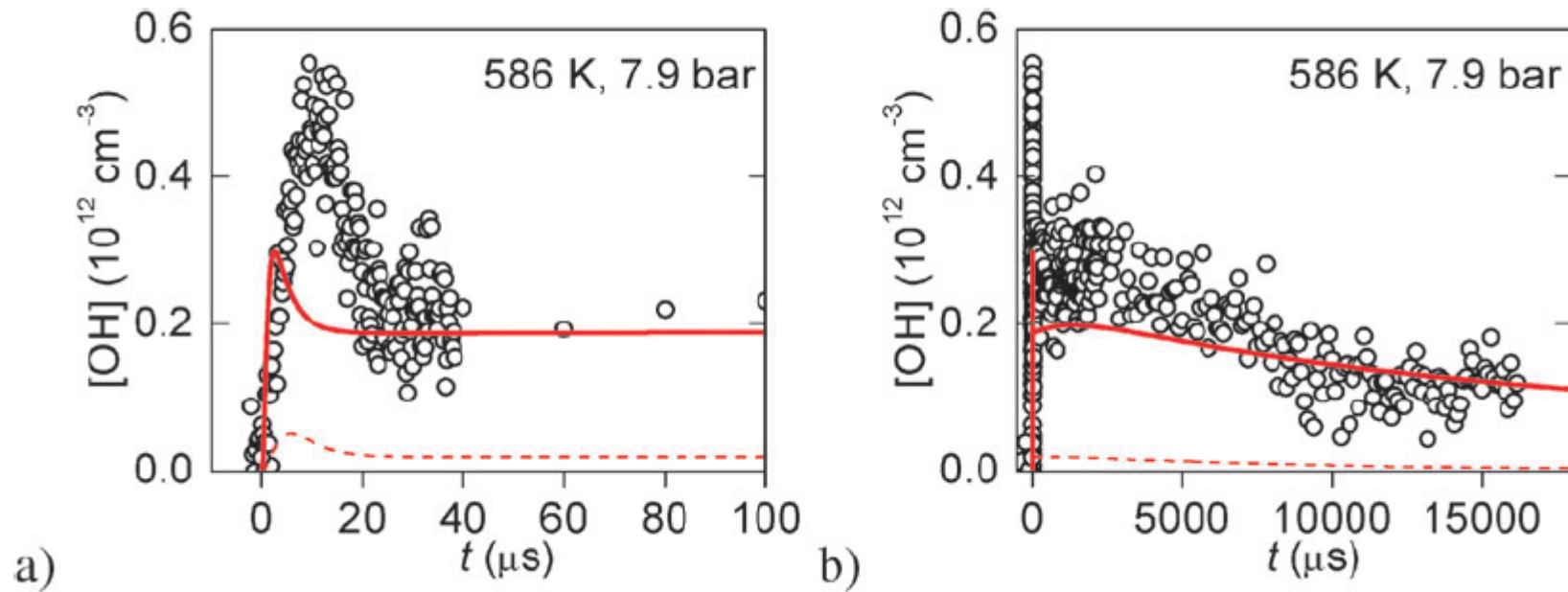
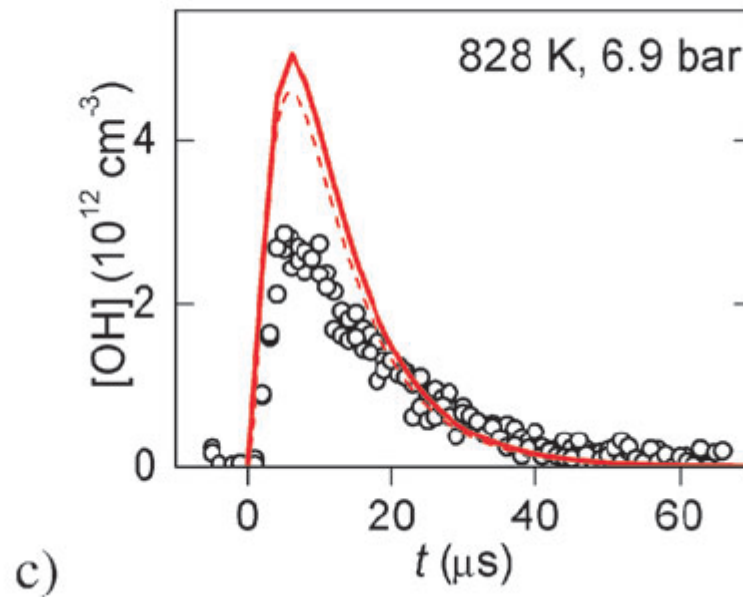


Fig. 5 Calculated OH concentration at 7.9 bar and 586 K using different models. The solid black line is the Knepp *et al.*¹³ model; the dashed black line is the Knepp *et al.* model, but without formally direct pathways. The dashed blue line is the Silke *et al.*⁴¹ mechanism, and the solid blue line is Silke *et al.* model, adding all rate coefficients from the ME calculation.

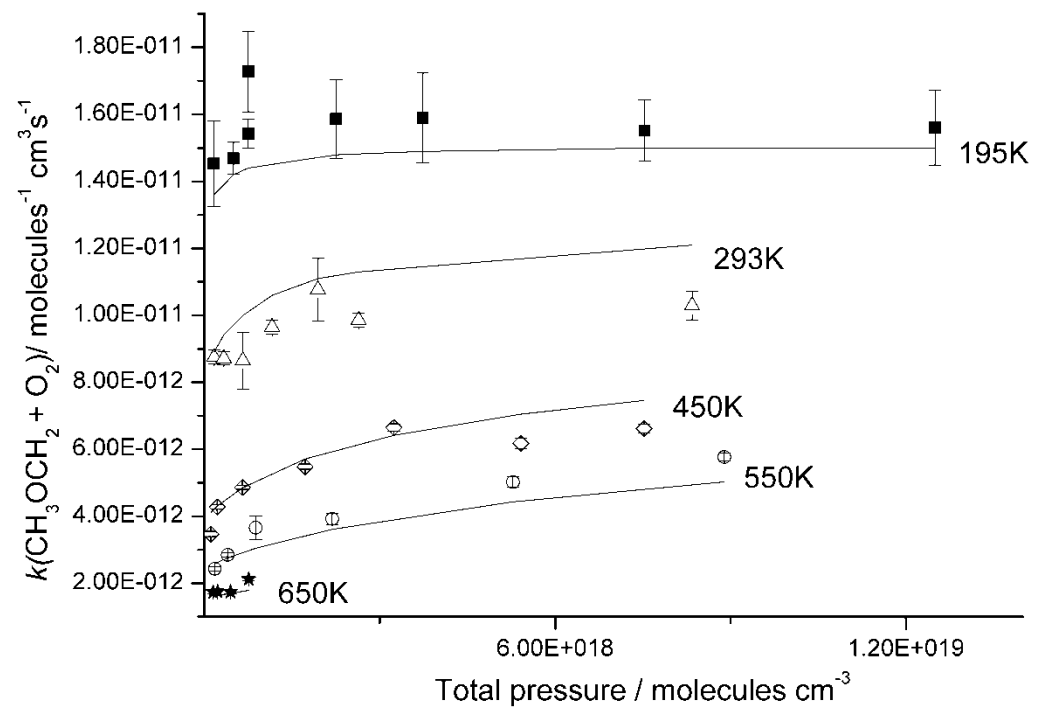
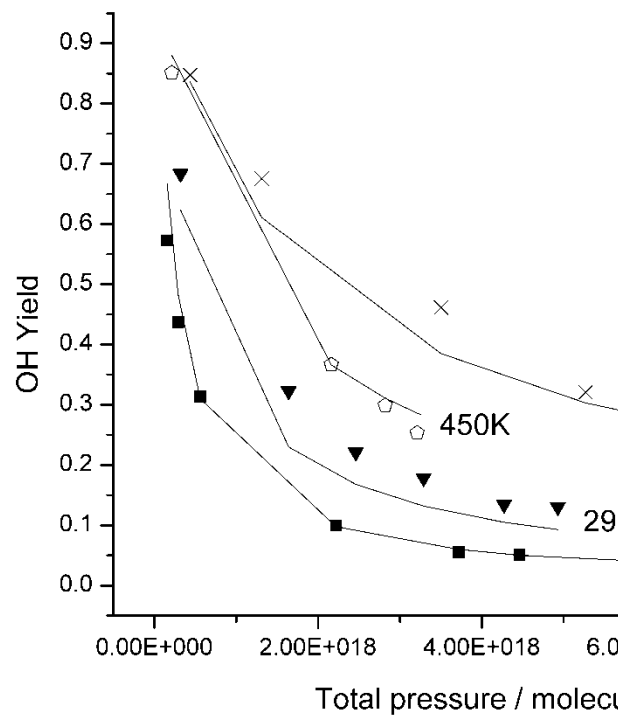


Effect of the chain branching on model calculations at (a)–(b) 586 K and (c) 828 K.

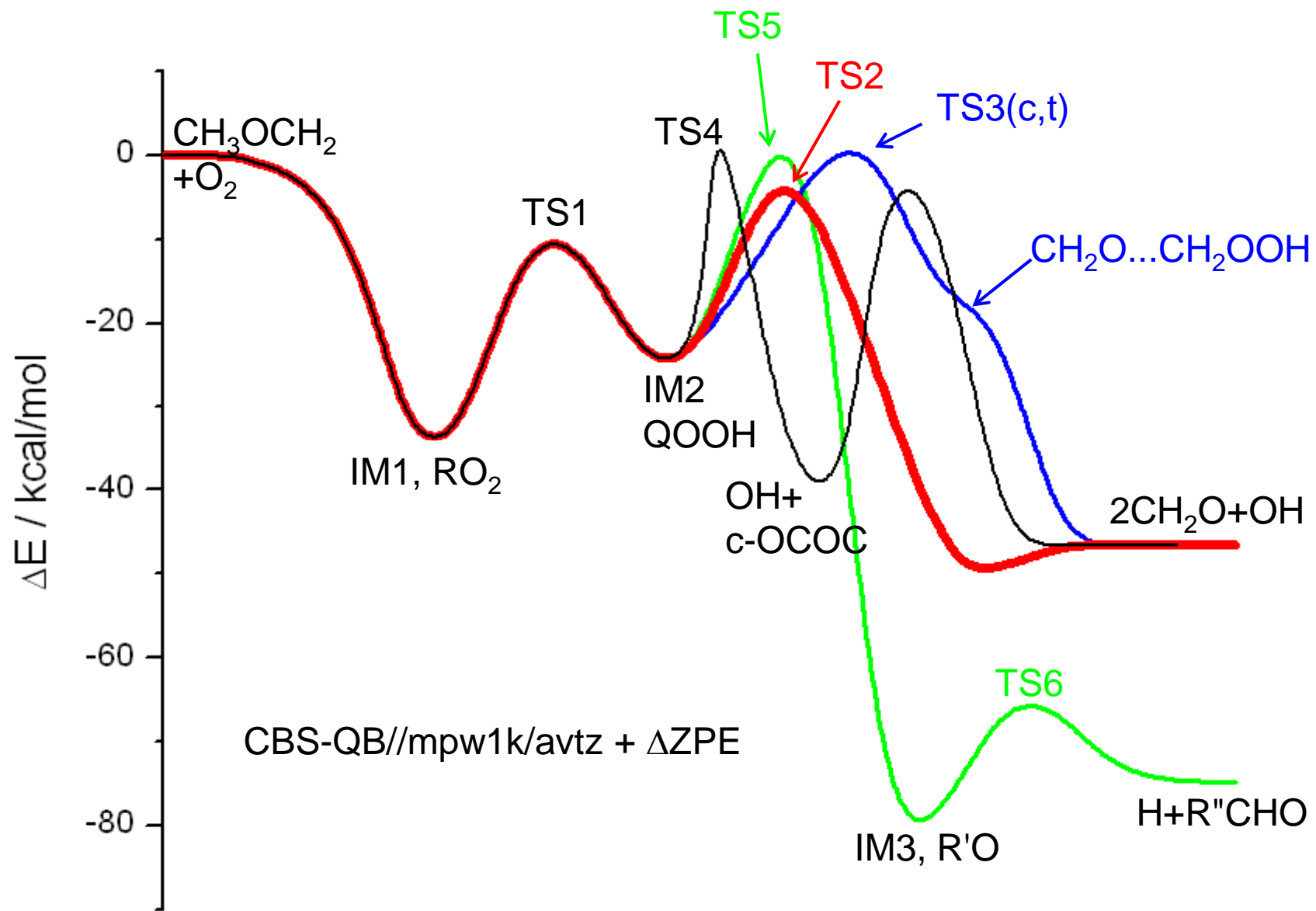
Evidence for chain branching at lower T



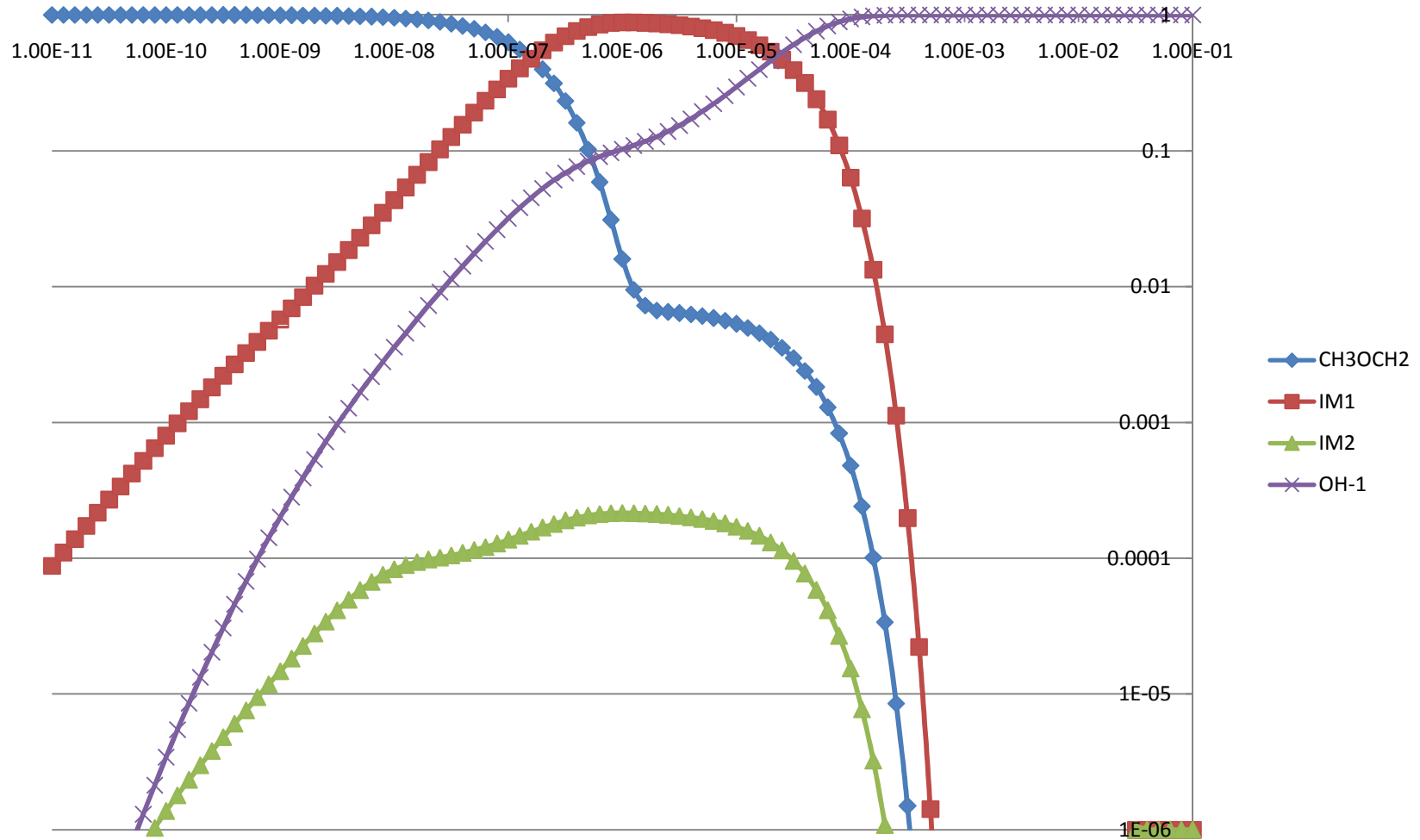
Dimethyl ether: $\text{CH}_3\text{OCH}_2 + \text{O}_2$ Eskola et al.



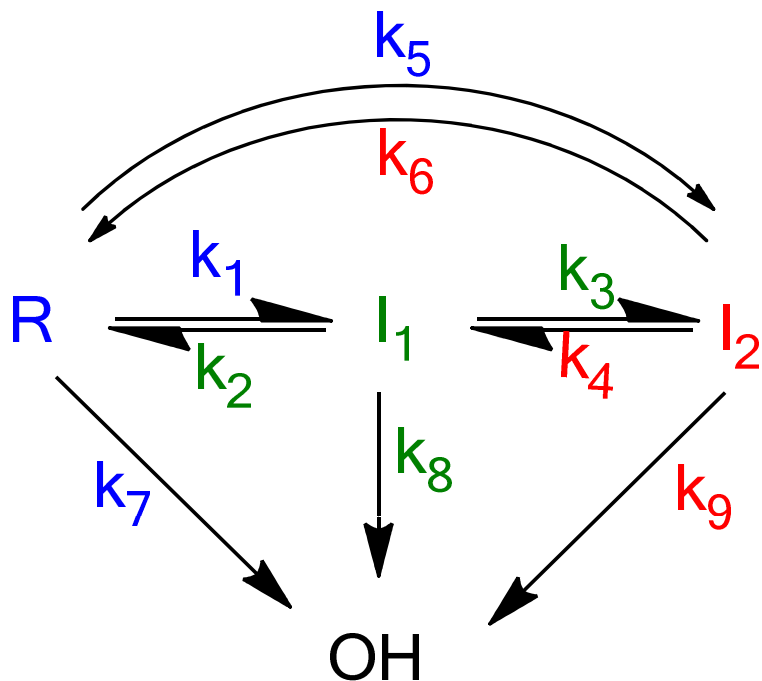
CH₃OCH₂ + O₂: major mechanism



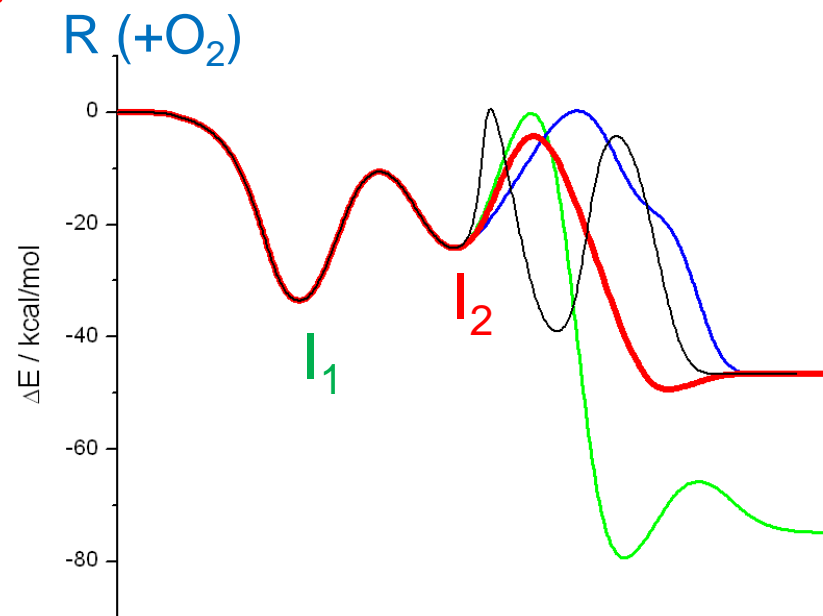
Species profiles, 550 K, 1 bar



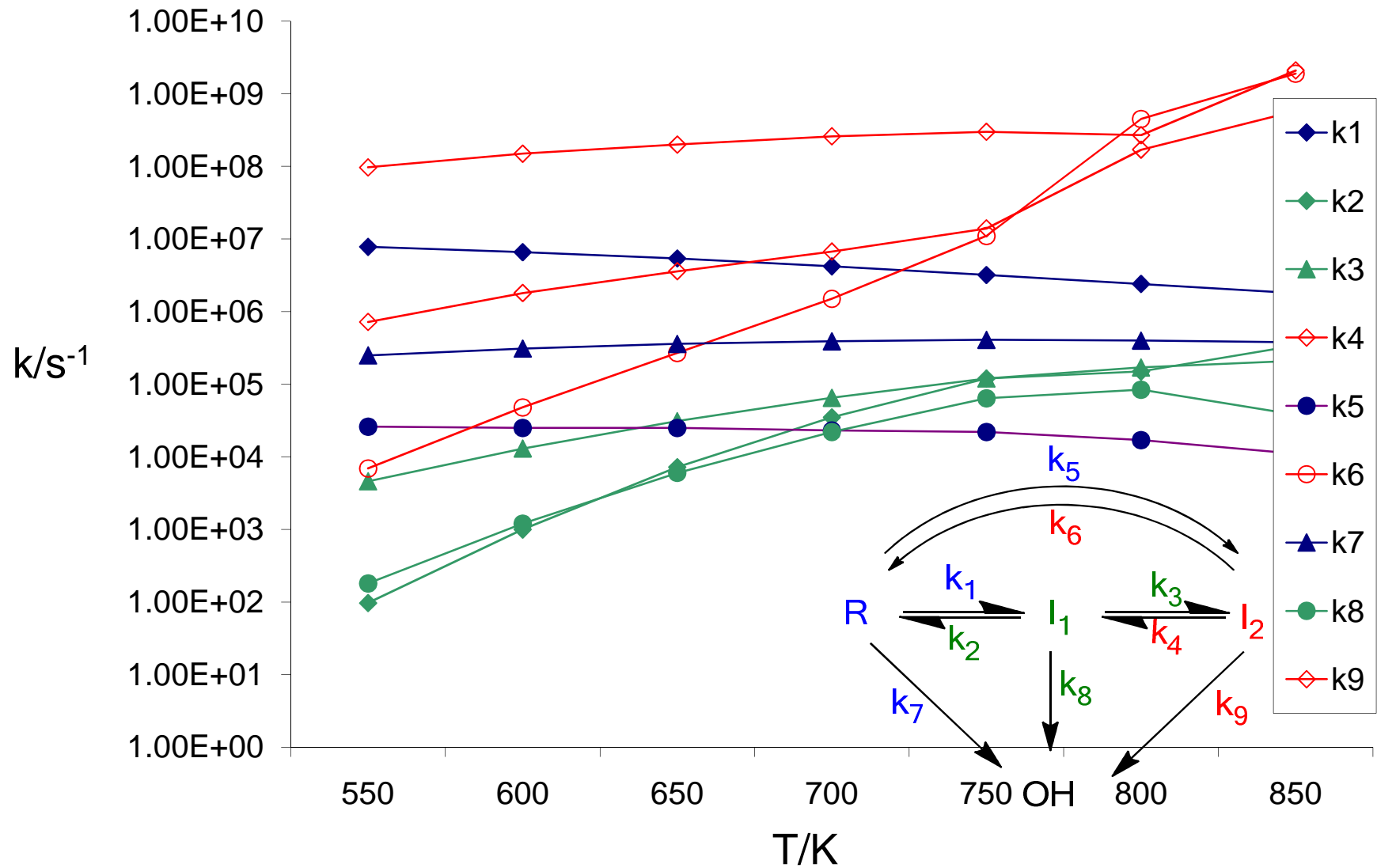
Master equation: rate constant analysis



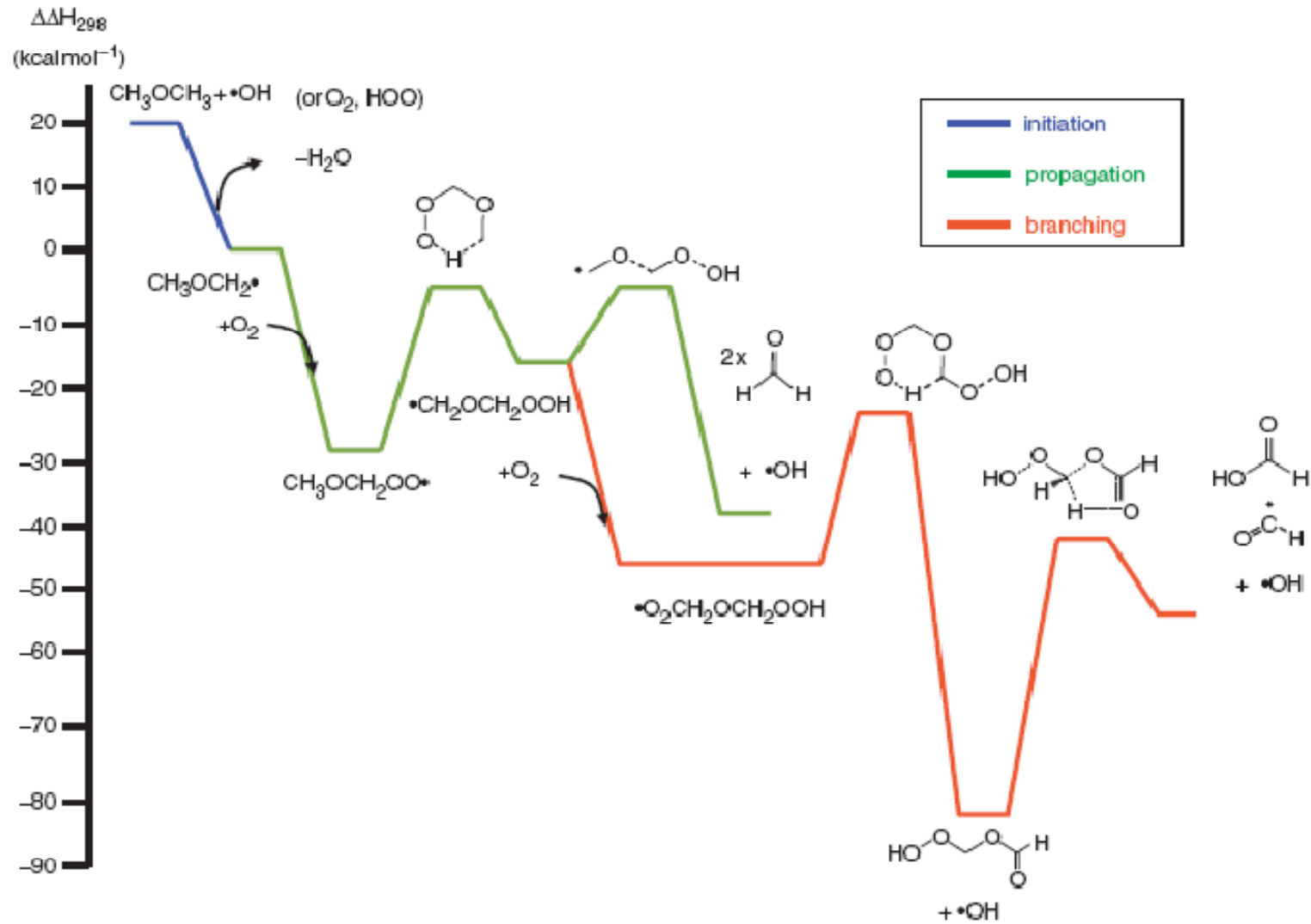
$I_1 = RO_2$
 $I_2 = QOOH$



Phenomenological rate coefficients from a Bartis Widom analysis



Routes to branching: $\text{CH}_3\text{OCH}_2 + \text{O}_2 (+ \text{O}_2)$



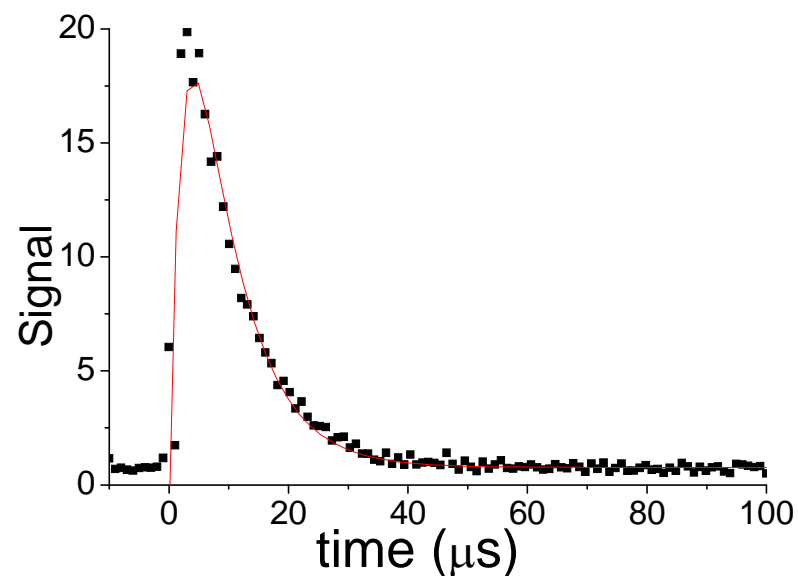
- Anderson and Carter: Molecular Physics 2008, 106, 367-396

Excited electronic states in combustion Chemistry of methylene (CH_2)

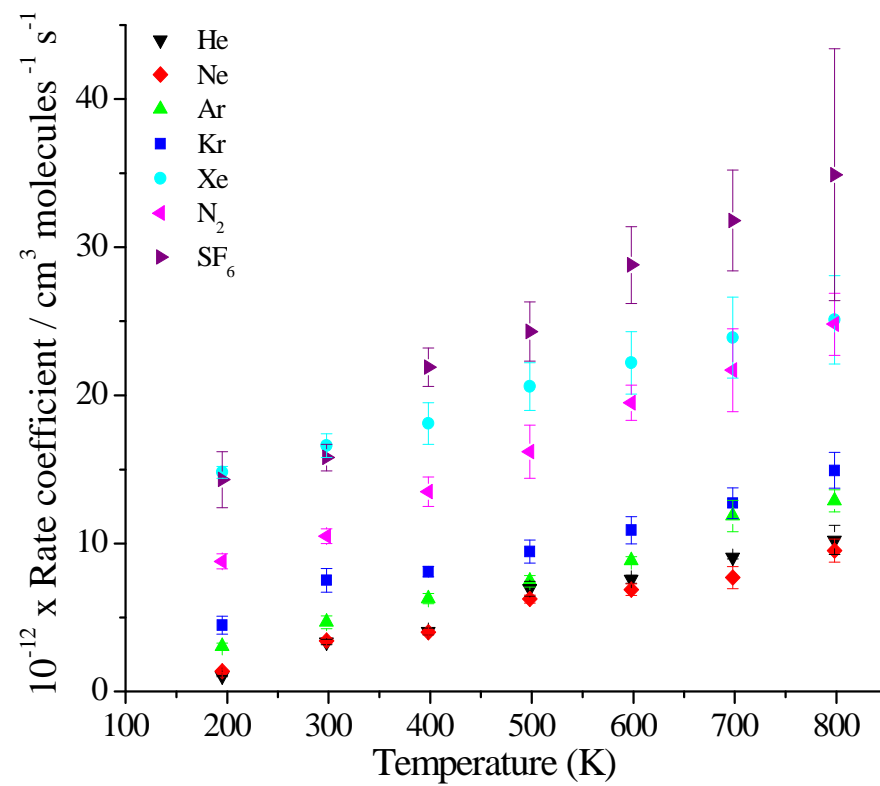
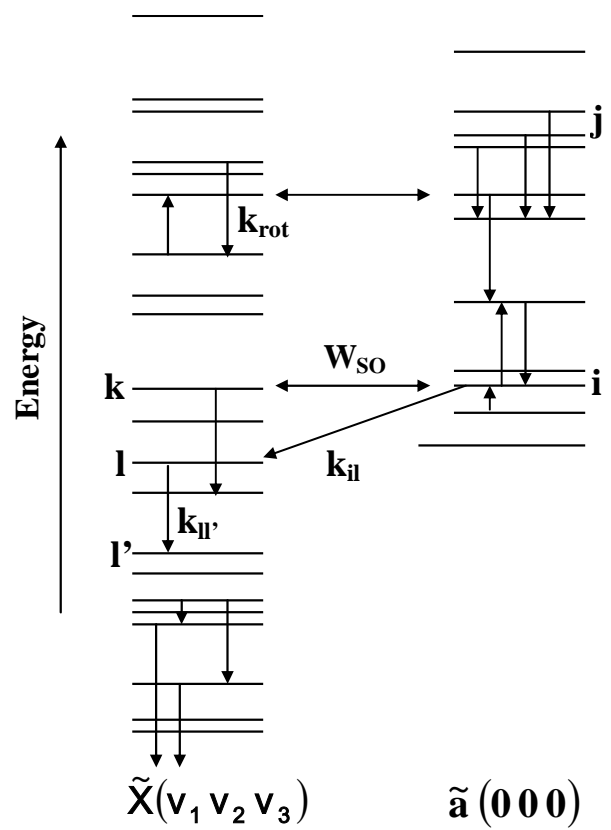
- CH_2 exists as a triplet ($^3\text{CH}_2$) and a singlet ($^1\text{CH}_2$), separated in energy by $\sim 9 \text{ kcal mol}^{-1}$.
- The upper state (singlet) is much more reactive. It is involved, e.g., in the production of C_3H_3 , a soot precursor and in the chemistry of Titan.
- The singlet is deactivated to the triplet on collision with unreactive (and reactive) gases.
- Our understanding of the mechanism of deactivation in reactive systems is limited, especially at combustion temperatures

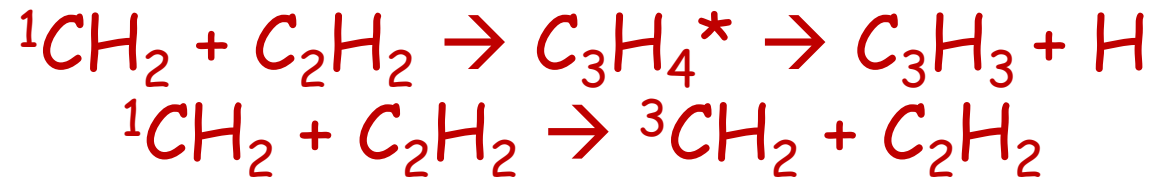
- Laser flash photolysis CH_2CO at (308 nm).
- Detection $^1\text{CH}_2$ by LIF, e.g. line from 3_{12} state in $a^1A_1(0,0,0)$ at 589.21 nm.
- Pressure 1 - 10 Torr. Rapid initial rotation relaxation of $^1\text{CH}_2(0,0,0)$.
- Collision induced intersystem crossing (CIISC) and reactions investigated for rotationally relaxed $^1\text{CH}_2(0,0,0)$

Methodology

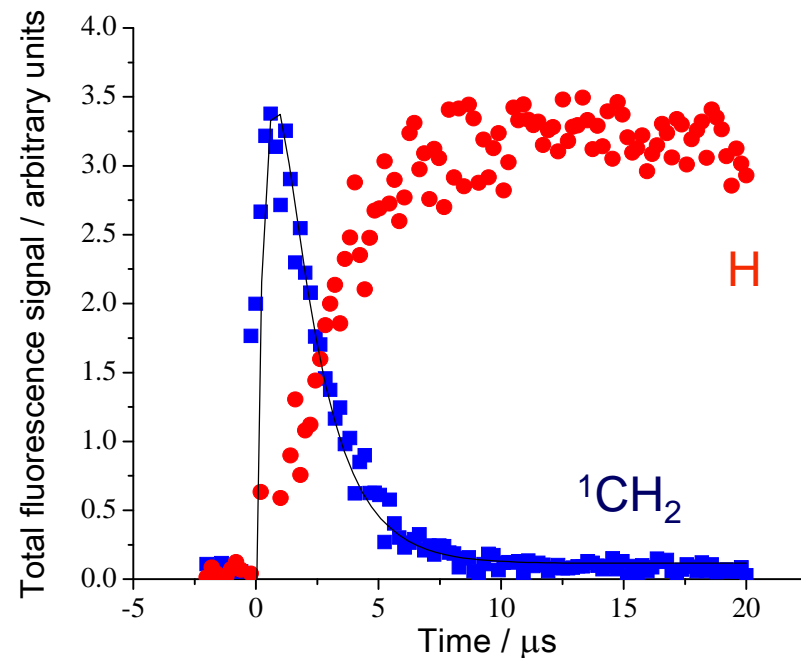


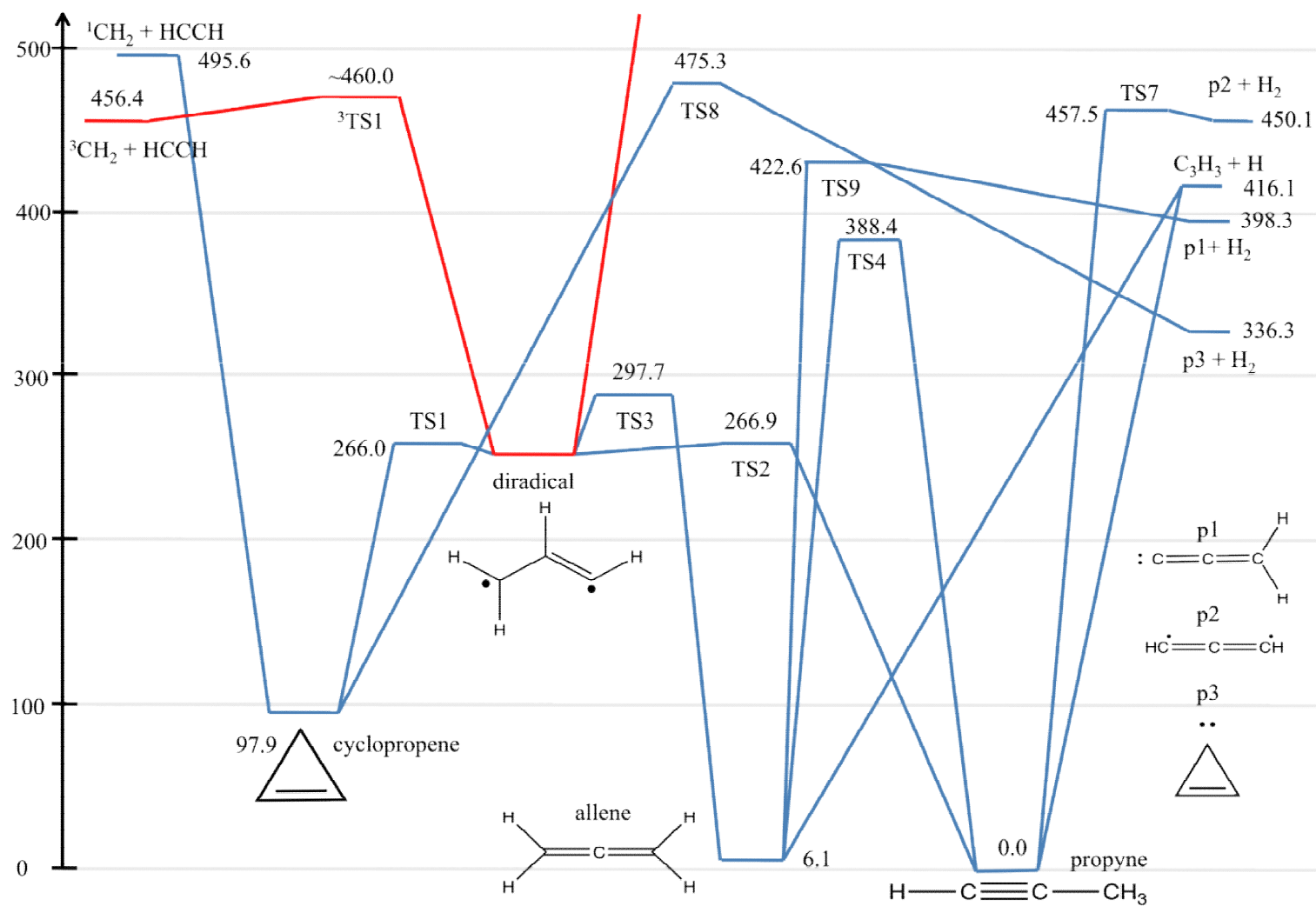
$^1\text{CH}_2 + \text{M} - \text{CIISC}$

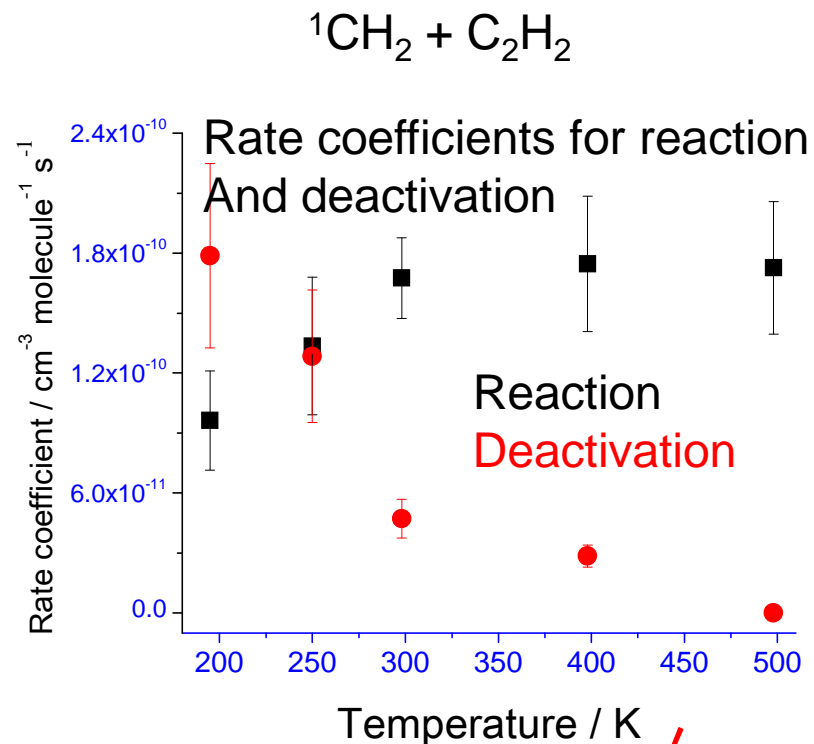
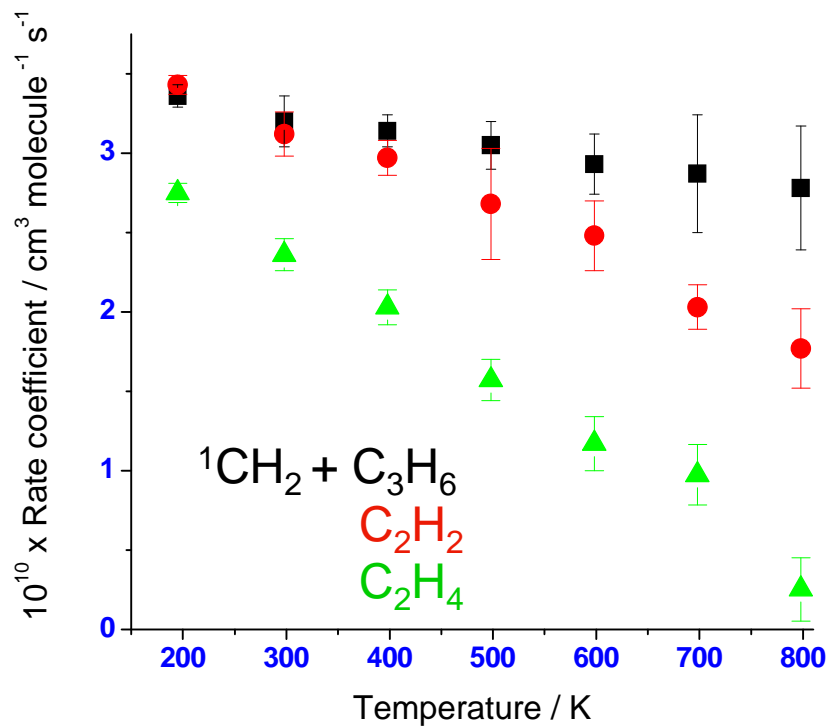




1. Kinetics from decay of CH_2
- the overall rate constant decreases as $T \uparrow$.
2. If same mechanism for deactivation as for Ar, then reactive channel becomes unimportant at higher T ???
3. Monitor H using VUV LIF; growth shows same kinetics as ${}^1\text{CH}_2$ decay
4. Calibrate H signal to determine what fraction of the ${}^1\text{CH}_2$ loss occurs by reaction and what fraction by deactivation.

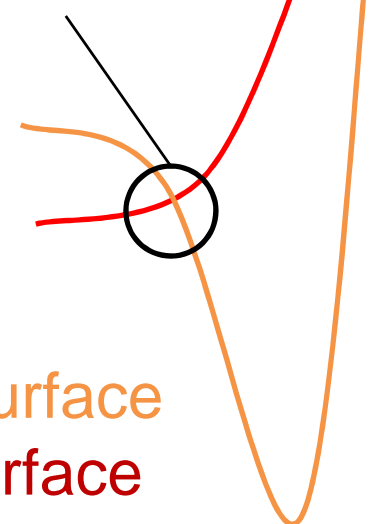






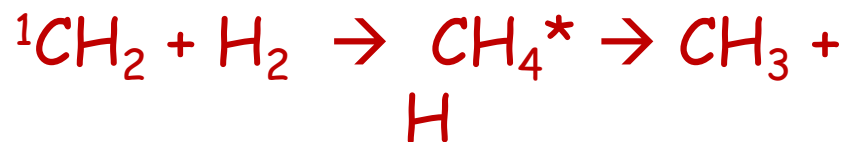
Rate coefficient for deactivation to the triplet now decreases with T . Doesn't fit in with the behaviour found for inert gases. What is the mechanism?

Surface crossing

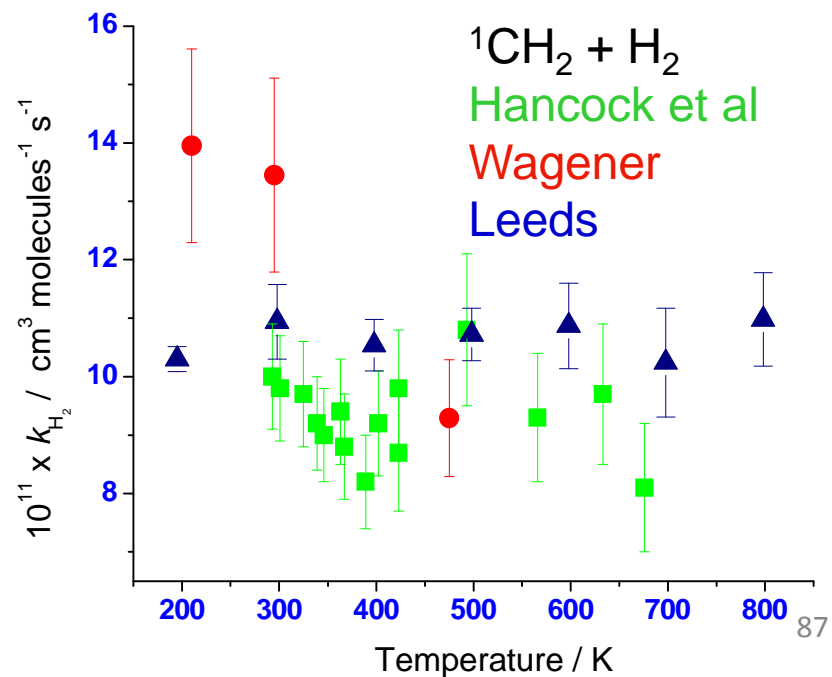
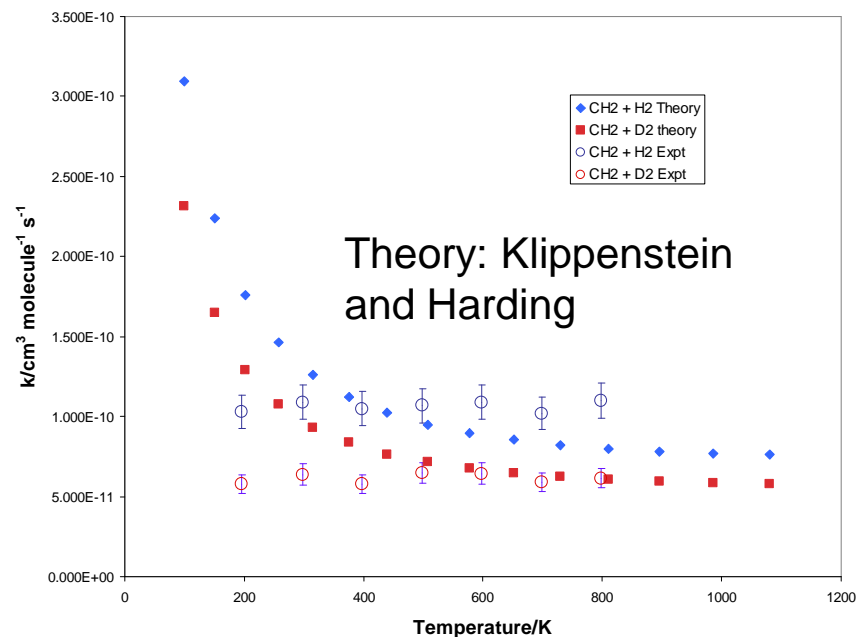


Singlet surface
 Triplet surface

Look at a simpler system

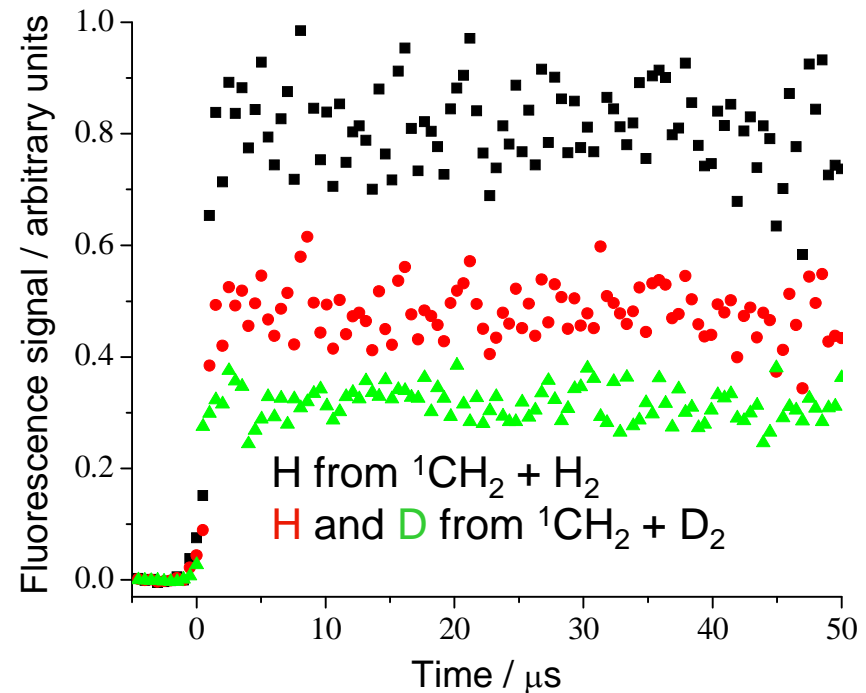


T / K	$10^{10} \times k_{\text{H}_2} / \text{cm}^3 \text{ molecules}^{-1} \text{ s}^{-1}$	$10^{11} \times k_{\text{D}_2} / \text{cm}^3 \text{ molecules}^{-1} \text{ s}^{-1}$
195	1.030 ± 0.021	5.77 ± 0.27
298	1.094 ± 0.064	6.39 ± 0.47
398	1.054 ± 0.044	5.77 ± 0.36
498	1.072 ± 0.045	6.49 ± 0.52
598	1.087 ± 0.073	6.45 ± 0.44
698	1.024 ± 0.093	5.91 ± 0.22
798	1.098 ± 0.080	6.14 ± 0.35



Absolute H and D atom yields from ${}^1\text{CH}_2 + \text{H}_2, \text{D}_2$

- k_{CIISC} again increases as T decreases. Similar behaviour for both collision partners.
- H vs D yields depend on dissociation of CH_2D_2^* . Theory gives a lower H:D ratio (~ 1.3 vs $1.6 - 2$)



T / K	${}^1\text{CH}_2 + \text{H}_2$	${}^1\text{CH}_2 + \text{D}_2$		
	a_{H}	a_{H}	a_{D}	$a_{\text{H}} + a_{\text{D}}$
195	0.71 ± 0.07	0.49 ± 0.07	0.24 ± 0.09	0.73 ± 0.12
298	0.85 ± 0.08	0.47 ± 0.05	0.28 ± 0.09	0.75 ± 0.10
398	0.92 ± 0.08	0.55 ± 0.07	0.34 ± 0.04	0.89 ± 0.10^{88}

Mechanism of $^1\text{CH}_2 \rightarrow ^3\text{CH}_2$ deactivation in reactive systems

- The triplet reacts with H_2 on a repulsive surface, while that for the singlet is attractive - an intersection occurs where isc may occur
- Harding calcs show the intersection occurs at large distances and at a small interaction energy
- Can the T dependence of ISC be explained in terms of Landau Zener theory?
- What is the role of the mixed states - if any?
- Do we include both the reaction and deactivation processes in the capture rate calculations?

